Electrical processes in heavy rain in the tropics

Lane-Smith, Derek R.

ELECTRICAL PROCESSES IN HEAVY RAIN IN THE TROPICS

Thesis submitted for the degree of

Doctor of Philosophy

by

Derek R. Lane-Smith

June 1969

ELECTRICAL PROCESSES IN HEAVY RAIN IN THE TROPICS

by Derek R. Lane-Smith

ABSTRACT

The thesis is based on research carried out in Sierra Leone over a period of several years. An asymmetric field mill and a 'wide-angle' shielded receiver have been developed for the measurement of electric field and precipitation current in tropical thunderstorms. A detailed field-mill theory is presented which analyses the effects of leakage currents, inadequate grounding, contact potentials, conduction current, 'pick-up' of fluctuating electric fields and noise in the amplifier. Principles are deduced for the optimum design of a precision field mill using either a phase sensitive detector or an asymmetric signal.

Measurements of precipitation current and its response to step changes in the field show that turbulent diffusion of splash droplets probably constitutes an important, even dominant, electrical process in heavy rain. The response of precipitation current to a lightning flash, averaged over many flashes, is large and has a delay of a few seconds. From the analysis of various models considered as a mechanism to explain the results it is deduced that charge carried on splash droplets is being diffused upwards by turbulence, transported by wind and is itself precipitating into the rain receiver.

An experiment was performed to measure the electric current due to evaporation. The results show that the current due to evaporation in the presence of an electric field is much smaller than that due to conduction in air.

The observation of a 'warm' thunderstorm cloud is reported. A project was developed to make visual and electrical measurements simultaneously on the same cloud. A time lapse film of tropical clouds, together with some electric field measurements beneath them, are used to discuss the flow pattern associated with a tropical thunderstorm and the mechanism by which it becomes charged.

Appendices include an analysis of the shielding effect of a vertical rod at ground potential, the description of some further instrumentation, including a data processing system designed by the author which uses a novel but effective method of detecting the occurrence of the peak of a signal, more detailed mathematical derivations of equations used in the main text and a filming schedule for the time-lapse photography.

ACKNOWLEDGMENTS

The author wishes to express his sincere gratitude to all those who have at one time or another rendered assistance in the work reported in this thesis.

The late Professor J. A. Chalmers, though over 2000 miles away most of the time, was always enthusiastic in his prompt replies to the letters which arrived far too infrequently from Sierra Leone. It was a privilege to be able to spend one term with him in Durham in the Autumn of 1966. The new design of field mill was completed at that time.

The summer of 1964 was spent in the department of Electrical Engineering at Manchester University designing and testing an analogue to digital converter for data processing. Professor D. Edwards was an apparently unlimited source of expertise and encouragement. Much of the author's enthusiasm for electronics has developed from that stimulating environment.

The research was carried out at Fourah Bay College

and the author is indebted to the faculty and the administration for the provision of a research hut, a grant and helpful cooperation. U.K. technical assistance and U.S. A.I.D. between them provided most of the test equipment without which the work would have been impossible. Dr. G. Williams of the Geography Department provided the meteorological records shown in Figures 3.4a, b and c.

The Sierra Leone Development Company offered facilities for a field site at Pepel where they maintain a port for shipping iron ore. They provided a room for equipment, free accommodation in the club house, complete with swimming pool, whenever it was necessary to change the recorder chart or service the equipment and full cooperation in preparing the room and erecting apparatus. The Sierra Leone Selection Trust gave the author rides in their aeroplane looking, unsuccessfully, for warm thunderstorms. Professor F.H. Ludlam lent a 16 mm. time-lapse movie camera to photograph clouds over Pepel.

Thanks are due to Dr. W.C.A. Hutchinson and Professor B. Vonnegut who read the thesis and made many helpful suggestions, to Mrs. S. Smith for her superb typing and to J. Radema who drew the diagrams.

TABLE OF CONTENTS

ABSTRACT i

ACKNOWLEDGMENTS iii

LIST OF ILLUSTRATIONS ix

CHAPTER I - Introduction 1

CHAPTER II - Instrumentation 5

2.1 Rate of Rainfall 5

2.2 Precipitation Current 7

2.22 The Effect of the Ground Rods 11

2.23 Calibration of the Electrometer 11

2.3 Electric Field 12

2.32 Sources of Spurious Signals and Noise 14

2.33 Design Variables 20

2.34 Choice of System 21

2.35 Conclusion 28

2.36 The Field Mill Type A 29

2.37 Field Mill Type B 30

2.38 Calibration of the Field Mills 31

2.4 Ancillary Electronics 32

2.41 Recorder Pen Switch 32

2.5 Site Topography 33

CHAPTER III - Results 35

3.1 Pattern of Electric Field Changes 35

3.2 Pattern of Precipitation Current Changes 37

3.3 Response of Precipitation Current to Electric Field Changes 37

3.4 Meteorological Records 40

CHAPTER IV - Analysis of Results 42

4.1 General Considerations and Nomenclature 42

4.2 The Whipple-Chalmers Model 45

4.3 A Droplet Diffusion Model 58

4.4 A Droplet Blanket Model 62

4.43 Splash Trajectories 66

4.44 Magnitude of Splash Effect. 67

4.5 Further Considerations 69

CHAPTER V - Evaporation Current 72

5.1 Zero Drift 72

5.2 Apparatus 72

5.3 Results 73

CHAPTER VI - The Pepel Project 74

6.1 The Warm Thunderstorm 75

6.2 Discussion of the Warm Storm 76

6.3 Experimental Project 78

6.4 Results 79

CHAPTER VII - Conclusions 82

7.1 Instrumentation 82

7.2 Precipitation Current 83

7.3 Splashing 85

7.4 Evaporation 87

7.5 Pepel Project 87

APPENDIX A - The Effect of the Grounded Rods .. 89

A.1 Background 89

A.2 Potential Gradient at the Ground . 90

APPENDIX B - Further Instrumentation 93

B.1 Single Drop Detector 94

B.2 Oscilloscope System 95

B.3 Analogue to Digital Converter 96

B.4 Peak Detection 99

B.5 Future Development 101

APPENDIX C - Mathematical Derivations 103

C.1 Nomenclature 103

C.2 Conduction Current 104

C.3 Hum and 'Pick-up' 106

C.4 Thermal Noise 107

C.5 Phase Sensitive Detector Type 1 .. 109

C.6 Phase Sensitive Detector Type 2 .. 110

APPENDIX D - 16mm Filming Schedule 112

D.1 Preamble 112

D.2 Schedule 113

REFERENCES 118

LIST OF ILLUSTRATIONS

Figure		Following Page
2.1a	Rate of Rainfall Circuit	6
2.1b	Rainfall Calibration Graph	7
2.2a	Rain Receiver Diagram	8
2.2b	Rain Receiver Photograph	8
2.21a	Splash Suppression Experiment	9
2.21b	Splash Suppression Results	10
2.32a	Exploded Diagram of Field Mill	14
2.34a	Phase Sensitive Detector, Type 1	22
2.34b	Diode Bridge Phase Sensitive Detector, Type 2	23
2.36a	Photograph of Field Mill Type A	29
2.36b	Pre-Amplifiers for Field Mill Type A	29
2.36c	Amplifiers and Detector for Field Mill, Type A	29
2.37a	Photograph of Field Mill Type B	30
2.37b	Photograph of Pepel Field Mill	30
2.37c	Pre-Amplifier for Field Mill Type B	31
2.37d	Detector for Field Mill Type B	31

Figure		Following Page
2.41a	Circuit of Recorder Pen Switch	33
2.5a	Freetown Peninsular	33
2.5b	Fourah Bay College	33
2.5c	Kortright Field Site	33
2.5d	The Research Hut	33
2.5e	Rain Receiver Site	33
2.5f	Field Mill Site	33
3.10a	Typical Electric Field Changes	35
3.20a	Record of Nov. 4, 1965, Storm	37
3.30a	Precipitation Current Changes after Lightning	37
3.30b	Precipitation Current and Electric Field Changes after Lightning	37
3.30c	Computed Characteristics of Three Storms .	39
3.4a	Meteorological Records for Oct. 24, 1965 ..	40
3.4b	Meteorological Records for Nov. 4, 1965 ..	40
3.4c	Meteorological Records for June 7, 1966 ..	40
4.22a	Graph of Median Volume Radius against Rainfall	47
4.22b	Graph of Mean Volume Radius against Rainfall	47
4.23a	Graph of Height Above Ground against Potential Gradient	54
4.23b	Table of Values for 4.23a	55
5.20a	Evaporation Current Experiment	72

Figure		Following Page
6.1a	Sierra Leone River	75
6.1b	A Warm Thunderstorm	75
6.4a	Growth of Electric Field with Cloud Height	81
6.4b	Table of Cloud Heights with Time and Frame Number	81
7.2a	Parameters from Three Storms	84
A.2a	Table of Values for A.2b	91
A.2b	Graph of Shielding Effect of Different Shaped Rods	91
B.2a	Trigger Pulse Amplifier	95
B.2b	Camera Control Circuit	95
B.3a	Block Diagram of A/D System	97
B.4a	Peak Detector	100
C.2a	Variation of Conduction Current and Displacement Current with Time	104

CHAPTER I

INTRODUCTION

Living and working in the tropics gives one the opportunity to study a wide range of phenomena which do not occur in temperate climates and which therefore are beyond the reach of the majority of interested scientists. This unique opportunity helps to compensate for the special difficulties which are a feature of life in the tropics.

Thunderstorms near Freetown have several significant differences from their temperate relatives. The freezing level is usually at around 6 km, the cloud base is often as low as 300m and the cloud top may range anywhere from 3 km to 20 km. Though they are often organized in groups or lines which sweep the whole country, they are also frequently seen as isolated storm clouds both small ones and also the big ones. The ratio of the

number of lightning strokes within the cloud to the number striking the ground is of the order 10.

Many storms feature intense localized rainfall with rates sometimes exceeding five inches per hour. Such heavy rain together with high electric fields provided the conditions for measurements described in this thesis.

The climate of Freetown is characterized by a dry season, November to April, and a wet season, June to September. The annual rainfall varies from around 70 inches in the Kissy area on the east side of the mountains (see Figure 2.5a) to over 300 inches in the Guma valley on the west. The meteorological station at Kortright in Fourah Bay College (see Figure 2.5b) has an annual rainfall of about 140 inches. During the dry season the air is laden with fine dust, possibly from the Sahara desert, which sometimes reduces visibility to less than one mile. The dust may carry a negative charge (Harris, 1967). At the changeover of the seasons, thunderstorms sweep across the country washing out the fine dust so that, after a night of storms, the visibility the following morning may extend nearly 100 miles, bringing into view the Futa Djallon mountains in Guinea.

It is not known whether the dust plays any part in the development or the electrification of the thunderstorms.

Measurements on tropical thunderstorm precipitation have been made by Sivaramakrishnan (1961, 1965 and 1967). The 1961 paper is concerned with the origin of electric charge carried by thunderstorm rain in the tropics. In heavy rainfall he finds the rain current density sometimes greater than the point discharge current density and also that, according to the Whipple-Chalmers (1944) process the rain drops were positively charged right from the cloud. He rejects any electrical effects due to splashing. The work of this thesis sheds new light on the problems raised by those results.

The high freezing level raises the possibility of warm thunderstorms. Several of these have been observed and reported and their significance discussed. The author's observation of a warm storm over Pepel (see Figure 6.1a) initiated the Pepel project described in Chapter VI.

An unexplained zero drift in the rain receiver caused an investigation of electrification by evaporation. This suggestion has been raised from time to time, starting with Volta (1782), see Chalmers (1967). Most reports, as that stated here, show no electrification

by evaporation or that it is small compared with conduction currents under the conditions of the experiment.

A considerable amount of time and effort at Fourah Bay College was spent preparing to make measurements which were, in fact, never made. Measurements on individual drops with a high speed data processing system were planned. A report is included in Appendix B.

CHAPTER II

INSTRUMENTATION

2.0 Instruments were developed to measure electric field, precipitation current and rate of rainfall. A new principle of operation was applied to the measurement of electric field and a detailed analysis of field mill design is presented.

Other instruments designed but not used to obtain the results considered in chapters III and IV are described in Appendix B.

2.1 Rate of Rainfall

A 'Casella' tipping bucket rain gauge was modified to give a direct recording of rate of rainfall on the potentiometric recorder.

Each flip of the bucket caused a momentary contact to be made in a mercury switch mounted on the arm supporting the bucket. A diode pump circuit, figure

2.1a, charged two capacitors which discharged through a diode network designed to give logarithmic response.

At low rainfall each flip of the bucket was clearly resolved as a separate event on the chart. Very high rates of rainfall, of the order 6" per hour or 4 x 10^{-5}m sec^{-1}, gave a large and nearly constant deflection.

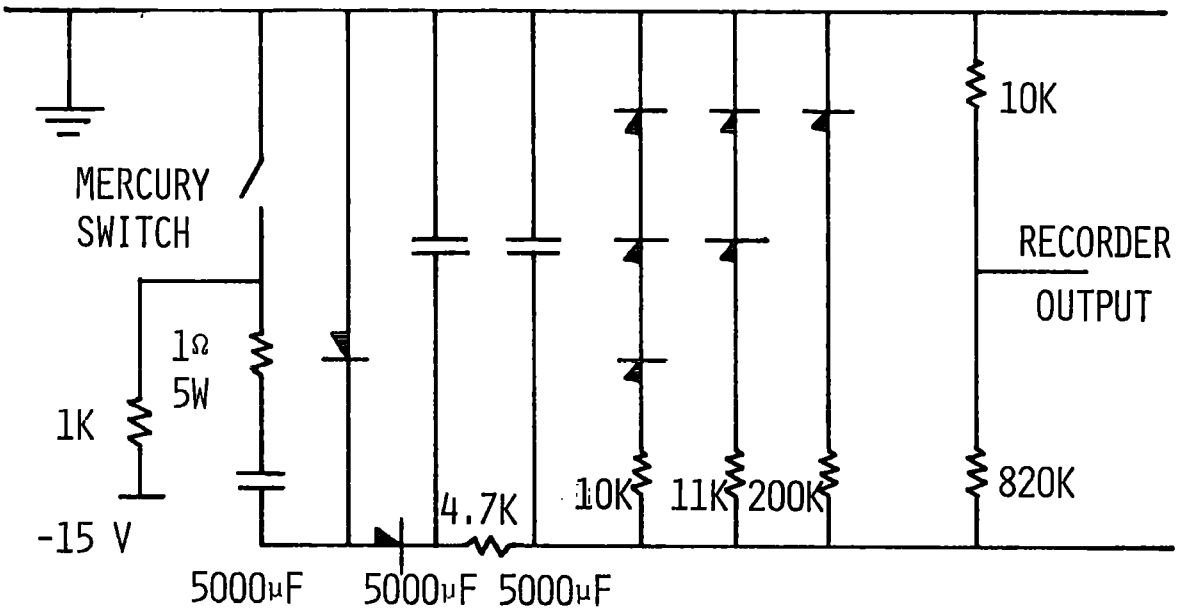

RATE OF RAINFALL LOGARITHMIC CONVERTER CIRCUIT

FIGURE 2.1a

The rain gauge was calibrated by allowing a burette to discharge slowly into the gauge and counting the number of flips of the bucket. Each flip was found to correspond to 0.02 ± 0.001 inches or 5.1 ± 0.5 x 10^{-5}m of rain.

The chart record was calibrated for high rates of rainfall by tipping the bucket at various steady and measured rates. A calibration graph of peak displacement against rate of fall was plotted, figure 2.1b. Calibration for lower rates of fall was not required because each tip of the bucket could be resolved.

2.2 Precipitation Current

The current from the surface of the earth downwards consists of displacement current proportional to the rate of change of electric field, the precipitation current brought to the surface on hydrometeors which have fallen from a cloud, a splashing current being a possible net flow of charge due to the emission of charged droplets from the ground and a conduction current due to the flow of ions to or from the surface and which will be taken to include point discharge current.

The parameter of interest was the charge on the rain rather than the net air-earth current and it was

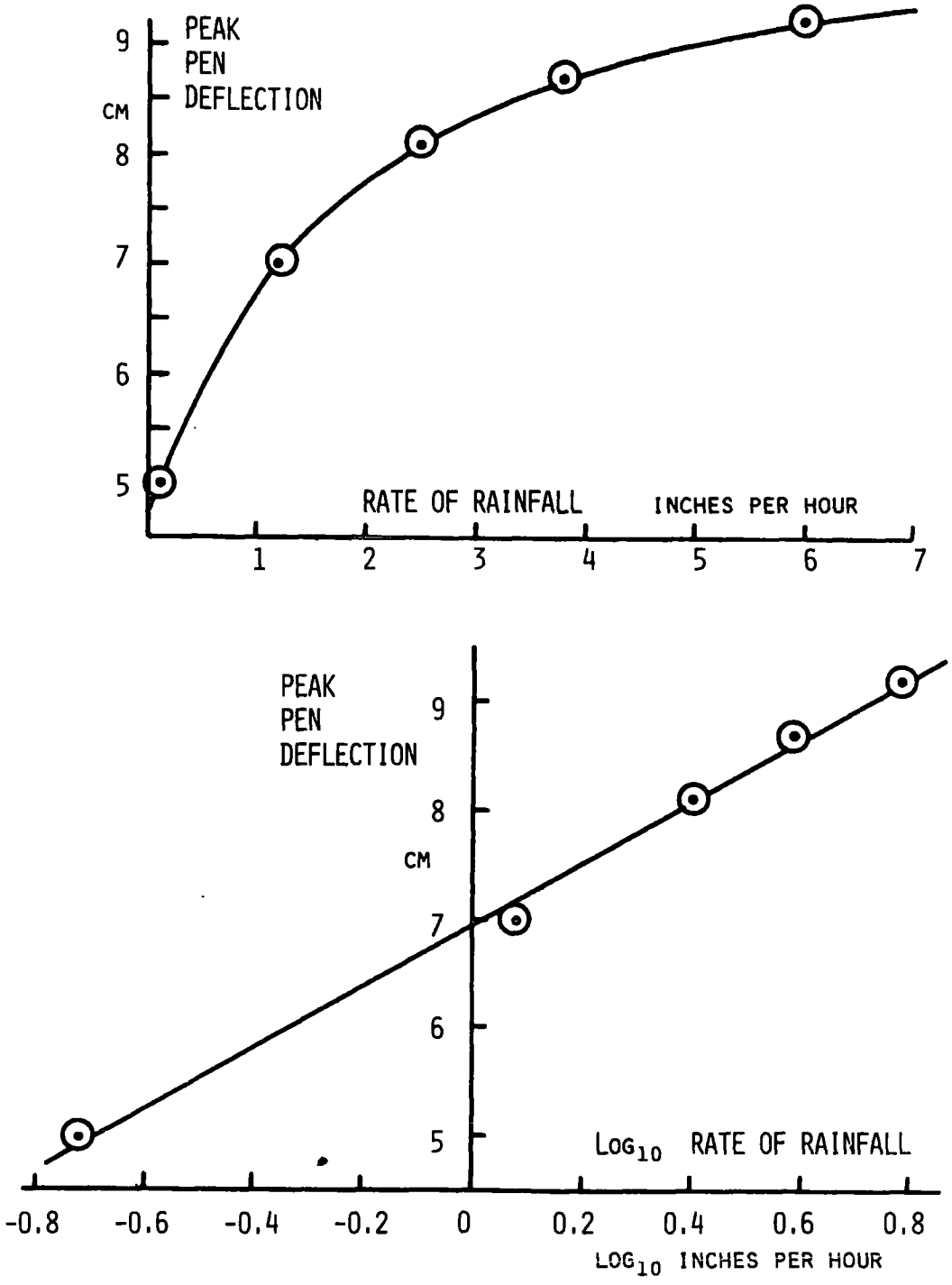

FIGURE 2.1b RATE OF RAINFALL CALIBRATION CURVES

decided, therefore, to try to measure this one parameter alone rather than to measure the combined effect and to measure and correct for the effect of the other parameters. Both methods are fraught with difficulties and there is some uncertainty in interpreting the results.

A rain receiver (see Figures 2.2a and 2.2b) was built to receive rain over a wide angle and which would be screened, as far as possible, from the effects of changing field, splashing and conduction currents.

The receiver was able to receive driven rain at angles up to 70^{o} to the vertical. The shielding was sufficient to make displacement currents negligible except during a lightning flash and conduction currents negligible at all times.

The aperture was 0.127 m diameter and was surrounded by wire mosquito netting from the lip to a distance of 0.6 m. The separation between the netting and the lid was not less than ½cm at 2cm from the lip and increased beyond that. Three wire rods, gauge 12 copper, 0.38 m high were fixed to the netting symmetrically round the aperture and 0.25 m from the lip. Three more rods, 1.2 m high, were placed symmetrically 1.2 m from

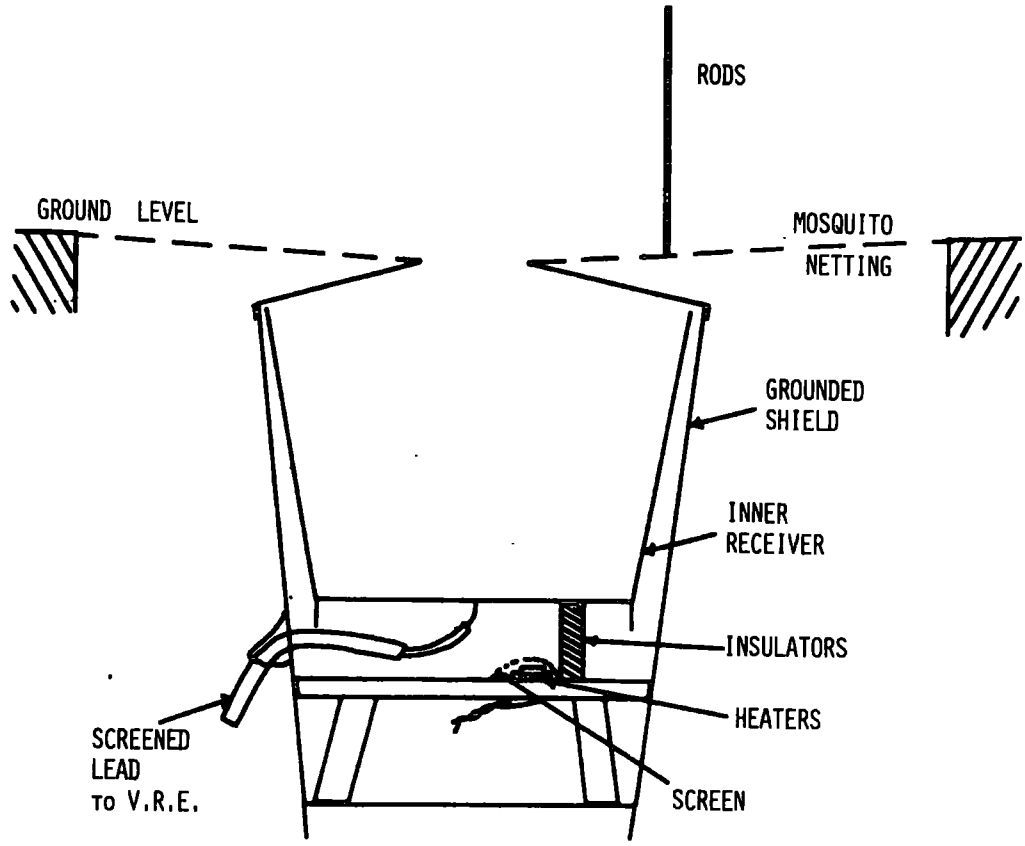

FIGURE 2.2a RAIN RECEIVER

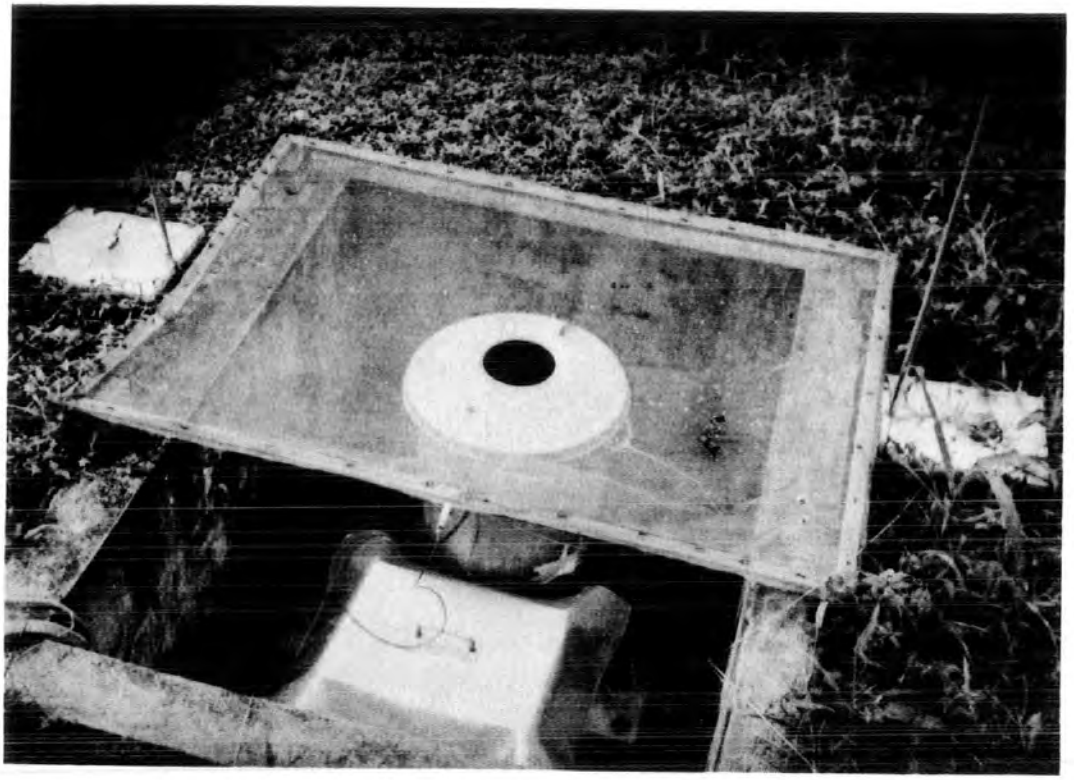

FIGURE 2.2B RAIN RECEIVER

the lip between the 38 cm rods.

The mosquito netting considerably reduced the splashing outside the receiver and the rods reduced the field at the lip of the receiver so that splashing there took place under low field conditions and the resultant change separation was small.

At high fields, no doubt, the rods emitted point discharge current but this only served to improve the screening of the receiver.

The receiver stood on polystyrene insulators which were kept warm by resistors carrying current behind a grounded screen. The output was fed to an Ekco type N616B vibrating reed electrometer.

The instrument was calibrated monthly during the rainy season. The insulators had to be cleaned about once every six months and until the V.R.E. became inoperative around August 1966 (it started to deposit change on the input circuit) the instrument gave excellent service.

2.21 Experiment to investigate the effectiveness of wire netting, with mesh about 8 wires to the cm, in reducing the effect of the splashing (Blanchard, 1949).

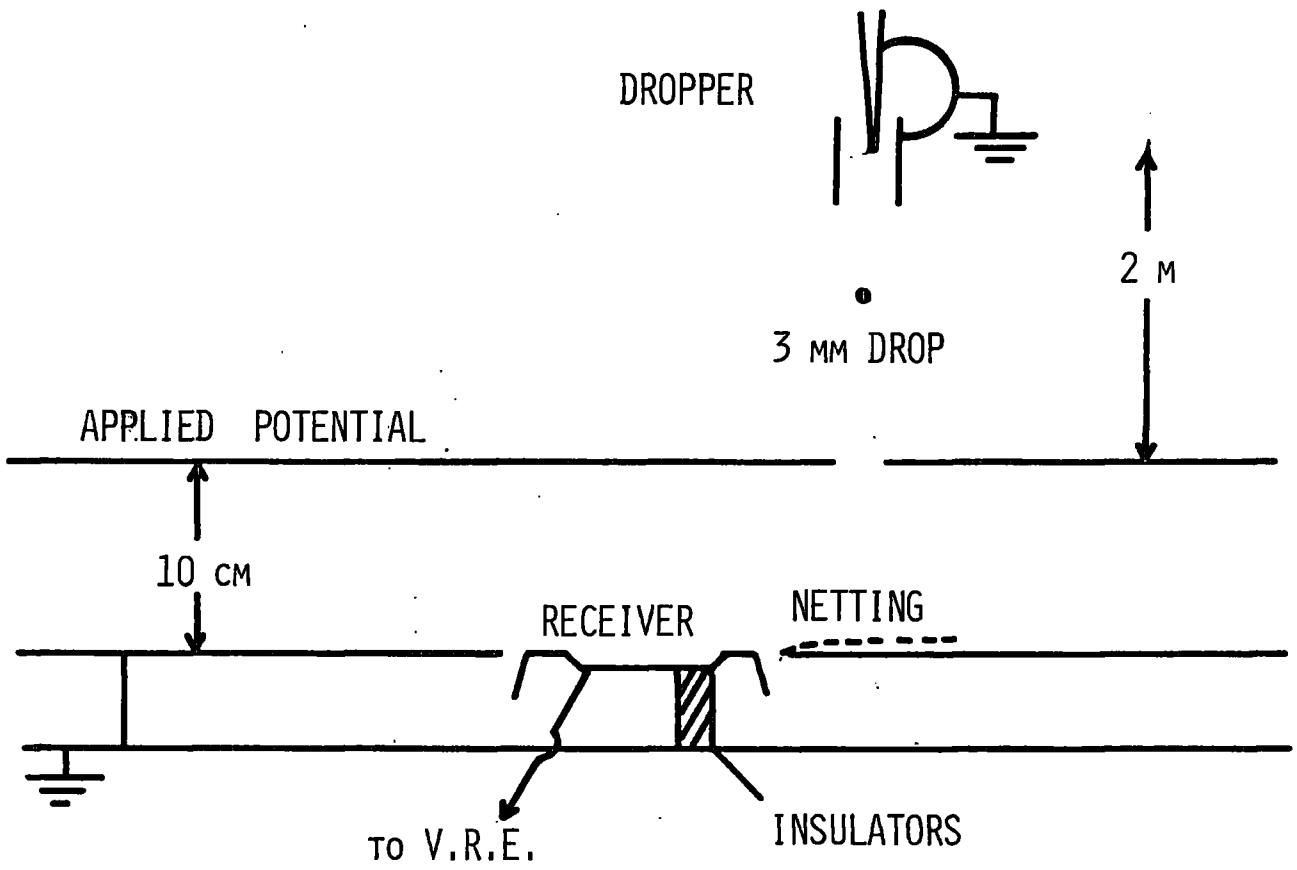

FIGURE 2.21a

SPLASH SUPPRESSION EXPERIMENT

Three-millimetre drops of nominally zero charge were dropped 1.8 m onto a grounded metal surface under various field conditions. About one third of the resulting droplets were caught on an insulated receiver connected to a V.R.E.

Netting was positioned beneath the dropper 0.5 cm above the ground plane and the measurements repeated.

The results, figure 2.21b, showed that in the configuration, the netting reduced the splashing effect by a factor of about four. It seems the netting acts in two ways. The drop does not splash on the wire but passes straight through and is shattered in the process. The resulting smaller drops, less than 1 mm diameter, are less effective in splashing on the surface below, so fewer droplets are produced. Secondly, the splashing that does occur below the netting takes place under zero field conditions so that the droplets carry very little charge (Lenard, 1892).

The effect of splashing into the rain receiver would be a "mirror image" effect (Simpson, 1949), with a time delay of less than one second. That this was not observed indicated that any splashing effect remaining was small.

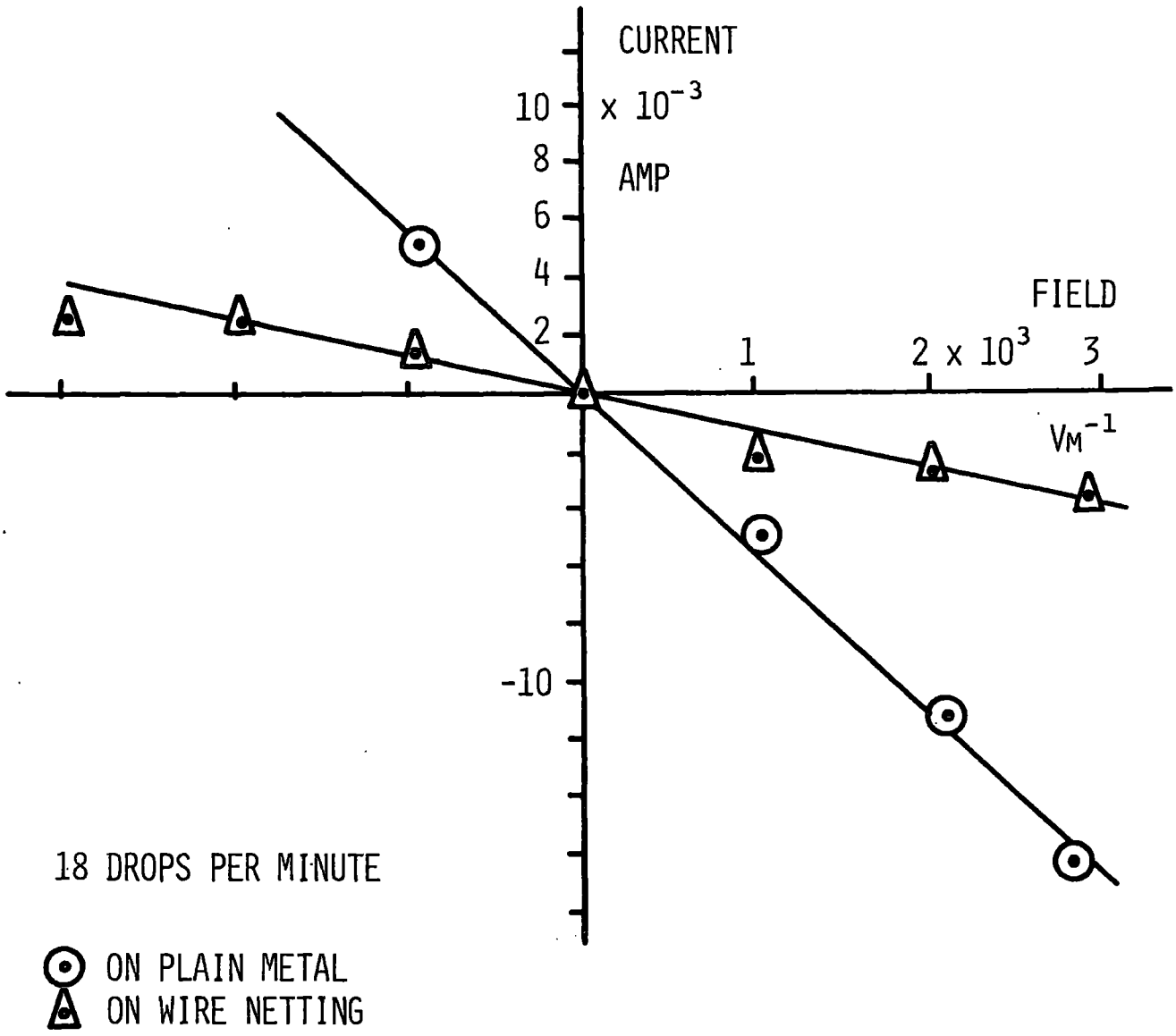

GRAPH OF SPLASH CURRENT AGAINST FIELD

FIGURE 2.21b

2.22 The Effect of the Ground Rods

The total effect of the rods was to reduce the field at the lip of the aperture by less than 10% in fine weather, see Appendix A. Away from the aperture the shield was more complete.

The probability that a drop would hit the top 1/10th of a rod instead of falling into the receiver was about 0.1%. The probability that the droplets from such an impact would subsequently fall into the receiver, assuming equal probability over an area of radius two feet, was about 1%. Both effects were assumed negligible. If the latter were significant, a similar mirror image effect to that due to splashing would have been evident.

2.23 Calibration of the Electometer

The Ekco was used in the voltage mode. That is, the potential difference across a selected input resistance, carrying the unknown current, was measured directly. It was necessary therefore to verify the accuracy of the voltage ranges and of the selected resistors.

The potential difference across the terminals of a standard Mallory cell was measured and the reading

was always equal to the known E.M.F. of the cell to within 2%.

The input resistors, 10^8, 10^{10} and 10^{12} ohm, were measured by discharging a capacitor. The special quality polystyrene capacitor of 0.5133 MF had a discharge time constant in dry air of several days. Values for the half life of the charge on the capacitor were 41.6 ± 2 seconds across the 10^8, 59 ± 2 minutes across the 10^{10} and more than a day across the 10^{12}. The corresponding values for the resistors are 1.15 ± .05 x $10^8\Omega$, 0.98 ± .04 x $10^{10}\Omega$ and of the order $10^{12}\Omega$.

The 15% error in the $10^8\Omega$ was not considered in the calculation of precipitation current because other uncertainties probably introduced greater errors and because it is merely a scaling factor.

The existence of a spider's web or other deterioration in the insulation of the receiver was first manifested by a drift in the zero. The leakage completed a circuit around which thermoelectric forces were able to drive a current causing the zero drift.

2.3 Electric Field

2.30 The design of a field mill and its associated

electronics was developed over a period of three or four years.

The useful measurements at Kortright, Fourah Bay College, made prior to August 1966 were made with a field mill, to be called type A, which used a phase sensitive detector for sensing the sign. After this date, a mill, to be called type B, was installed which generated an asymmetric wave form for sign discrimination (Lane-Smith, 1967). In addition, a field mill of type B was set up at Pepel and gave six months continuous service.

2.31 Some of the design factors for a field mill system are first discussed before a description is given of the actual instruments used.

The field mill (Harnwell and van Voorhis, 1933; Lane-Smith, 1967) is used to measure an electric field. Spurious signals may arise in the field mill system due either to a potential difference between the rotor, or screen, and the stator of the field mill, pick-up on the stator and the lead to the amplifier, or noise in the amplifier.

The factors which may be varied in the design of a field mill include the area of stator exposed, the

rotor rotation rate and signal frequency, the input impedance of the amplifier, and the detection system used. These factors and their effect on the signal-to-noise ratio are considered.

2.32 Sources of Spurious Signals and Noise

Consider a field mill, figure 2.32a, which alternately exposes and screens an area A of an insulated plate. Let the rotor run between the insulated stator and a ground shield. Let both the rotor and the shield have n identical equi-spaced sectors removed and let the separation between the shield and the stator be d. The amplifier input, in effect, consists of a resistance R in parallel with a capacitance C.

2.32 (i)

Calculation of the signal due to a potential difference between the stator and the rotor or shield.

This potential difference may be caused by the combined effect of static charge on the insulators, leakage onto the stator from a supply potential in the amplifier, poor grounding of the rotor, contact potential difference between the stator and shield and air conduction current onto the stator.

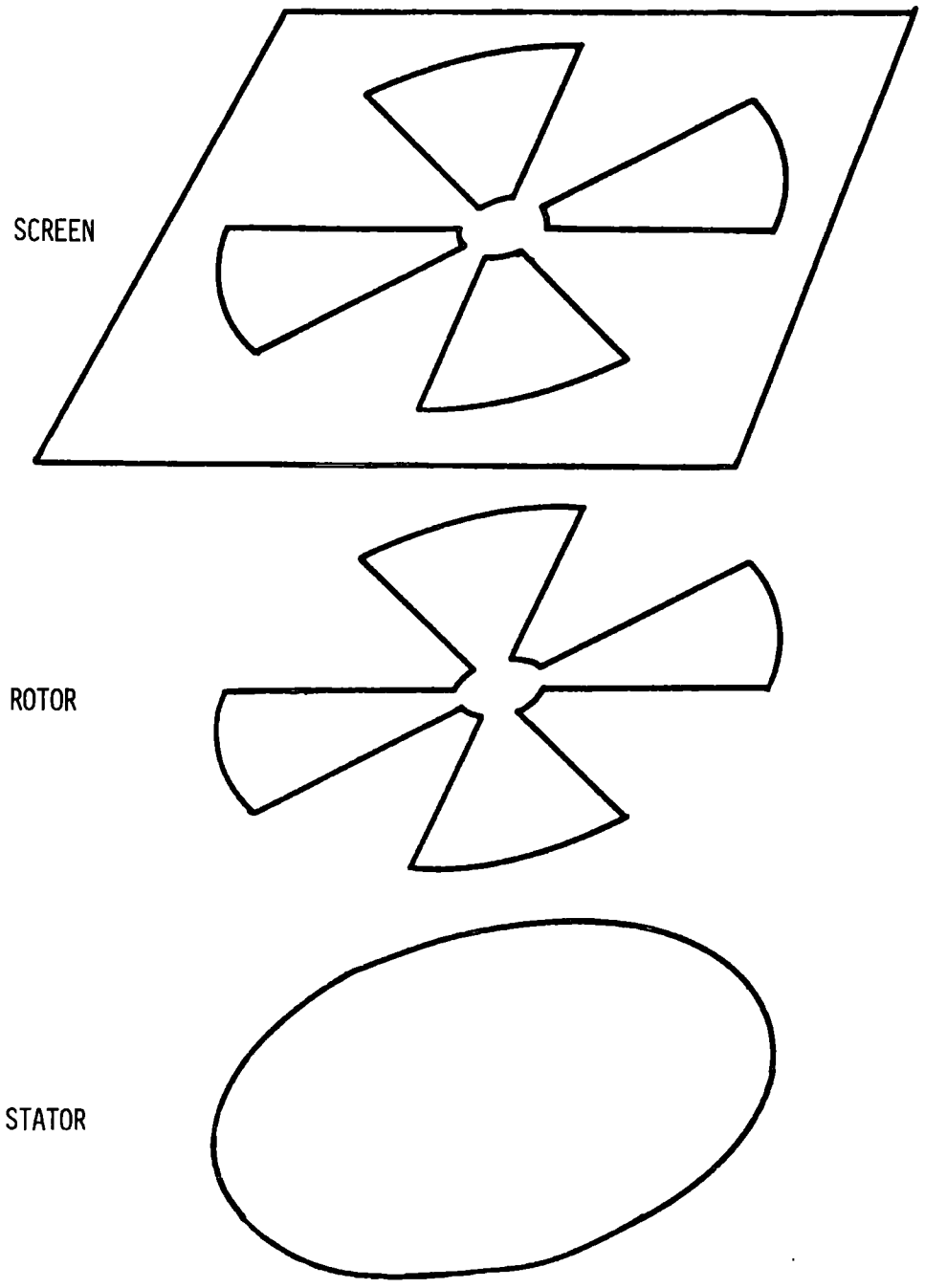

FIGURE 2.32a EXPLODED DIAGRAM OF FIELD MILL

The effect of a potential difference V between the shield and the stator is identical to that produced by a field of V/d. If errors are required to be less than 0.1 volt per metre and d is of the order 10^{-2}m, V should be less than 1 mV.

If the stator is isolated from the amplifier by a good quality capacitor, leakage current onto the stator is not likely to exceed 10^{-12} amperes in which case the resistance to ground of the stator should not be greater than 10^{9} ohm. R will be this resistance in parallel with the input resistance of the amplifier.

If the leakage current onto the rotor from the motor supply is of the order 1 mA, the resistance to ground of the rotor should be less than 1 ohm. The brushes may be allowed to jump off the rotor for a time not exceeding δT where

$$I\delta T/c' = \delta V \qquad (1)$$

where I = Leakage current onto rotor

c' = Capacitance of the rotor

δV = Allowed potential change of the rotor

if			
I	=	10^{-3} Amp	10^{-6} Amp
c'	=	10 pF	100 pF

	δV	=	10 mV	0.1 V
then	δT	=	10^{-10} secs	10^{-5} secs

This condition which appears very stringent may be relaxed if the amplifier or detector do not respond to high frequency spikes.

If the shield, rotor and stator are all made of stainless steel, contact potentials would probably remain well below 1 mV.

The current, I_2, being supplied to the stator by conduction in the air is given by

$$I_2 = KEa \qquad (2)$$

where K = Conductivity of air

E = Electric field

a = Area of plate exposed

If $a = 2tA/T$ $(o<t<T/2)$ and $a = 2A(1 - t/T)$ $(T/2<t<T)$ where A is the total plate area exposed and T is the periodic time of the signal, the effect of I_2 can be approximated to a combination of -- a) a current 90^{o} out of phase with the field signal and of amplitude KEA/2 together with, -- b) a signal due to an applied potential on the stator of KEAR/2.

The ratio γ of the signal to the spurious signal

due to I_2 is given by (see Appendix C)

$$\gamma(a) = 2\varepsilon_o/KT = 10^5 \text{ approx.}$$

where ε_o = Permittivity of free space (10^{-11} F m^{-1})

K = conductivity of air (10^{-13} $ohm^{-1}m^{-1}$)

T = Signal period = 10^{-3} secs

and $\gamma(b) = 2d/KAR = 10^3$ at least.

Even if $\gamma(b)$ were significant, changes in sensitivity due to changes in K would still be negligible.

2.32 (ii)

Pick-up on the stator and signal lead.

If earth loops are avoided, pick-up in the input lead is due to fluctuating electric fields, mainly at the supply frequency, which introduce current at the input proportional to de/dt. Let the charge, q, introduced by given by

$$q = He\cos\omega t$$

where $e\cos\omega t$ is the field at time t,

and H is a constant.

The response of the amplifier depends on the relationship between RC and ω(Lane-Smith, 1967). If RC is much larger than the periodic time of both the field signal and the hum pick-up, the signal-to-noise ratio, γ,

is given by (see Appendix C)

$$\gamma_{(c)} = \varepsilon_o EA/He$$

If the signal frequency is much higher than the hum frequency and 1/RC lies between, then

$$\gamma_{(c)} = \varepsilon_o EA/He\omega CR$$

so the smaller the value of RC, the better the signal-to-noise ratio.

A notch filter at supply frequency or a high pass filter would further improve the hum rejection.

2.32 (iii)

Amplifier noise.

If the first stage of the amplifier is a silicon planar Field-Effect transistor (F.E.T.), the two main sources of noise will be Johnson noise in the gate leak resistor and the equivalent of shot noise in the channel current.

The Johnson noise can be considered as an E.M.F., e_1, in series with the gate leak resistor, R_g, then

$$\overline{e_1^2} = 4kT\ B\ R_g \qquad (3)$$

where k = Boltzmann's constant

T = Absolute temperature

B = Power bandwidth

This E.M.F. is decoupled by the input capacitance and the voltage applied to the gate of the F.E.T., e_2, is given by

$$\overline{e_2^2} = \overline{e_1^2} \,/\, (1 + \omega^2 C^2 R^2) \tag{4}$$

If the signal and most of the noise is at a frequency high compared with 1/RC, the signal-to-noise ratio, $\gamma(d)$ becomes (see Appendix C)

$$\gamma(d) = \varepsilon_o \, EA_f \sqrt{R} \,/\, \sqrt{kTB} \tag{5}$$

where f = the signal frequency.

All other things being constant, $\gamma(d)$ varies as $\sqrt{R}$. For typical values and with a bandwidth of 10^3 Hz, $\gamma(d) \simeq \sqrt{R}$.

The F.E.T. shot noise can be expressed in terms of a noise characterization resistance, R_n, such that the noise is equivalent to that produced by a fluctuating potential difference between the gate and source, e_3, given by

$$\overline{e_3^2} = R_n \, 4kT \, B \tag{6}$$

R_n varies with frequency and with channel current but a typical value would be of the order 10^7 ohm (Blaser and MacDougall, 1964). This noise is not decoupled

by the input capacitance, so the signal-to-noise ratio becomes (for RC much bigger than the signal period)

$$\gamma(e) = \varepsilon_o EA / \sqrt{4kT\ B\ R_n}\ C \qquad (7)$$

For a given signal frequency, the range of acceptable input time constant, P (= RC), is limited and may be considered here as an invariant. P/R may be substituted for C in equation (7) giving

$$\therefore \quad \gamma(e) = \frac{\varepsilon_o EAR}{\sqrt{4kTBR_n} \cdot P} \qquad (8)$$

If the following values are substituted in equation (8),

$E = 1\ V\ m^{-1}$

$A = 10^{-2} m^2$

$T = 300^{o}K$

$B = 10^{3}$ Hz

$P = 10^{-2}$ secs

then $\gamma(e) = 10^{-6}R$

Miller feedback over the first stages can be used to stabilize the charge sensitivity of the pre-amplifier but it does not change the signal-to-noise ratio.

2.33 Design Variables

The two most important sources of spurious signal are pick-up and shot noise in the first amplifier stage.

The signal-to-noise ratio for the hum pick-up is proportional to 1/P, where P is the periodic time of the signal or the time constant, RC, whichever is the greater. The signal-to-noise ratio for the shot noise is proportional to AR / $P\sqrt{B}$. For best performance, P should be as small as possible and AR / $\sqrt{B}$ as large as possible.

The maximum signal frequency is limited, mechanically, to the order 10^3 Hz, RC therefore is limited to around 10^{-2} secs. A will be limited by the permitted moment of inertia of the rotor, $10^{-2}m^2$ may well be difficult to exceed. R is limited by leakage currents and by the electronics to a value around 10^8 ohms. B is determined by the system used and the response time required; the minimum value would be about 10 Hz.

Using the best figures, for a field of 1 Vm^{-1}, a signal-to-noise ratio of over 10^2 appears quite feasible.

2.34 Choice of System

Three basic systems available are -- a) a simple rectification of the signal with an applied field to offset the zero for sign discrimination, -- b) a phase sensitive detector, or -- c) an asymmetric signal carrying information on both magnitude and sign of field

(Lane-Smith, 1967).

2.34a

Offset Zero.

Among the disadvantages of system (a) are --i)it accepts the full bandwidth of noise and, -- ii) changing the range involves setting up a new zero displacement. This system will not be discussed further.

2.34b

Phase Sensitive Detector.

The output, V, of the normal type of phase sensitive detector (see, for example, Chaplin and Owens, 1957) as shown in figure 2.34a for signal period T and a response time nT may be approximated to

$$V = \frac{1}{nT} \sum_{p=1}^{n} \int_{(P-\frac{1}{2})T}^{pT} (e_t - e_{(P-\frac{1}{2})T}) \cdot dt$$

The variation of output with phase makes this detector unsuitable for the present application. If $e_t = e_o \sin \{\frac{2\pi t}{T}\}$ and if Vo is the output when the chopping signal is in phase with the field signal, then the out-

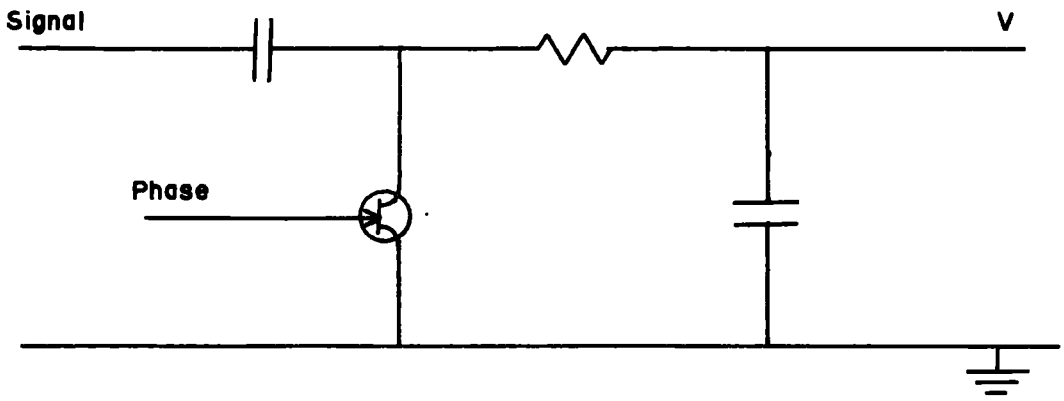

FIGURE 2.34A PHASE-SENSITIVE DETECTOR, TYPE I

put with a differential phase change of δ becomes (if δ is small) (see Appendix C),

$$V = Vo\ (1 - \frac{\pi}{2} \sin \delta)$$

which means that a 1% or 3.6^{o} change in phase produces a 10% change in the output. Similarly, variations in the mark-to-space ratio cause significant changes in the output, though these can be reduced by a form of negative feedback (Lane-Smith, 1965).

It is difficult to set up a phase reference signal whose phase is accurate or stable to within 1%. A slight offset of the rotor or a small differential phase change in the amplifiers may introduce errors of this magnitude and so make this type of detector unacceptable.

The output, V, of a diode bridge type of phase sensitive detector (see, for example, Beneteau and Riva, 1963 or Moody, 1956) as shown in Figure 2.34b for signal period T and a response time nT may be approximated to

$$V = \frac{1}{nT} \sum_{p=1}^{n} \int_{(P-\frac{1}{2})T}^{pT} e_t \cdot dt$$

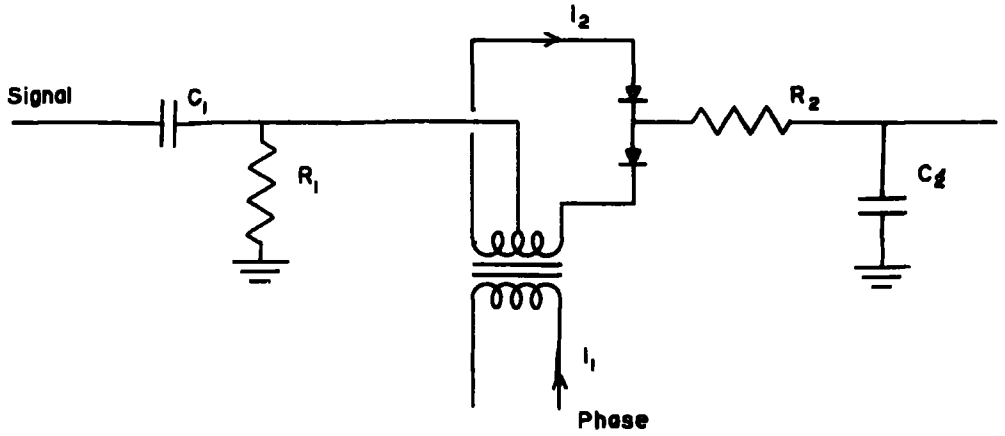

I_1 is a voltage limited square wave current drive

such that $I_2 >> \frac{\hat{e}}{R_2}$ where $\hat{e}$ is the peak value of the signal voltage

$C_1R_1 >>$ T where T is the signal period

$C_2R_2 >>$ T $\quad R_2 >> R_1$ and $\hat{e}_{min/R_2} >>$ Diode reverse current

A full diode bridge could be used instead of the centre tap on the transformer.

FIGURE 2.34B A DIODE BRIDGE PHASE-SENSITIVE DETECTOR

The output with a small phase differential δ now becomes (see Appendix C),

$$V = Vo\ (1 - \frac{\delta}{2} \sin\delta)$$

which means that a 1% or 3.6^{o} change in phase produces only a 0.2% change in the output.

In addition, the diode bridge detector responds less to subharmonics of the signal frequency.

If the detector response time tends to infinity and the phase signal has a mark-to-space ratio of 1, then the output of the diode bridge detector to signals of all frequencies is given by

$$V = \tfrac{1}{2}(h\ V_f + \frac{h_3 V_{3f}}{3} + \frac{h_5 V_{5f}}{5} + ...)$$

where $V_f = \overline{|e_f|}$ is the mean of the modulus of the signal at frequency f

f = fundamental frequency of phase switching

h_1, h_3, h_5 ... are factors, lying between $-\pi/2$ and $+\pi/2$, whose value depends on the relative phase of the switching and the signals at frequencies f, 3f, 5f, ...

With a finite response time, nT, the frequency

response is a fourier transform of the response time about each of the 'resonant' frequencies. This approximates to a bandpass of ± δf either side of f, 3f, 5f, ... where $\delta f = \frac{1}{nT}$ provided δf is smaller than the lowest frequency passed by the amplifier.

Thus if a low pass filter is inserted between f and 3f, the phase sensitive detector responds only to noise at frequency f and bandwidth 2δf. This improves the signal-to-noise ratio by a factor of 10 or more. Tuned amplifiers may be used (Gathman and Anderson, 1965) but there may be little improvement in the signal-to-noise ratio and a drift in the signal frequency may cause a change not only in the sensitivity but also in the phase shift of the amplifier.

2.34c

Asymmetric Signals.

The output, of the asymmetric detector with a response time nT can be approximated to

$$V = G\,(e_+ - e_-)nT$$

where G is a constant

e_+ is the peak positive swing during the previous time, nT

e_- is the peak negative swing during the

previous time, nT.

Landon (1941) has shown that the amplitude of white noise has a gaussian distribution so that the probability, P(e)·de of the voltage at any instant lying between e and e + de is given by

$$P(e)\cdot de = (2\pi\overline{e^2})^{-\frac{1}{2}} \cdot \exp(-e^2/2\overline{e^2})\cdot de$$

and the probability that it will be bigger than e_m is

$$\int_{e_m}^{\infty} P(e)\cdot de$$

The value of $\int_{e_m}^{\infty} P(e)\cdot de$ can be determined numerically for various values of the ratio $\frac{e_m}{\sqrt{\overline{e^2}}}$.

$\frac{e_m}{(\overline{e^2})^{\frac{1}{2}}}$	$\int_{e_m}^{\infty} P(e)\cdot de$
3	0.0015
4	3×10^{-5}
6	3×10^{-7}

2.34 (i)

Zero Shift

In a time, nT, the total number of independent sam-

ples is of the order BnT, where B is some representative frequency bandwidth. If nT = 10^{-1} secs and B = 10^3 Hz, BnT = 10^2 and the most probable peak value of e will be $2.2\sqrt{\overline{e^2}}$. During twice this period that most probable peak value would be $2.45\sqrt{\overline{e^2}}$ so the most probable difference between the positive and negative peak values during a time in which the order of 100 independent samples may be observed is $0.25\sqrt{\overline{e^2}}$. This compares favourably with the expected zero shift in a phase sensitive detector whose bandwidth is 1/20th of the 10^3 Hz used in this example.

2.34 (ii)

Sensitivity

In the presence of an asymmetric signal, the contribution of the noise of one sign will be sampled over a longer period than that of the opposite sign. The difference will depend on the amplitude of the signal.

For small signals, whose amplitude, V, is of the order $\sqrt{\overline{e^2}}$, the noise would reduce the effective signal by about $0.5\sqrt{\overline{e^2}}$. For larger signals, the noise contribution increases to a maximum of about $2\sqrt{\overline{e^2}}$ for signals whose amplitude, V, is greater than $50\sqrt{\overline{e^2}}$. These factors demand that noise levels be kept steady and a

detailed calibration curve be plotted if the field mill is to be used at the limit of its sensitivity.

2.34 (iii)

Asymmetric Pick-up

The detector cannot cope with this type of interference. If the hum signal includes any harmonics of fixed phase relative to the fundamental then this is detected as a shift in the zero reading. By using a high signal frequency this effect can normally be kept small.

2.35 Conclusion

A fast mill with a high input impedance amplifier will give the best signal-to-noise ratio in all systems. For maximum sensitivity, a bandpass amplifier with a phase sensitive detector of the preferred type is better than the asymmetric field mill but at the cost of considerably increased complexity. Either design is sensitive to signals whose amplitude is of the order $\sqrt{e^2}$ and can be built to have a zero stable to well below 1 volt per metre.

For normal continuous recording, the mill may be placed well above ground level. This increases the ex-

posure factor, and hence the sensitivity, but also eliminates any shielding due to space charge near the ground.

2.36 The Field Mill Type A

The mill, Figure 2.36a, consisted of a segmented stator and a similar rotor. A phase signal was obtained from an electrostatic probe mounted between the blades of the stator and electrically screened from it. The mill was mounted upside down, 1.2 m above the ground at a spot clear from obstructions down to an angle of 20^{o} to the horizontal. The pre-amplifiers, Figure 2.36b, were mounted near the mill while the main amplifiers and detector, Figure 2.36c, were indoors with the recorder.

The electrostatic probe was the only method conveniently available to obtain a phase signal. The three main disadvantages were:

i) that the varying potential of the probe induced a spurious signal on the stator,

ii) that the phase relationship between the probe and the field signal had both an uncertainty in average value and a rapid fluctuation which caused considerable difficulty

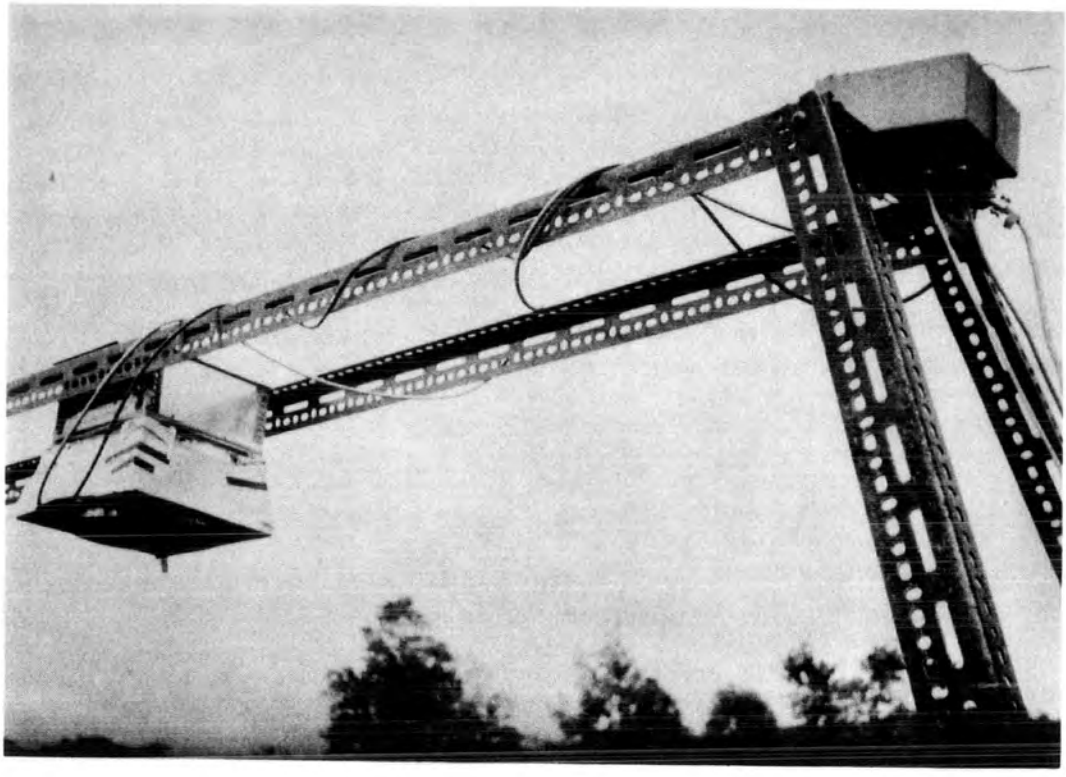

FIGURE 2.36A FIELD MILL TYPE A

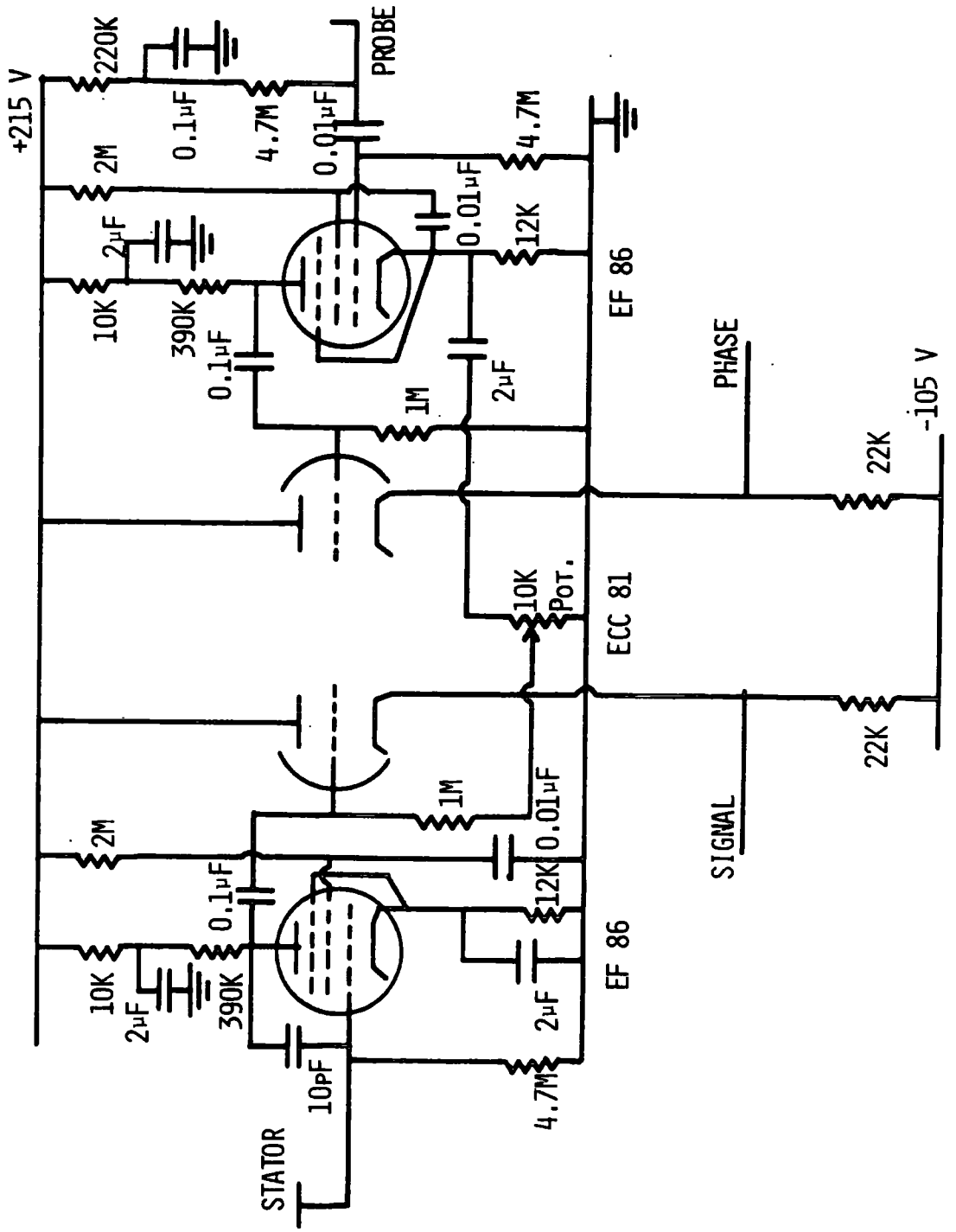

FIGURE 2.36b FIELD MILL TYPE A PREAMPLIFIER

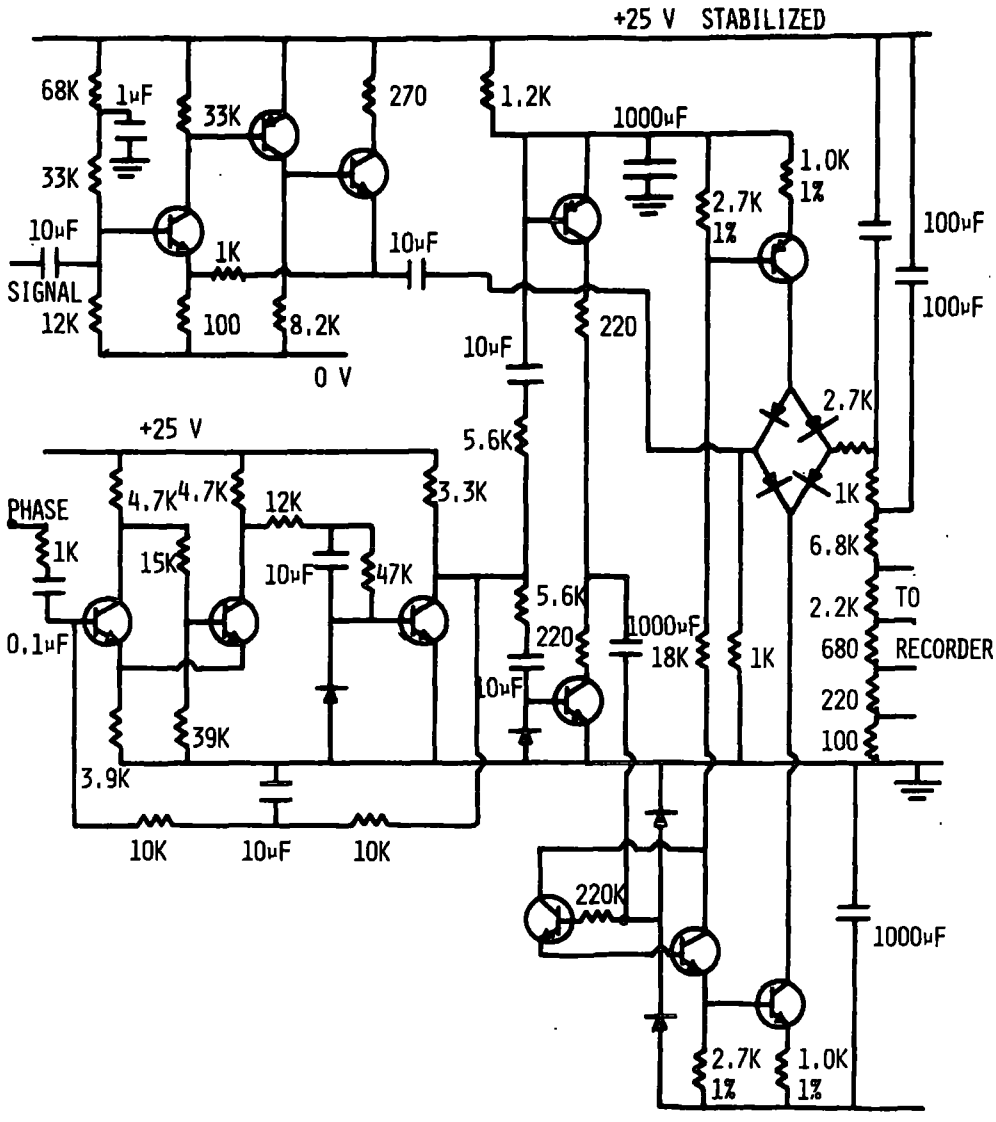

FIGURE 2.36c FIELD MILL TYPE A AMPLIFIERS AND DETECTOR

in the design of the phase-sensitive detector and,

iii) that the phase signal was not square and the mark to space ratio was not necessarily one.

Various forms of feedback were devised and incorporated to adjust the mark to space ratio of the phase signal from the limiter to one (Lane-Smith, 1965) and to make the detector insensitive to variations in the mark to space ratio.

Mounting the mill upside down 1.2 m above the ground enabled the mill to operate in heavy rain but eliminated the effect of space charge within 1.2 m of the ground.

2.37 Field Mill Type B (Lane-Smith, 1967)

This mill was developed to avoid the complications of generating and processing a phase signal and yet still retain sign discrimination with the zero stability and range switching facilities of the phase sensitive system.

The Kortright Mill, Figure 2.37a, was mounted with the axis of rotation horizontal and facing away from the usual storm winds. The Pepel mill, Figure 2.37b,

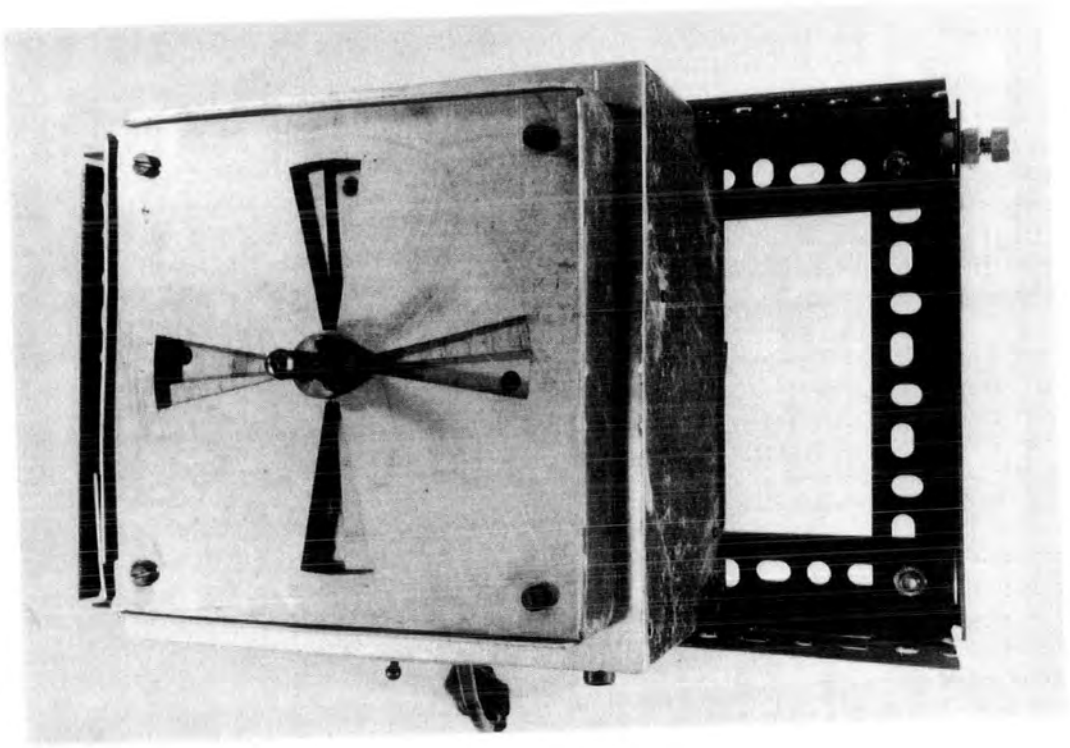

FIGURE 2.37A FIELD MILL TYPE B

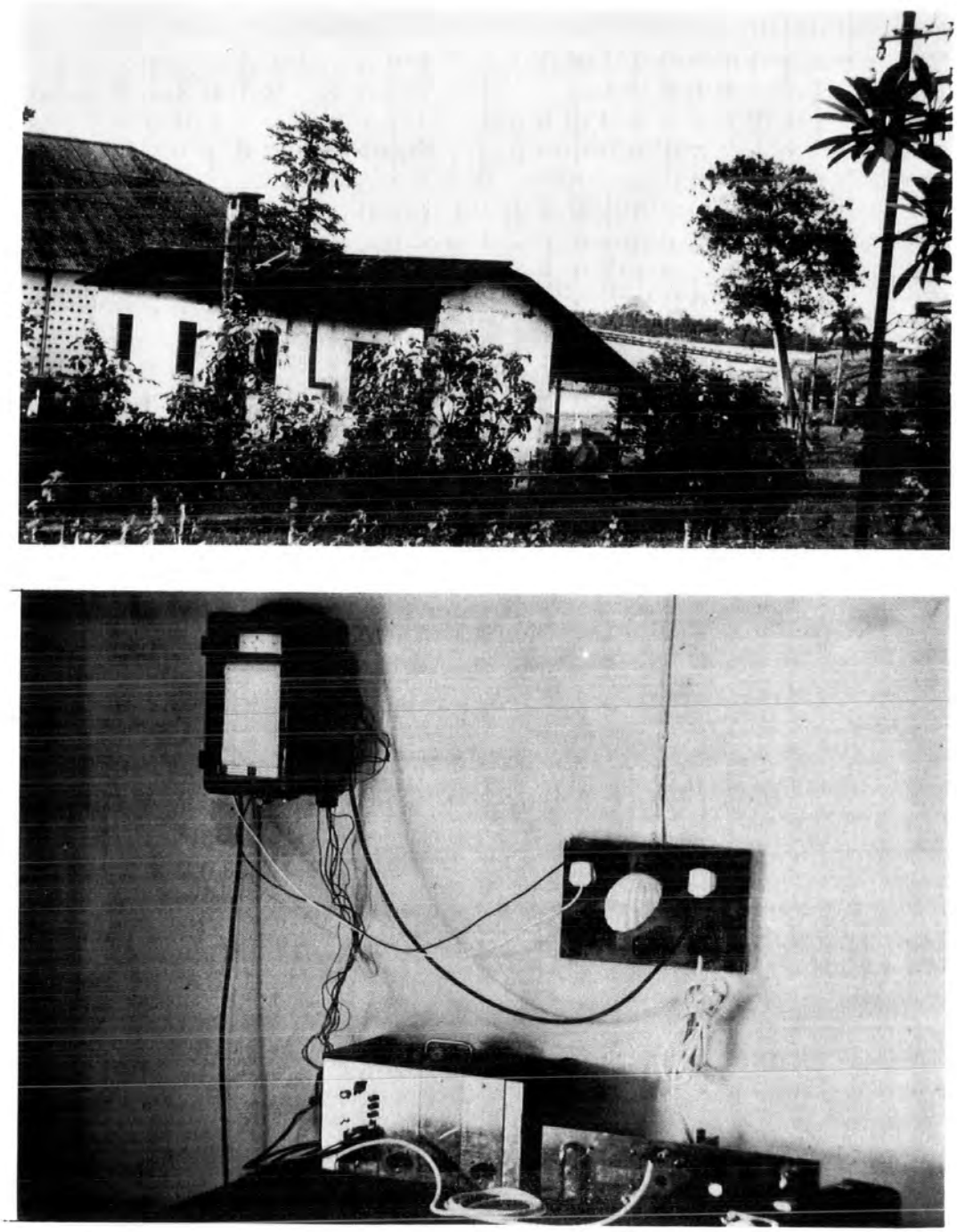

FIGURE 2.37B PEPEL FIELD MILL SITE

was high on the end wall of an outhouse, sheltered by the roof overhang.

The pre-amplifiers were high impedance charge amplifiers. One, for the Kortright mill, is shown, Figure 2.37c. The detectors were similar to that shown in Figure 2.37d.

2.38 Calibration of the Field Mills

A calibration mill of type B was placed 20 feet away from the Kortright Mill on flat ground at the centre of a grounded plate six feet square with the rotor in the plane of the plate. A covering plate was supported 10 cm above the grounded plate and insulated from it. Various measured potential differences were applied to the plates and the output of the mill recorded.

After the initial calibration, the covering plate was removed and the outputs of the calibration mill and the Kortright mill recorded simultaneously.

A satisfactory calibration could be made only when after the initial calibration, the ambient field varied over the range of interest--that is, from zero to several thousand volts per metre--without the onset of precipitation. Nature rarely co-operated in providing these conditions.

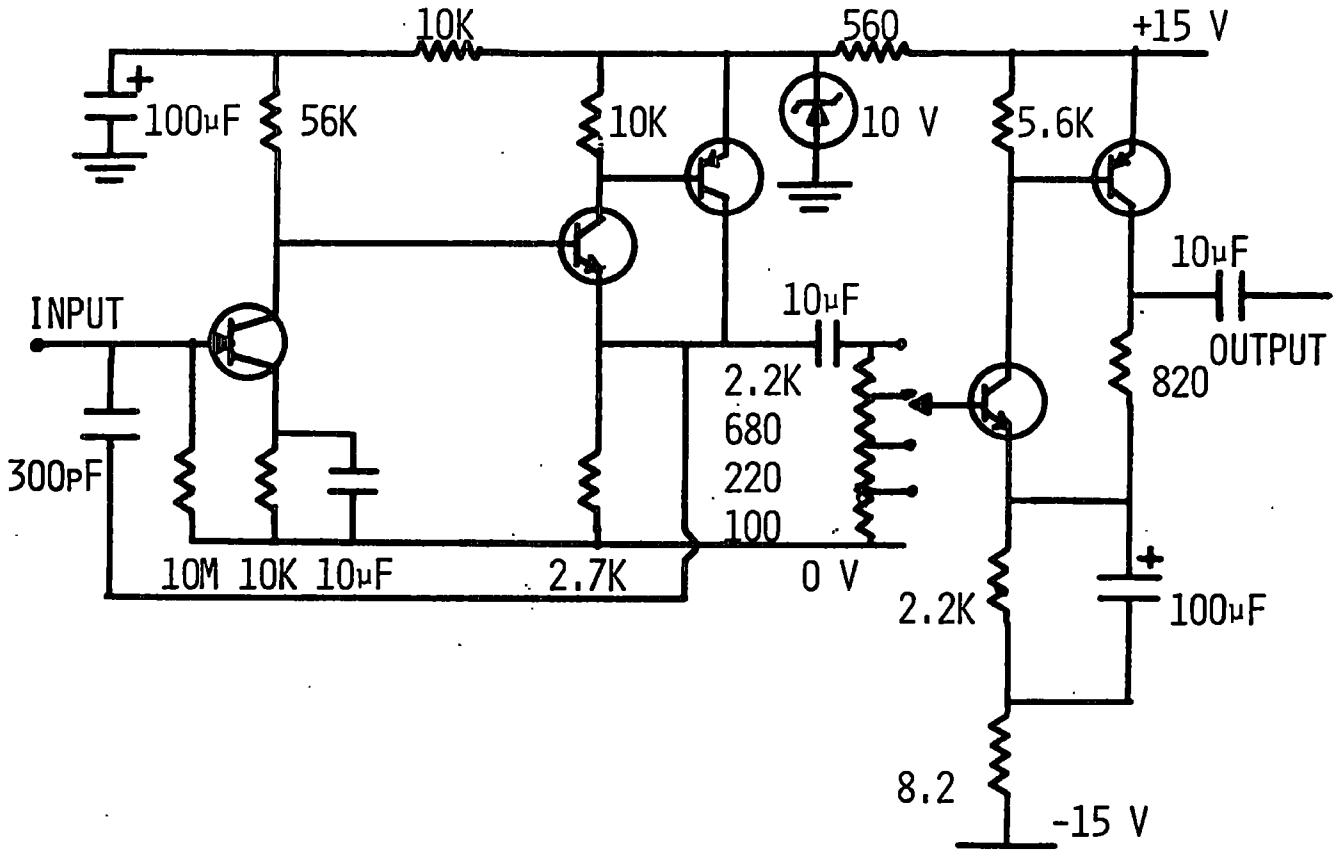

FIGURE 2.37c

PREAMPLIFIER FOR FIELD MILL TYPE B

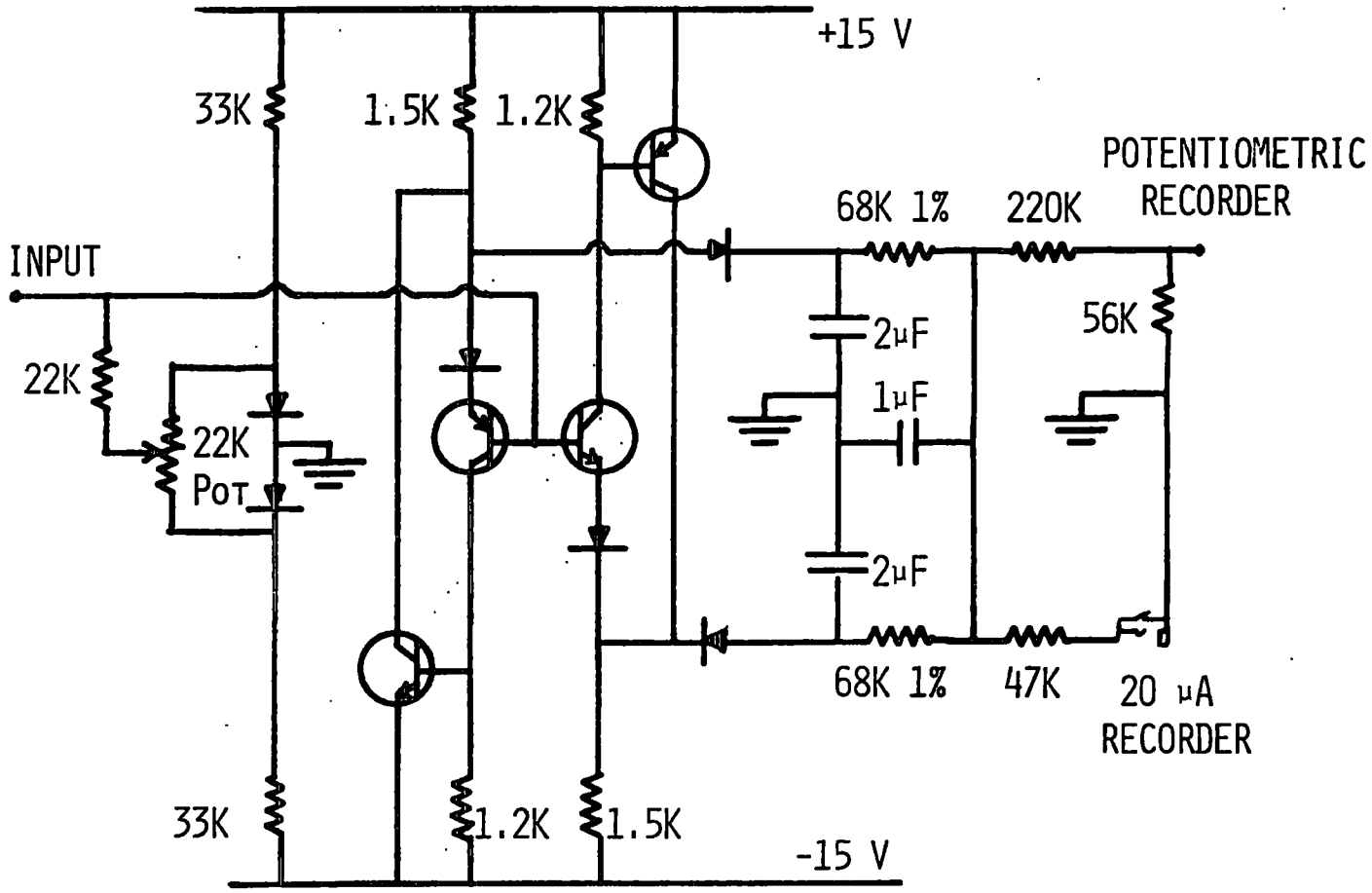

FIGURE 2.37d

DETECTOR FOR FIELD MILL TYPE B

Inaccessibility and the lack of any open space without overhead power lines or telephone cables or trees prevented the calibration of the field mill at Pepel. A very rough estimate of the sensitivity was made, but the value of the results is primarily qualitative, not quantitative.

2.4 Ancillary Electronics

2.40 It was necessary to design and build all power supplies and various other electronic devices of which one, to double the capacity of the two pen Bristol recorder, is described.

2.41 Recorder Pen Switch

The main pen recorder used for data recording was a Bristol 'Dynamaster', potentiometric, two pen recorder. It had fixed ranges, variable speed and was equipped with a pen lifter.

A circuit was designed to lift the pens, switch to two different channels, lower the pens for a short time and repeat the procedure to return to the other channels. The time spent in one pair of channels was much longer than the total time spent switching and recording on the other channels. In this way, two para-

meters could be recorded in effect continuously while two others were sampled at intervals. The main records were of electric field and precipitation current while the sampled parameters were rate of rainfall and wind speed. The circuit is shown in Figure 2.41a.

2.5 Site Topography

Freetown, Sierra Leone, at 8° 28' North and 13° 13' West, is at the NNW end of a peninsula about 10 miles wide and 30 miles long, Figure 2.5a. Fourah Bay College, Figure 2.5b, lies along a spur overlooking Freetown. The field site, Figure 2.5c, was on gently sloping ground at about 1100 feet above sea level. The hut, figure 2.5d, contained all the recording equipment and an electronics workshop where the equipment was built and tested. The rain receiver together with the head unit of the V.R.E. was mounted in a concrete pit about 1.8 m by 1.2 m by 1 m deep in an area level to a radius of 2 m, Figure 2.5e, which was about 18 m from the hut. 6 m further down the slope, the field mill was mounted on a Dexion frame 1.2 m above the ground, Figure 2.5f.

Thunderstorms invariably approached from the N.E., down the Sierra Leone River and were lifted by the hills

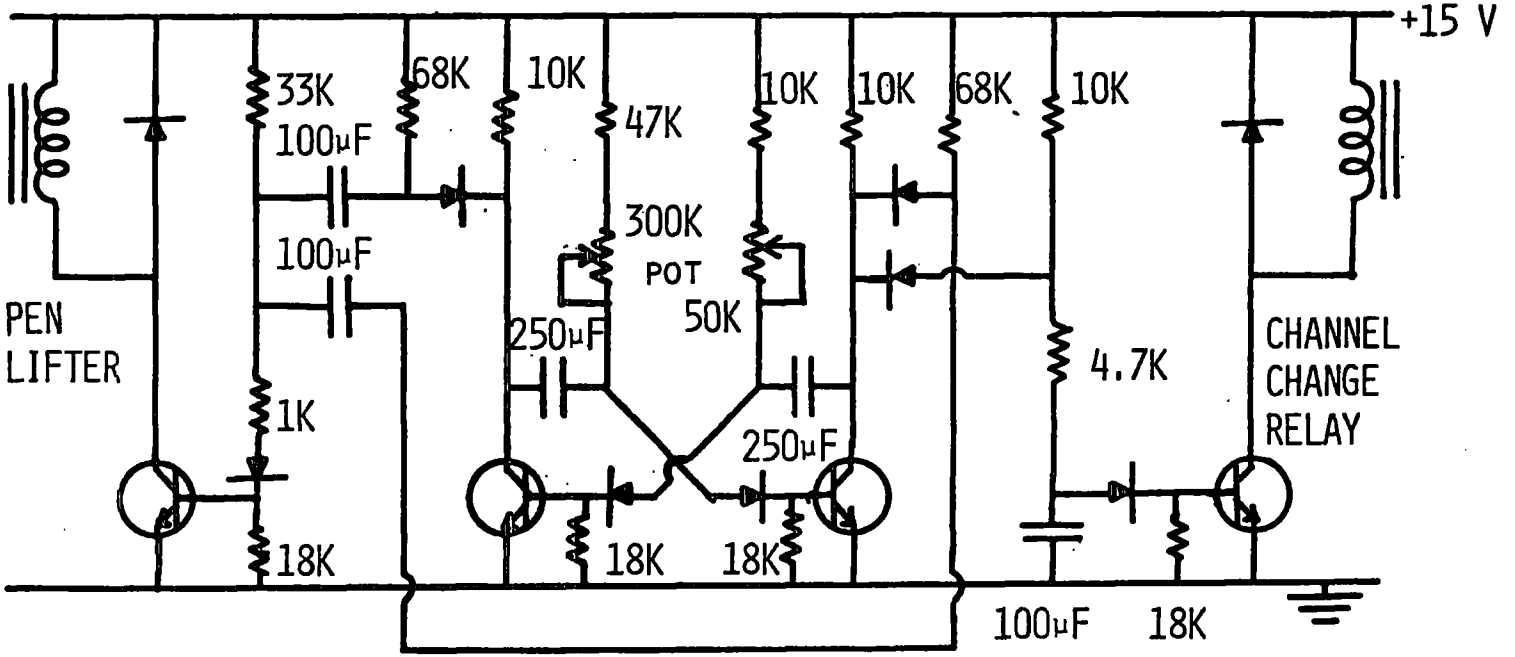

FIGURE 2,41a

PEN RECORDER SWITCHING CIRCUIT

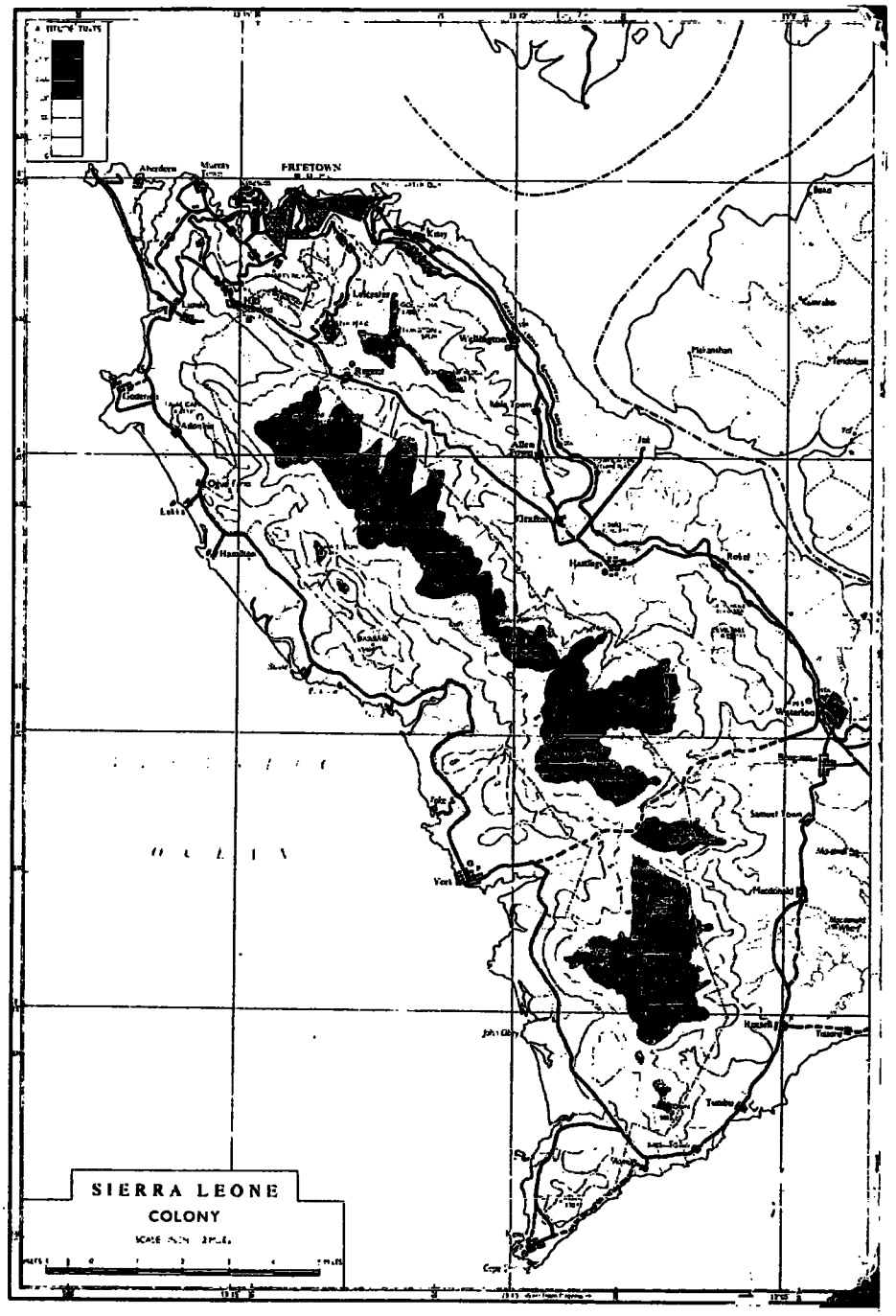

FIGURE 2.5A FREETOWN PENINSULA

SCALE: GRID LINES ARE 6 MILES APART

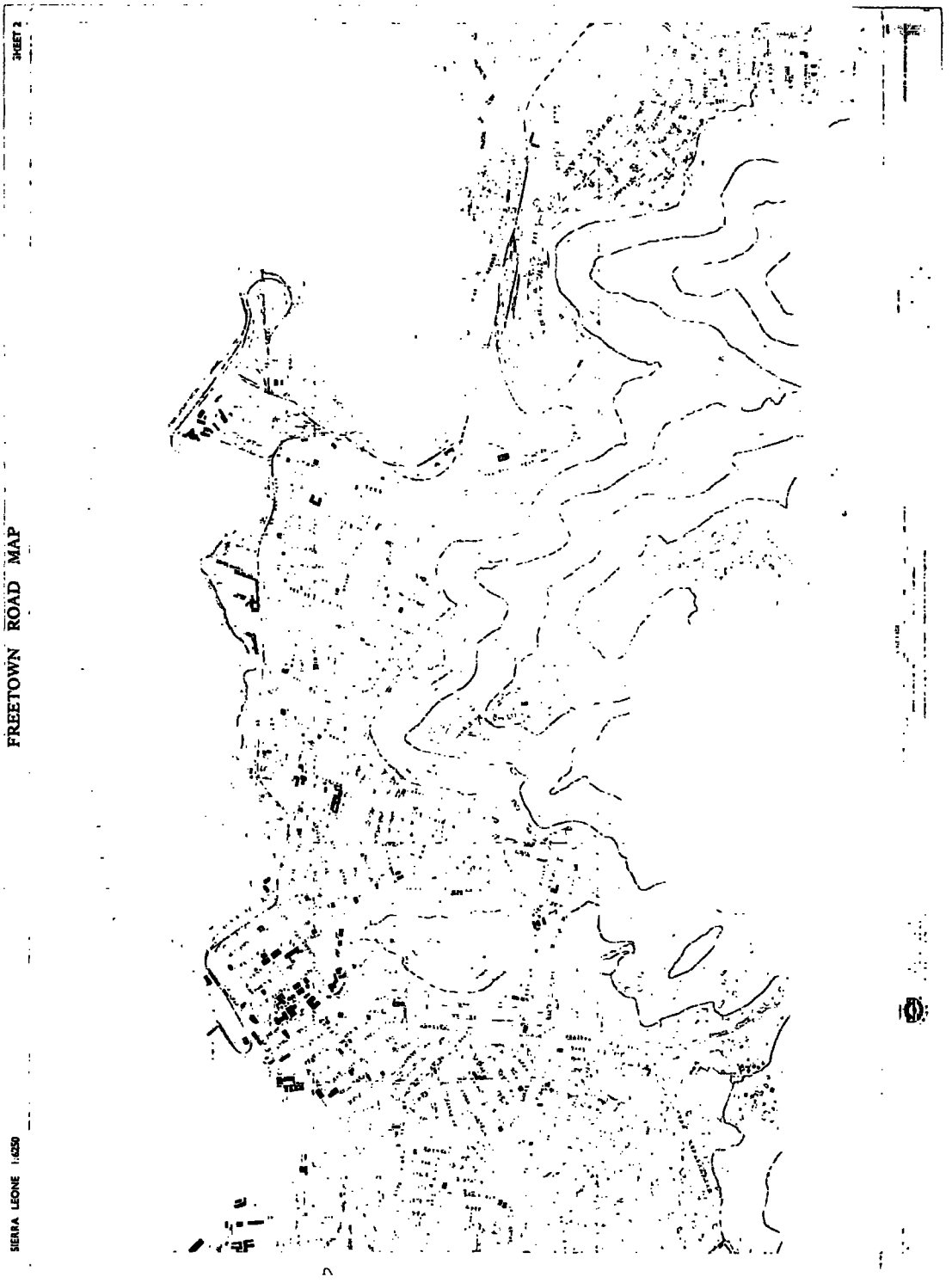

FIGURE 2.5B FOURAH BAY COLLEGE

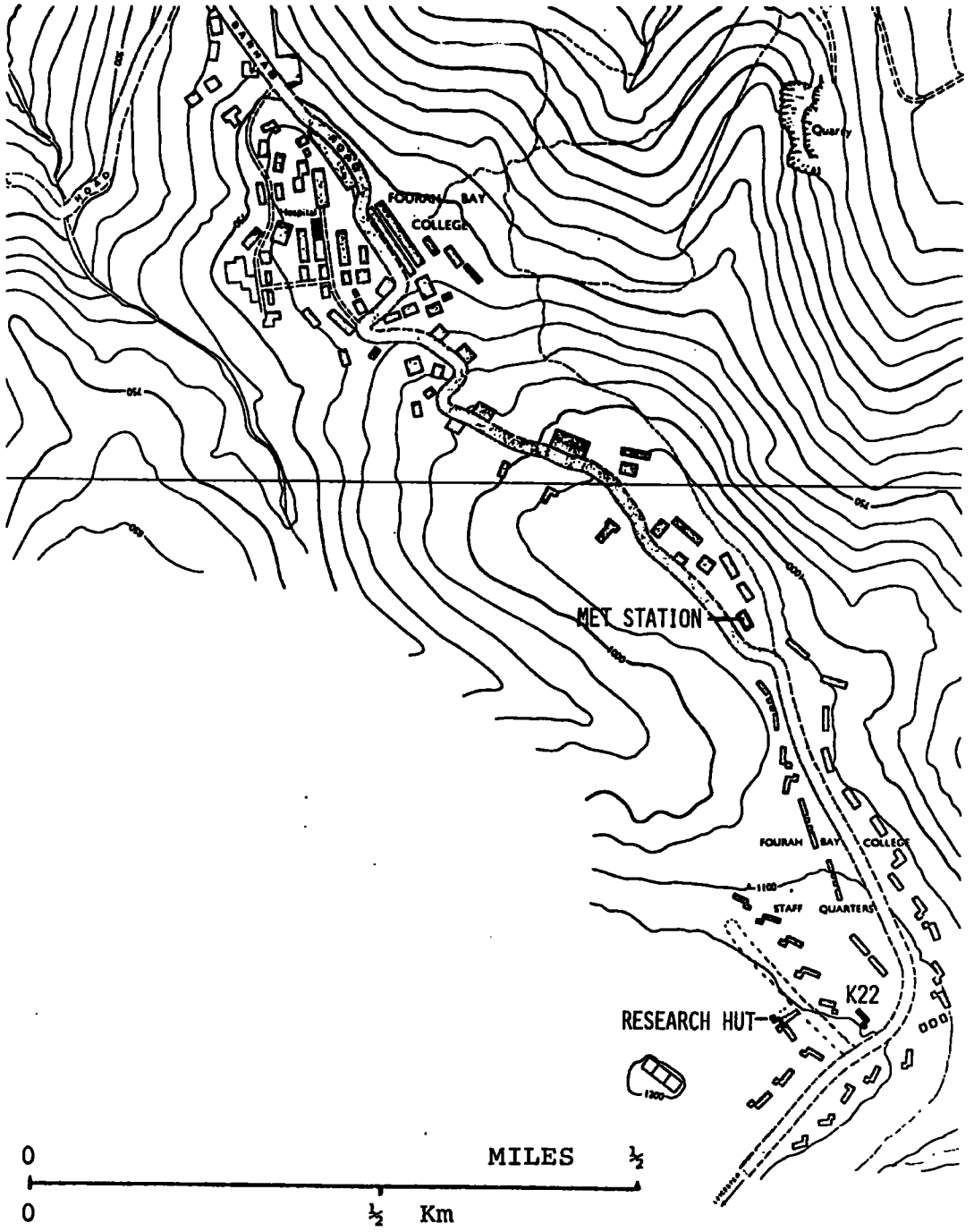

FIGURE 2.5c KORTRIGHT FIELD SITE

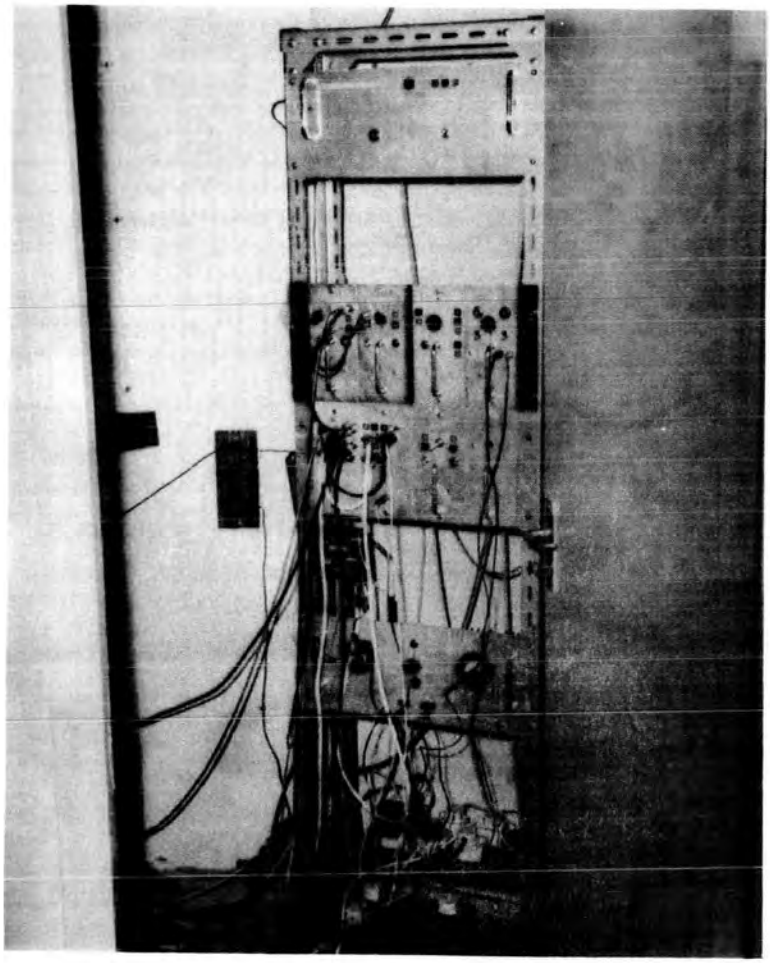

FIGURE 2.5D THE RESEARCH HUT

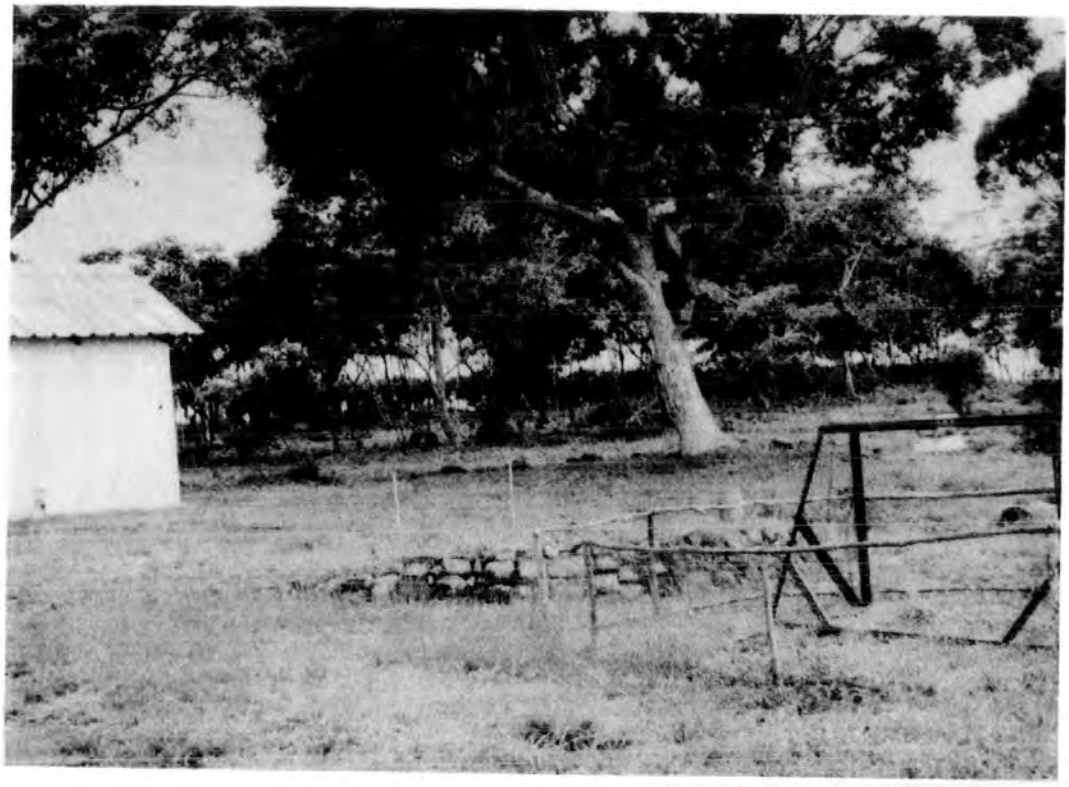

FIGURE 2.5E RAIN RECEIVER SITE

FIGURE 2.5F KORTRIGHT FIELD MILL SITE

of the Freetown peninsula . The prevailing wind during a storm was, therefore, North-Easterly so that the tarmac drive close to the field site, Figure 2.5c, was always upwind of the rain receiver.

CHAPTER III

RESULTS

3.0 It is difficult to interpret the value of the electric field at the ground because of indeterminate shielding charges both at the ground and around the cloud. However, when there is a discontinuous change in the field, due to a lightning discharge, there is almost no instantaneous redistribution of the shielding charges. It is more useful, therefore, to examine first the pattern of changes associated with a lightning flash than to look for a more general relationship of some parameter with the electric field.

3.10 Pattern of Electric Field Changes

During a typical storm the electric field may vary somewhat as in Figure 3.10a. For the storm of November 4, 1965, the average change in electric field at a flash was about 3000 V/m when the storm was about 1.5 km away. The average interval between flashes was

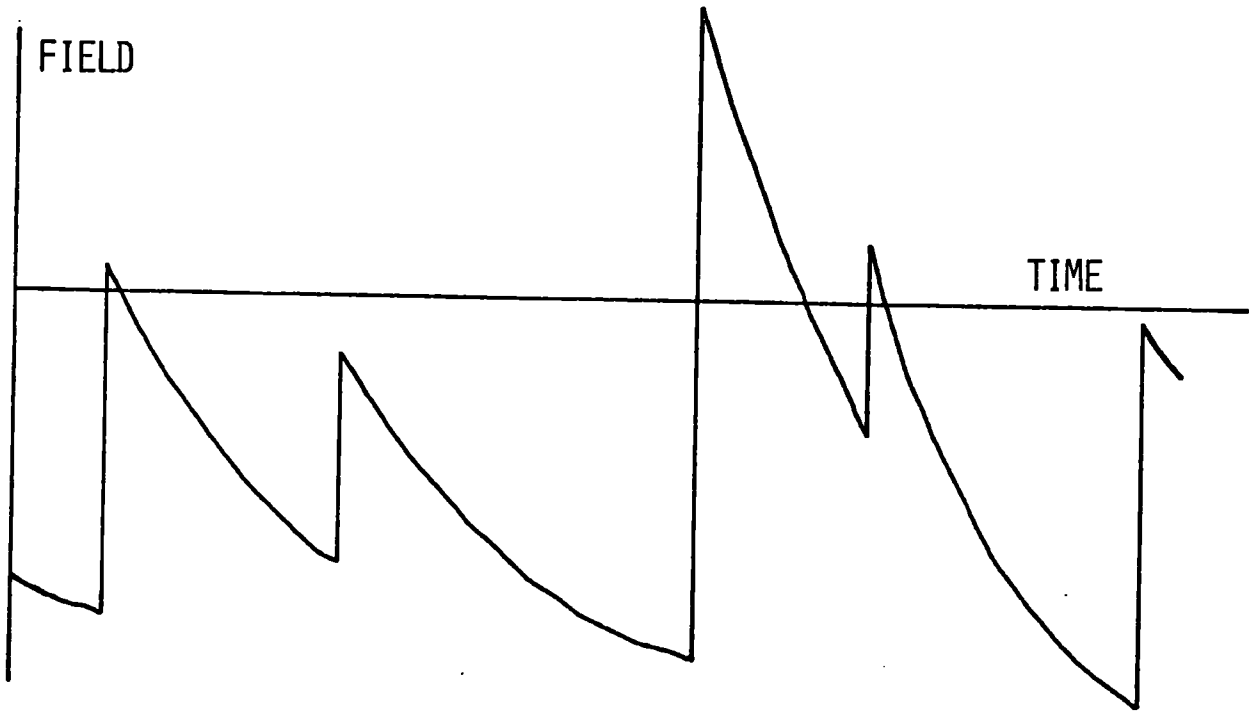

PATTERN OF ELECTRIC FIELD CHANGES

FIGURE 3.10a

30-40 secs.

As the time constant for the recovery of the electric field was about 30 secs, the field never fully recovered. To measure the recovery time constant it is necessary to calculate the relationship between the fully recovered field and the average field just before a flash. Consider the idealized case with identical discharges at equal time intervals superimposed on a steady fully recovered field.

Let the recovery time constant be ζ.

Let the time interval between flashes be τ.

Let the discharge amplitude be A.

Let the fully recovered field be V_o.

Then, after a time τ, the field has some value $V_o + \delta$ given by

$$V_o + \delta = V_o + (A + \delta)\, e^{-\tau/\zeta}$$

During the storm of the 4th November 1965, Figure 3.30b, τ and ζ were both about 30 secs. Thus $e^{-\tau/\zeta}$ is about 1/3 which makes δ about ½A.

If the field following several lightning flashes is averaged, the mean follows an exponential decay faithfully for the first 20 secs, Figure 3.30b, but after that the effect of subsequent flashes disturbs

the mean away from the exponential curve. If the first part of the curve is extrapolated towards the estimated 'fully recovered' electric field, the time constant, ζ_1, is 31 ± 3 secs.

3.20 Pattern of Precipitation Current Changes

The precipitation current during a storm varied rapidly and over a wide range. There was some evidence of a 'mirror image' effect (Simpson, 1949), in that the current tended to be of opposite sign to the field, but the only other regular feature apparent was the response to a sudden change in electric field due to a lightning discharge, Figure 3.20a.

3.30 Response of Precipitation Current to Electric Field Changes

The record of precipitation current after a lightning flash averaged over many events, looks like Figure 3.30a.

The first step is displacement current due to incomplete shielding of the rain collector. This can be evaluated by measuring the response of the precipitation current record to a lightning flash when no rain is falling. When the displacement current is subtracted the current appears as in Figure 3.30b.

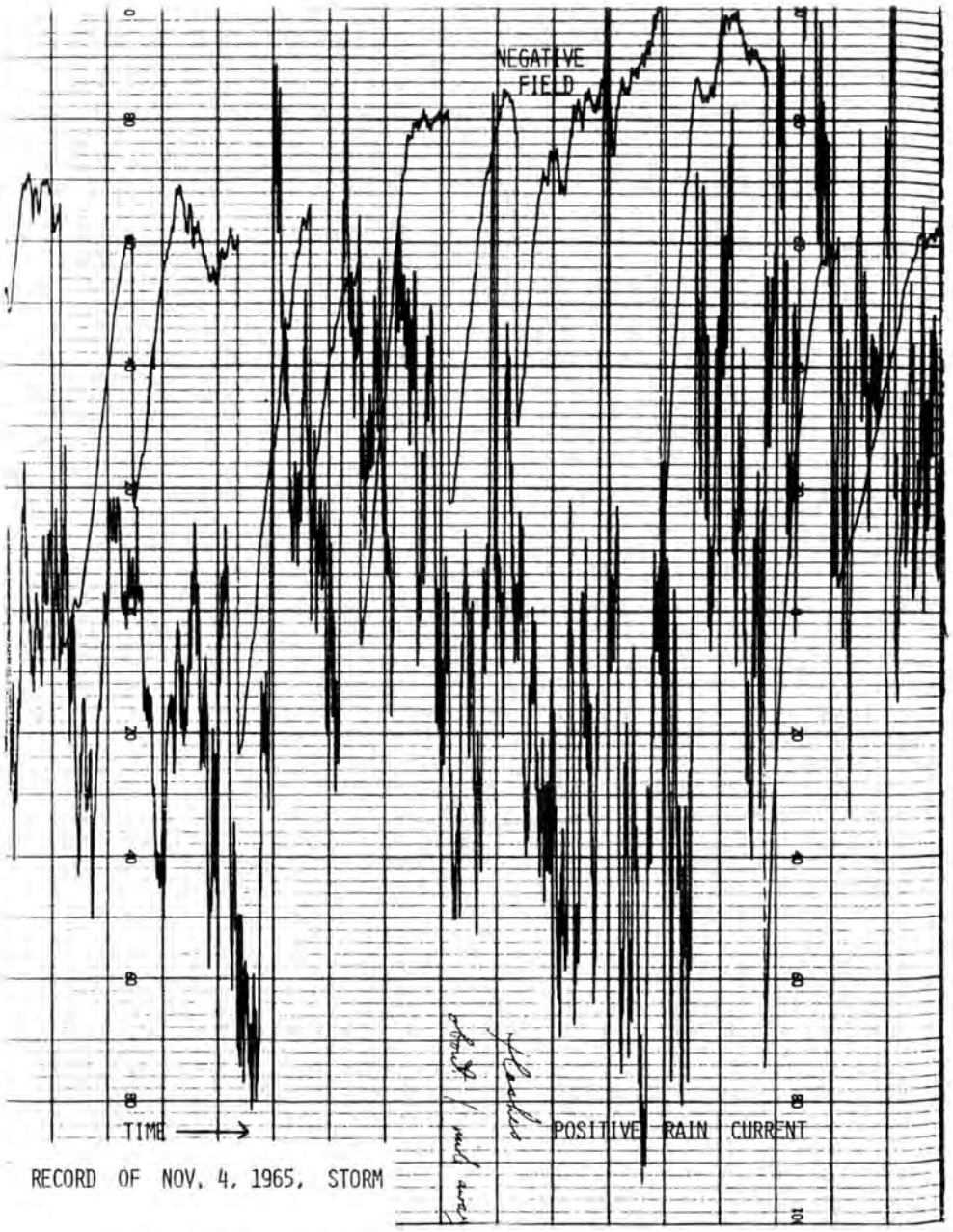

RECORD OF NOV. 4, 1965, STORM

TIME 2 DIVISIONS PER MINUTE

FIELD 5000 Vm^{-1} FULL SCALE DEFLECTION

CURRENT 5×10^{-11} AMP FULL SCALE DEFLECTION

FIGURE 3.20A

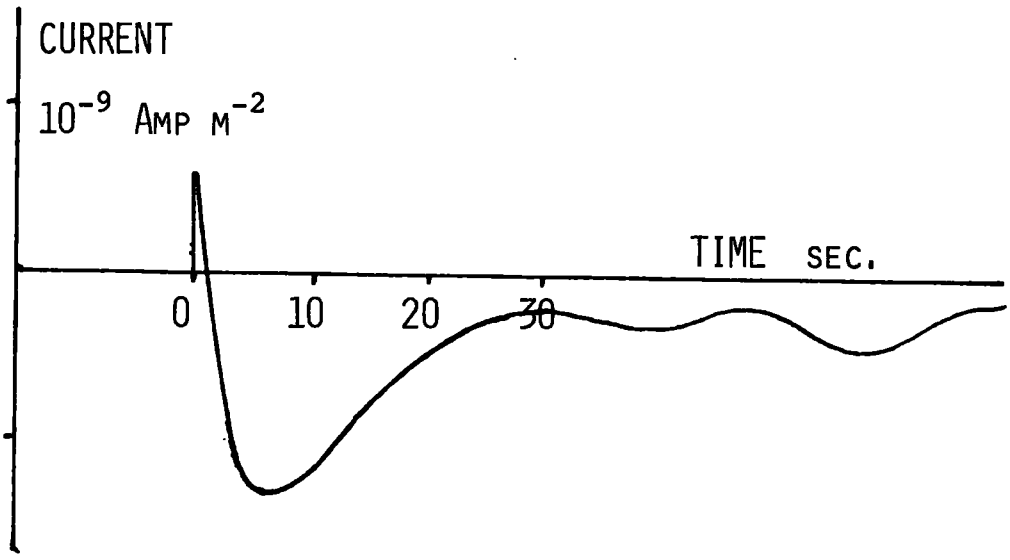

PRECIPITATION CURRENT CHANGES AFTER LIGHTNING

FIGURE 3.30A

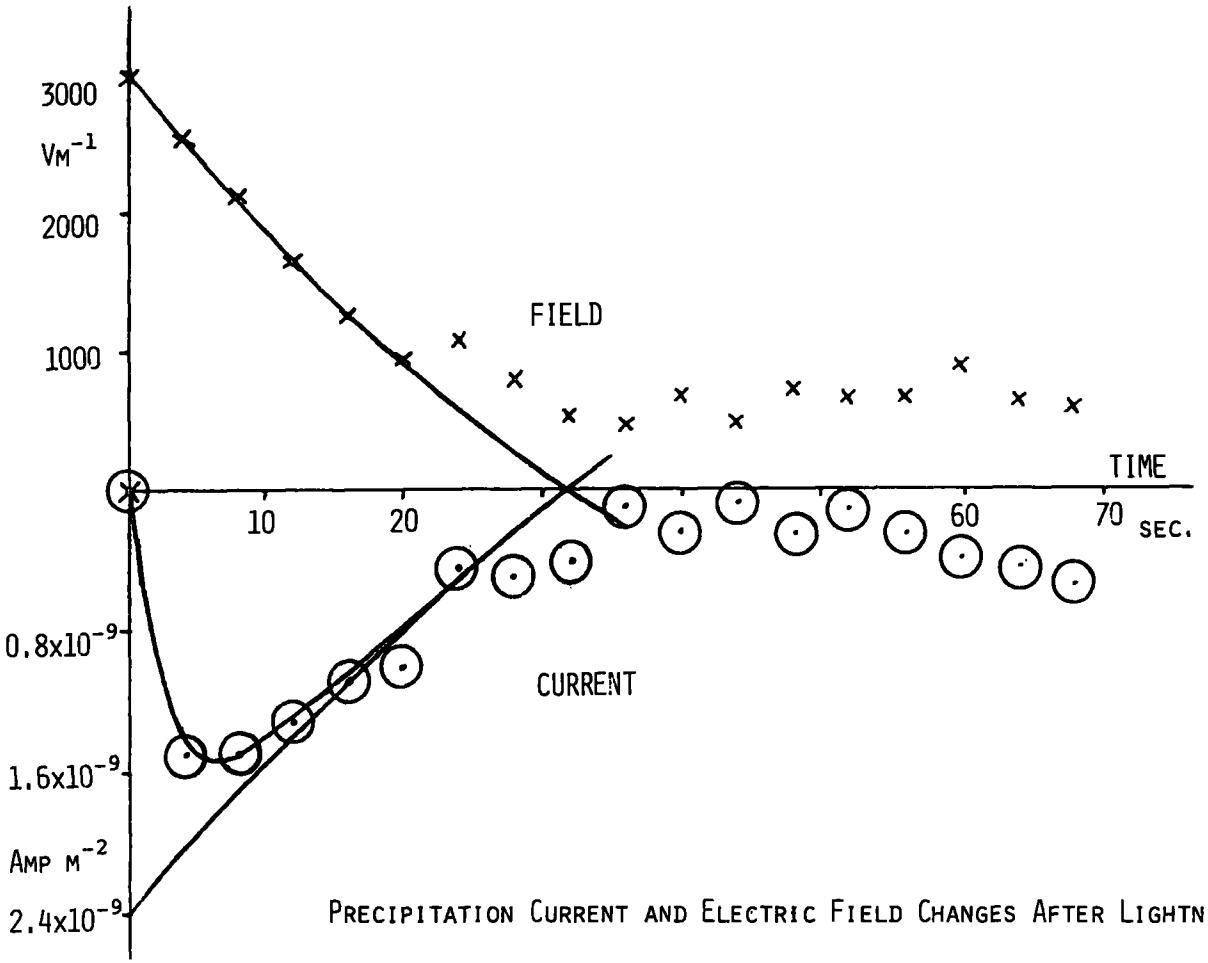

FIGURE 3.30B

PRECIPITATION CURRENT AND ELECTRIC FIELD CHANGES AFTER LIGHTNING

ANALYSIS OF THIRTEEN STROKES AT A RANGE OF APPROXIMATELY ONE MILE, FROM THE RECORD OF THE STORM ON NOVEMBER 4, 1965.

Three effects are evident. First, from 10-25 secs, the current is decaying with an exponential time constant ζ_1 equal to the recovery time constant of the electric field. Subsequent step changes displace the average current from the exponential curve in a similar manner to the effect on the electric field. During the first 10-15 seconds, however, the precipitation current which must remain constant during the fraction of a second of the lightning flash, approaches the exponential decay curve with another, shorter time constant, ζ_2.

From the graph for the storm on November 4, 1965, it is possible to deduce that $\zeta_2 = 3 \pm 0.3$ secs, and that the longer decay curve if extrapolated back to a time $\tau = 0$, at the lightning flash would read a precipitation current change of $2.6 \pm 0.2 \times 10^{-9}$ Amp metre^{-2} for an electric field change of 3000 V/M, during heavy rain of the order 1.4×10^{-5} m sec^{-1} or 2 inches per hour. The electric field just before a flash averaged about -2000 Vm^{-1} and the rate of recovery of electric field after a flash when the field was crossing zero was -125 Vm^{-1} sec^{-1}.

A computer was used to analyze three storms and to plot the averaged responses of field and current to

a lightning flash.

The results are tabulated in Figure 3.30c.

Analysis of Three Storms

Date	Oct.24,1965	Nov.4,1965	Jun.7,1966
Time of Start G.M.T.	16.05	15.07	14.15
Rainfall	about 1.4 x 10^{-5} m sec^{-1}	about 1.4 x 10^{-5} m sec^{-1}	2.0 ± 0.1 x 10^{-5} m sec^{-1}
Average step change in E due to lightning	4,960 V m^{-1}	3,000 Vm^{-1}	1,780 Vm^{-1}
Corresponding change in i_o, rain current	$4.9.10^{-9}$ Amp m^{-2}	$2.6.10^{-9}$ Amp m^{-2}	$7.05.10^{-9}$ Amp m^{-2}
Time constant ζ_2 for change in rain current	3.36 secs	3.2 secs	2.5 secs
Rate of Change of E after flash at E = 0	-179 Vm^{-1} sec^{-1}	-125 Vm^{-1} sec^{-1}	-228 Vm^{-1} sec^{-1}
Average field E before flash	-3,150 Vm^{-1}	-2000 Vm^{-1}	-780 Vm^{-1}

Figure 3.30c

3.4 Meteorological Records

Measurements taken at the Kortright meteorological station, Figure 2.5b, about half a mile from the field site, are available for the period of the storms, figures 3.4a, b and c. The records are transcribed to show on one sheet, over the duration of the storm, rainfall, wind speed and direction, pressure and, for October 24 and November 4, the relative humidity and temperature. At 15.00 on June 7, 1966, the dry bulb temperature was 70.1°F, the wet bulb 70°F, the relative humidity 99% and the vapour pressure 24.9 millibars.

All records show a lull in wind before the storm, a sudden increase in wind speed just as the rain started, or perhaps a minute or two before and continuous high winds for half an hour afterwards. Notice, too, that the wind backs from S.W. to S.E., from which direction the storms will have come. The October 24th record shows the characteristic temperature drop just before the storm but not the pressure signature which, however, is clearly shown on the June 7 record.

The rate of rainfall at the Kortright meteorological station was approximately one inch per hour or 0.7×10^{-5} m sec^{-1} on October 24, the same on November

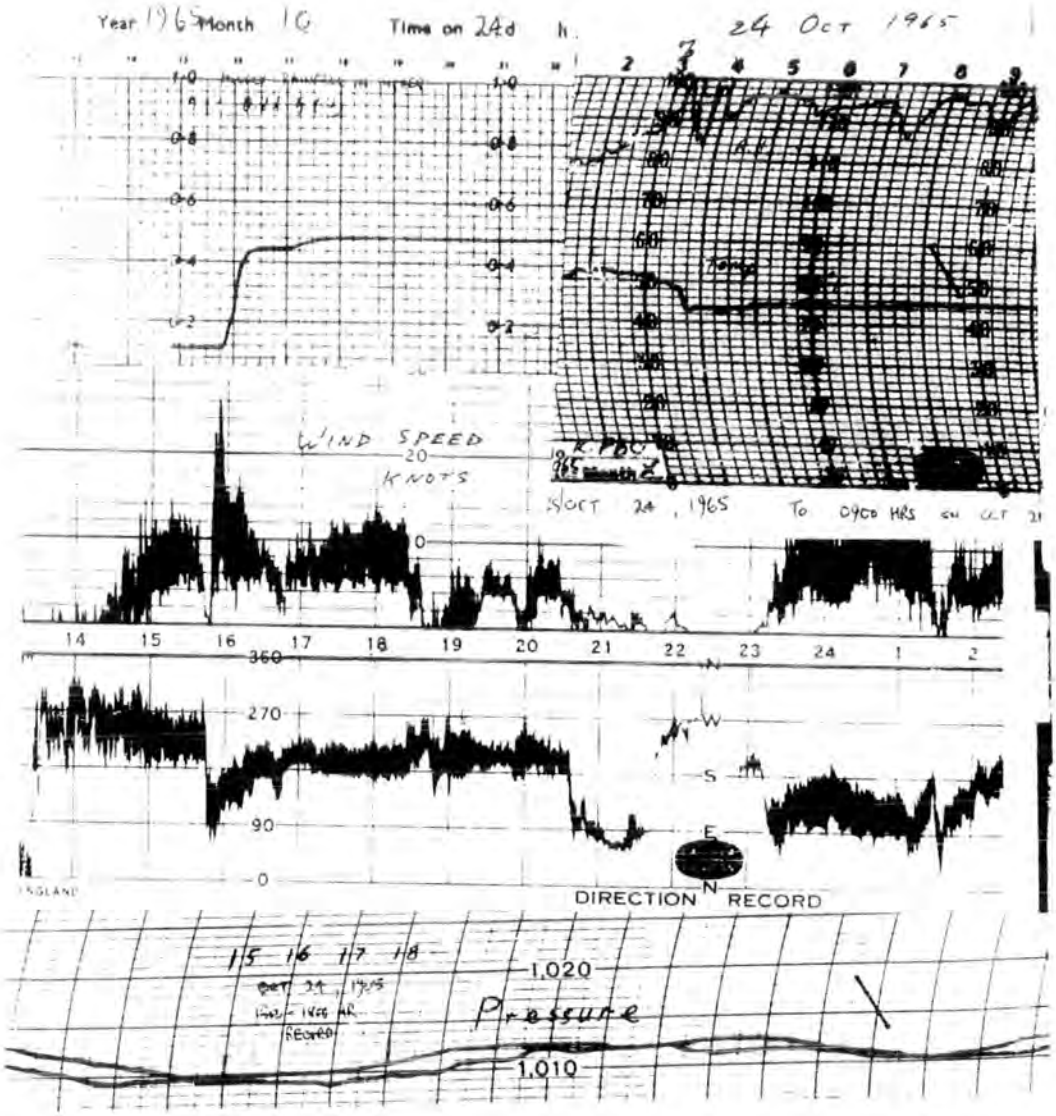

FIGURE 3.4A MET RECORDS FOR 24 OCTOBER 1965

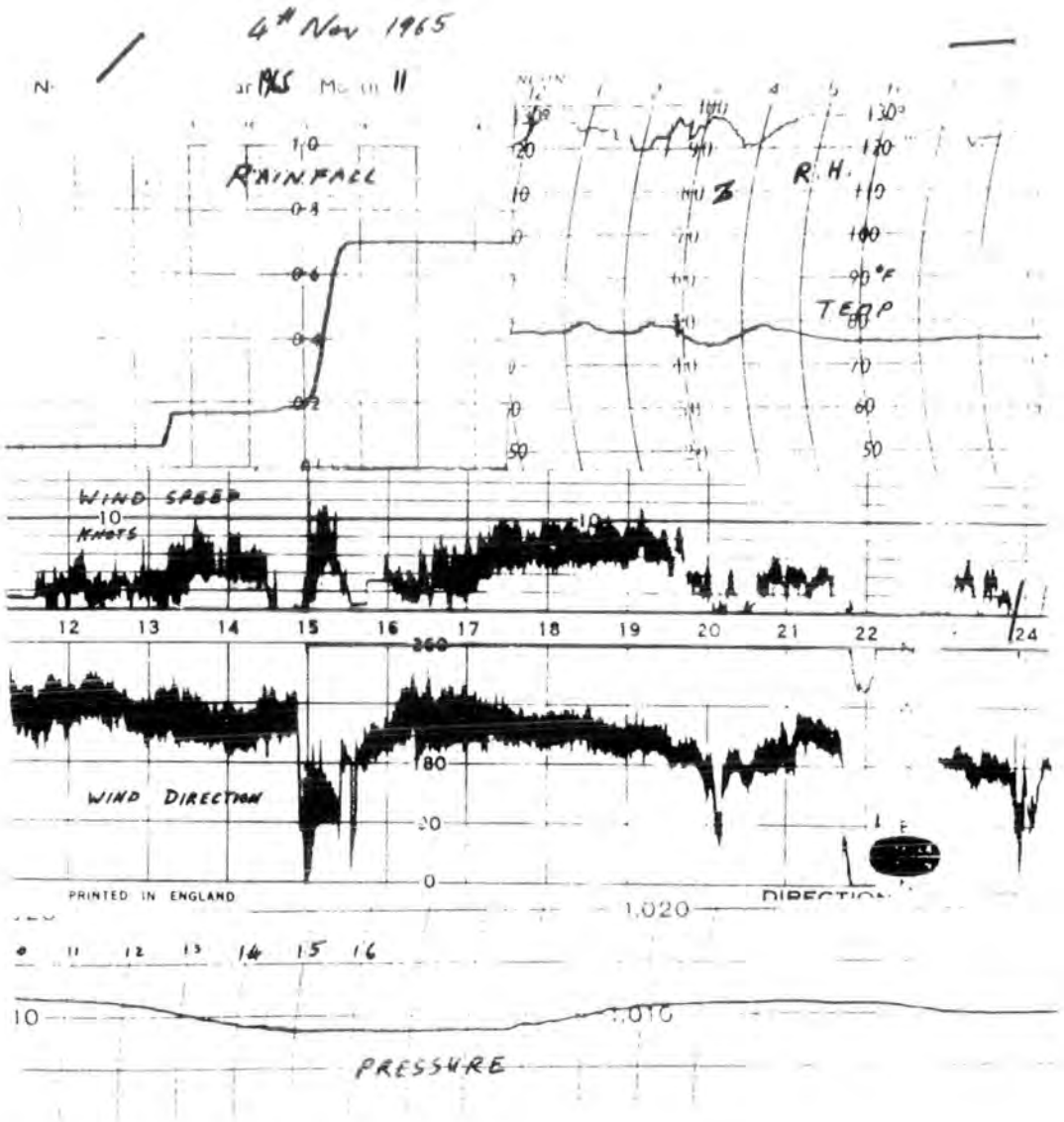

FIGURE 3.4B MET RECORDS FOR 4 NOVEMBER 1965

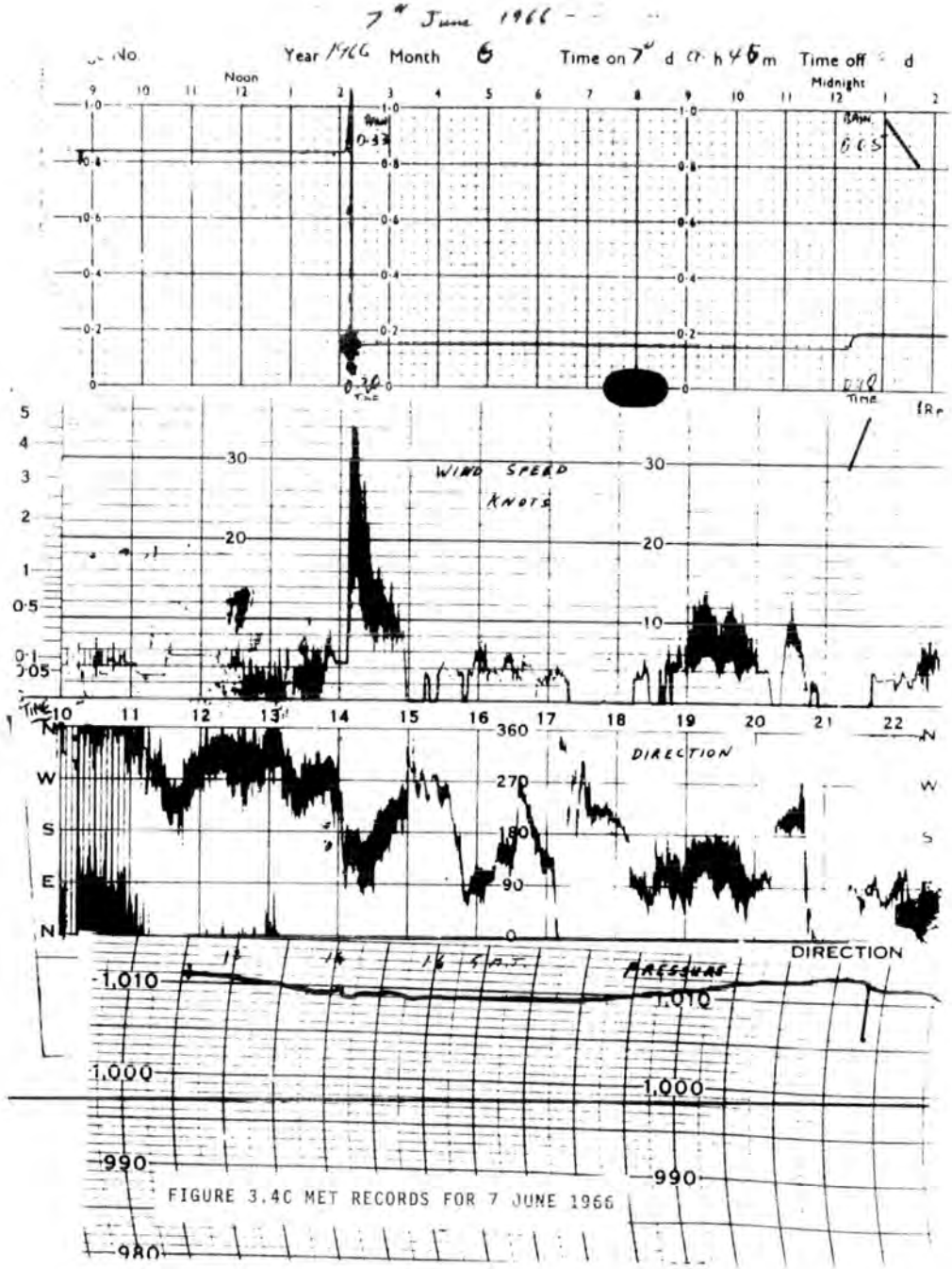

FIGURE 3.4C MET RECORDS FOR 7 JUNE 1966

11 and 1.6 inches per hour or 1.1×10^{-5} m sec^{-1} on June 7. These values, which are lower than the field site measurements do not necessarily mean that the latter are in error. The field site, further up the hill than the meteorological station, is likely to have a higher and heavier rainfall.

CHAPTER IV

ANALYSIS OF RESULTS

4.10 General Considerations and Nomenclature

4.11 The first and obvious interpretation of the changes in the precipitation current is that they are due simply to splashing; that is, charged droplets produced by splashing at the rim of the receiver and nearby, fall straight into the receiver. However, the time of a splash trajectory would always be much less than 1 second and the effective time constant would be just a few tenths of a second. The observed time constants were an order of magnitude greater than this and so cannot be interpreted in this way. Furthermore, a more intensive rainfall would give a longer time constant because of the expected higher splash trajectories but the opposite was observed.

During a heavy rainfall, drops will fall with a velocity of around 8 m sec^{-1} so that during the last few

seconds of their fall they are entirely below the cloud. The change in precipitation current after a lightning flash must, therefore, be caused by the capture of charge by the rain drops within the last few metres above ground.

4.12 Various models and mechanisms to explain the charge capture are examined. As far as possible, a common nomenclature is adopted as follows. The suffix 'o' denotes 'at the earth's surface.' The suffix '1' denotes 'at that height at which $Q = 4\pi\varepsilon_o\ 3a^2F$.'

Symbol			Units
a	=	radius of an average rain drop	m
b	=	a diffusion coefficient defined by equation 4.31(ii)	m^2sec^{-1}
e	=	the charge on a small ion	coulomb
h	=	rate of capture of droplets by one drop	sec^{-1}
i	=	NUQ = rain current density into the ground	amp m^{-2}
m	=	mass of an average droplet	Kgm
n	=	number density of positive small ions	m^{-3}
q	=	average charge per droplet	coulomb
r	=	radius of the average droplet	m

t	=	time	sec
z	=	height above ground	m
E	=	potential gradient,	Vm^{-1}
H	=	rate at which rain drops sweep up droplets	$m^{-2}sec^{-1}$
I	=	vertical current density due to charges residing on droplets	amp m^{-2}
J	=	vertical current density due to movement of ions	amp m^{-2}
L	=	thickness of droplet blanket	m
M	=	mass of an average rain drop	Kgm
N	=	number density of rain drops	m^{-3}
P	=	$3\pi a^2N$	m^{-1}
Q	=	charge on a rain drop	coulomb
R	=	rate of rainfall	m sec^{-1}
S	=	number density of droplets	m^{-3}
T	=	surface tension of water	Joule m^{-2}
U	=	velocity of a rain drop	m sec^{-1}
F	=	$-E$	V m^{-1}
β	=	rate of flow of droplets upwards	$m^{-2}sec^{-1}$
γ	=	$(\pi a^2NU\nu/rb)^{\frac{1}{2}}$	m^{-1}
ε_o	=	permittivity of air	F m^{-1}
ζ	=	number of droplets produced by one drop	
η	=	viscosity of air	Kgm $m^{-1}sec^{-1}$

λ	=	rate of injection of droplets	$m^{-3}sec^{-1}$
ν	=	efficiency of droplet capture by drops defined by equation 4.31(i)	
ρ	=	density of water	Kgm m^{-3}
σ	=	space charge on suspended droplets per unit area of ground	coulomb m^{-2}
τ	=	time constant for rain current response to lightning	sec
ϕ	=	q/E	F m
χ	=	change in i_o reading by displacement current in receiver	amp m^{-2}
ψ	=	time constant for recovery of displacement current	sec
ω	=	mobility of ions	$m^2V^{-1}sec^{-1}$

4.20 The Whipple-Chalmers Model

4.21 A model for the interpretation of these results may be considered which is similar to that set up by Chalmers (1951). The space charge is assumed to reside entirely on small ions which migrate upwards because of the vertical potential gradient. Rain drops capture the ions according to the theory of Whipple and Chalmers (1944). However, it is not necessary to assume that the negative charge causing the field resides entirely on rain drops in the base of the cloud and that these drops subsequently sweep out the entire positive

space charge above a certain height. An alternative mechanism which could operate is that the cloud's negative charge may reside on cloud droplets. Positive charge if it arrives may also be captured by droplets. The positive and negative charges may neutralize one another or may be separated by advection and convection. With this relaxation in the constraints of the model calculations above the cloud base become meaningless.

From Whipple and Chalmers (1944) the rate of charging a rain drop is given by

$$\frac{dQ}{dt} = \frac{\pi n e \omega (3a^2F - \frac{Q}{4\pi\varepsilon_o})^2}{3a^2F}$$

$$\text{giving} \quad \frac{dQ}{dz} = \frac{-\pi n e \omega (3a^2F - Q/4\pi\varepsilon_o)^2}{3Ua^2F}$$

The maximum charge a drop can acquire is given by

$$Q_1 = 4\pi\varepsilon_o 3a^2F_1$$

which increases continually with height. If the average drop ever reaches this value, then its charge will be greater than $4\pi\varepsilon_o 3a^2F_o$.

At the ground $Q_o = i_o/NU = 4\pi a^3 i_o/3R$.

For the rain to be saturated, that is for z_1 to be positive, Q_o must be greater than $4\pi\varepsilon_o 3a^2F_o$ or i_o

greater than $9R\varepsilon_o F_o/a$.

4.22 Typical values for the storm of November 4, 1965, gave

$$i_o = 2 \times 10^{-9} \text{ amp m}^{-2}$$

$$F_o = 3 \times 10^{3} \text{ Vm}^{-1}$$

and $$R = 1.5 \times 10^{-5} \text{m sec}^{-1} \text{ (2 inches per hour)}$$

The measurements of rain drop sizes vary considerably with the type of rain and the method of measurement, see for example Fletcher (1962).

A recent measurement in tropical thunderstorm rain (Kelkar, 1968a) shows a distribution of median volume radius a, with rainfall, R, as in Figure 4.22a. The dotted lines indicate the spread in experimental results.

In another paper (Kelkar, 1968b) he draws a graph of the total number of raindrops reaching the ground m^{-2} sec^{-1} against rainfall from which can be calculated a mean volume and a mean volume radius as shown in Figure 4.22b together with some results from Humphreys (1929).

Because of the experimental uncertainty and because the final argument can be demonstrated by orders of magnitude, it is valid to simplify the raindrop spec-

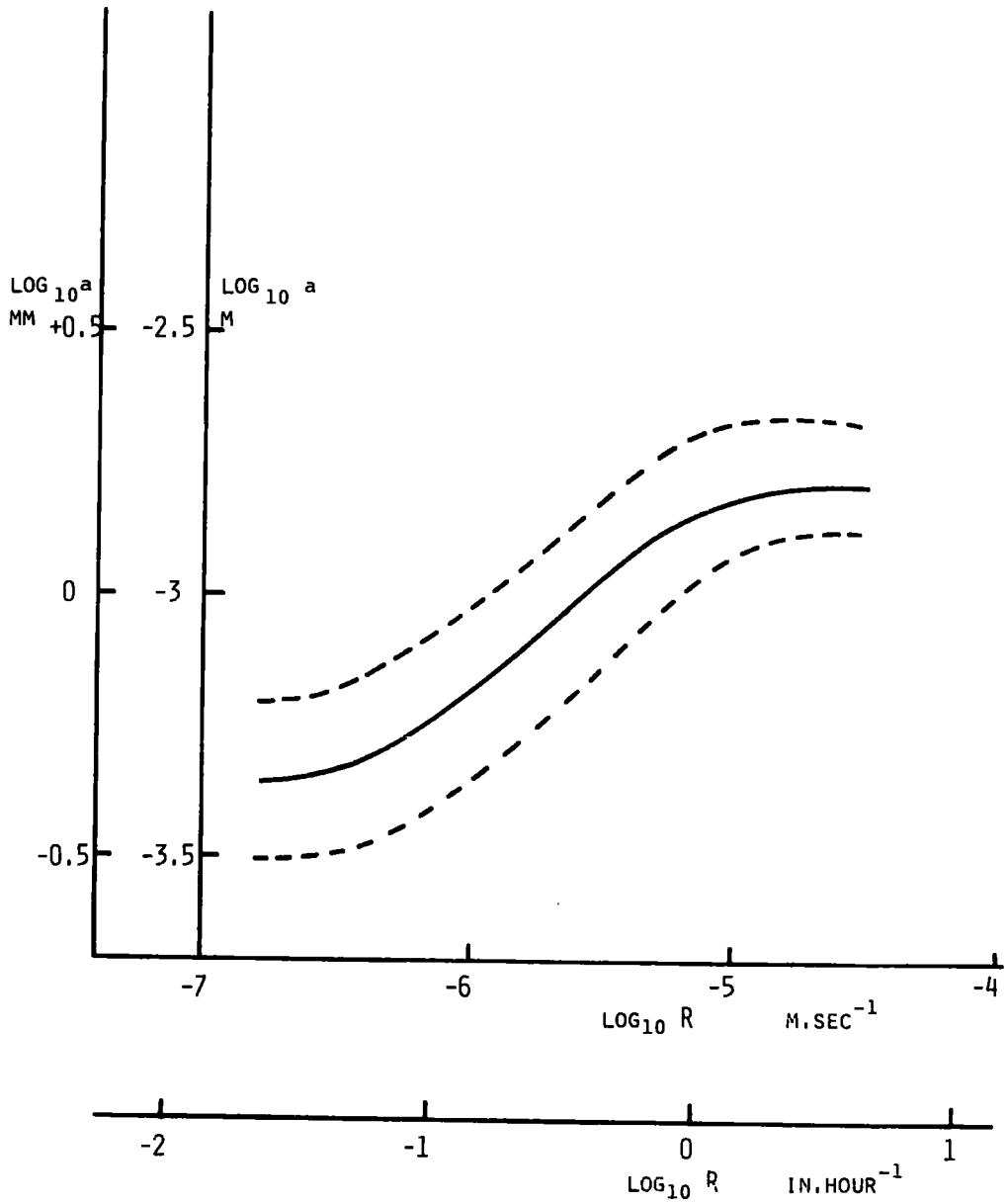

FIGURE 4.22a GRAPH OF MEDIAN VOLUME RADIUS AGAINST RAINFALL

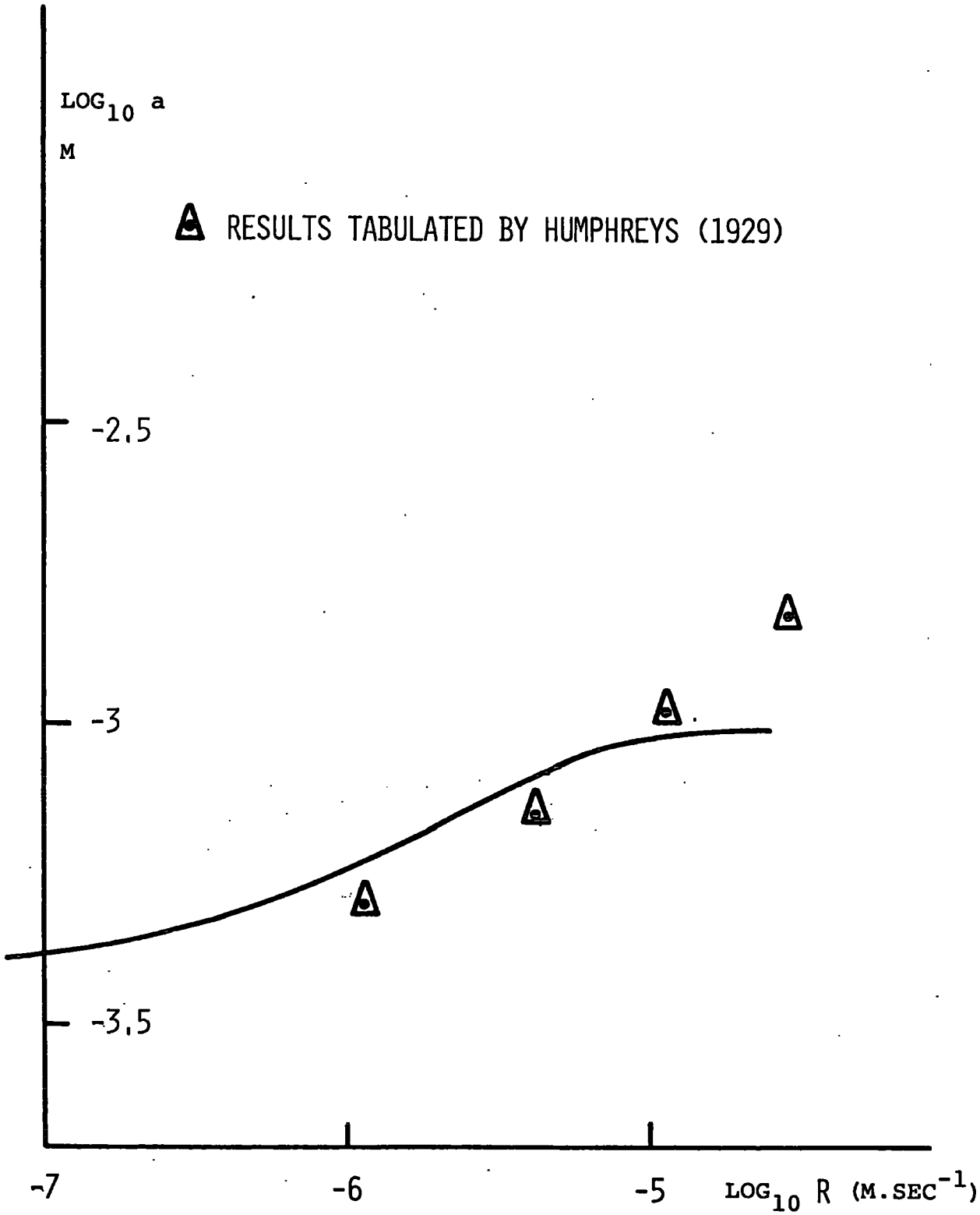

GRAPH OF MEAN VOLUME RADIUS AGAINST RAINFALL, FROM KELKAR (1968b)

FIGURE 4.22b

trum by considering it to consist of drops all one size. Dividing the rainfall by the number of drops reaching the ground per unit area per sec should give a mean weighted towards the faster drops. As the result is actually smaller than the median volume radius, a radius between the median from Figure 4.22a and that from Figure 4.22b would seem suitable for the purpose of this study.

$$\text{When } R = 1.5 \times 10^{-5} \text{ m sec}^{-1},$$

$$a = 1.1 \pm 0.2 \times 10^{-3} \text{ m}$$

$$\text{and } \frac{9R\varepsilon_o F_o}{a} = 3.3 \times 10^{-9} \text{ amp m}^{-2}$$

which is greater than i_o but sufficiently close to make it likely that some of the rain drops are charge saturated, though the proportion is uncertain.

Sivaramakrishnan (1961) found the charge on thunderstorm rain to exceed the value at which it would continue to gain charge all the way down to ground level, sometimes by a factor of five or six times.

4.23 The relaxation time for the change in precipitation current after a lightning flash, about 3 seconds, is much less than the typical interval between flashes, about 30 seconds. The precipitation current, therefore,

may be considered to have reached steady conditions just before a flash.

To evaluate these steady conditions it is necessary to first determine the vertical potential gradient profile. It will be shown that the profile is nearly independent of any assumption regarding the capture of ions by rain drops.

Over the region in which $Q > 4\pi\varepsilon_o 3a^2F$

$$\frac{dF}{dz} = \frac{1}{\varepsilon_o}(ne + NQ)$$

where NQ is constant.

Now, $R = NU\frac{4\pi a^3}{3}$

if $R = 1.5 \times 10^{-5}$ m sec^{-1}

$U = 7.0$ m sec^{-1} (Fletcher, 1962)

and $a = 1.1 \times 10^{-3}$ m,

then $N = 390$ m^{-3}

and $NQ = i_o/U = 2.9 \times 10^{-10}$ coulomb m^{-3}

Also, $ne\omega F$ = constant = A.

At ground level, $n_o e\omega F_o = J_o$.

Wormell (1953), Smith (1951) and Simpson (1949) all estimated J_o under a storm to be of the order 0.02 amp km^{-2}. Schonland (1928) estimated 0.16 amp km^{-2}.

An estimate of the current at the time and place

of the experiment can be made using a modification of Smith's method.

The recovery of electric field after a lightning flash is due to two effects: the recovery of the cloud dipole moment and the dissipation of space charge shielding the ground. Far distant flashes, measured at a site where no rain is falling and where the electric field is small, are not affected by local space charge and the recovery time constant is that of the cloud. Measurements on distant storms show this to be of the order of 2 minutes. Nearby flashes have recovery time constants of the order 25 secs or less which shows that the second process dominates.

It is assumed that the rate of dissipation of space charge when $F_o = 0$, just after a flash is equal to the rate just before the flash when F_o was steady. As this dissipation takes place -- i) by ion capture by rain drops and, -- ii) by conduction current into the cloud at heights where the field remains large and negative, the error in this assumption will be small but always in a direction to cause underestimation of J_o.

It is further assumed that the shielding space

charge is mainly higher than the field mill, mounted 1.2 m above the ground. For the Whipple-Chalmers model this is a good assumption. That the results show this assumption to be poor (paragraph 4.43) is evidence against this model.

From the record of the storm on November 4, 1965, the rate of recovery of electric field after a flash when $F_o = 0$, varied from 60 Vm^{-1} sec^{-1} at either end of the storm to about 230 Vm^{-1} sec^{-1} at the position of closest approach of the storm centre which was then about 1.5 km away. The maximum negative field over the same period varied by a factor of only 2.

The corresponding current densities required to maintain the space charge are 4.5×10^{-10} amp m^{-2} and 2×10^{-9} amp m^{-2}. These are an order of magnitude less than the figures quoted by Wormell (1953) which will be because the measurements were taken 1.5 km from the storm centre and because the mill was 1.2 m above the ground.

$$\begin{aligned} \text{If} \quad J_o &= 2 \times 10^{-9} \text{ amp } m^{-2} \\ \text{and} \quad \omega &= 2 \times 10^{-4} \ m^2 \ V^{-1} \ sec^{-1} \\ \text{then} \quad ne &= \frac{10^{-5}}{F} \\ \text{and} \quad \frac{dF}{dz} &= 1.12 \times 10^{11} \left(\frac{10^{-5}}{F} + 2.86 \times 10^{-10}\right) \end{aligned} \tag{4.23i}$$

for the region where $Q > 4\pi\varepsilon_o 3a^2F$.

At ground level,

$$F_o = 3 \times 10^3 \ Vm^{-1}$$

and $$\frac{dF}{dz} = 350 \ Vm^{-2}$$

At some height, z, the field is given by solving equation 4.23(i).

$$2.86 \times 10^{-5}F - \ln(1 + 2.86 \times 10^{-5}F) = 9.4 \times 10^{-4}z + A$$

where A is a constant.

If $F_o = 3 \times 10^3 \ Vm^{-1}$ when $z = 0$

then $A = 0.087 - \ln 1.087$

$= 0.0033$

and $$2.86 \times 10^{-5}F - \ln(1 + 2.86 \times 10^{-5}F) = 9.4 \times 10^{-4}z + 0.0033.$$

This relationship is displayed in Figure 4.23a and Figure 4.23b.

4.24 The assumption that no charge will be swept out by the rain is invalid at all times because of the spread in values of Q. The magnitude of this effect can be estimated by putting Q = 0, when

$$\frac{dQ}{dz} = \frac{-\pi ne\omega}{U} \cdot 3a \ F$$

$$ne\omega F - NUQ = \text{constant}$$

$$= J_o - i_o$$

$$\simeq 0$$

$$NUQ = ne\omega F = J$$

$$NU\frac{dQ}{dz} = \frac{dJ}{dz}$$

$$\frac{dQ}{dz} = \frac{-3\pi a^2 e\omega}{U} nF$$

$$\frac{dF}{dz} = \frac{1}{\varepsilon_o}(ne + NQ)$$

$$-3\pi a^2 NJ = dJ/dz$$

giving $J = J_o \exp(-Pz)$

where $p = 3\pi a^2 N$

and $J = J_o$ when $z = 0$

$$\varepsilon_o\frac{dF}{dz} = J_o \exp(-Pz)\{\frac{1}{\omega F} + \frac{1}{U}\}$$

$$\frac{\omega F \cdot dF}{(1 + \omega F/U)} = \frac{J_o}{\varepsilon_o} \exp(-Pz)\cdot dz \qquad (4.24i)$$

integrating (4.24i)

$$UF - (\frac{U^2}{\omega}) \ln(1 + \frac{\omega F}{U}) = J_o (\frac{1 - \exp(-Pz)}{\varepsilon_o P}) + B$$

where B is a constant. (4.24ii)

When $z = 0$, $F = F_o$

therefore, $B = UF_o - \frac{U^2}{\omega} \ln(1 + \frac{\omega F_o}{U})$

Given the various constants, it is simple now to calculate the variation of electric field with height

and also the variation of n and Q.

If $J_o = 2 \times 10^{-9}$ amp m^{-2}

$F_o = 3 \times 10^3$ Vm^{-1}

$a = 1.1 \times 10^{-3}$ m

$N = 390$ m^{-3}

so that $p = 4.45 \times 10^{-3}$ m^{-1}

$U = 7$ m sec^{-1}

$\omega = 2 \times 10^{-4}$ m^2 V^{-1} sec^{-1}

$\varepsilon_o = 8.9 \times 10^{-12}$ Fm^{-1}

At $z = 0$, $\omega F_o/U = 0.086$

and $B = 808$ V sec^{-1}.

Substituting values for the storm of November 4, 1965, equation (4.24ii) becomes

$$1 - \exp(-4.5 \times 10^{-3}z) = 2.0 \times 10^{-5}\{24.5 \times 10^4(2.86 \times 10^{-5}F - \ln(1 + 2.86 \times 10^{-5}F)) - 808\}$$

This can easily be solved for z on substituting values for F. Some values are displayed in Figure 4.23b and plotted in Figure 4.23a.

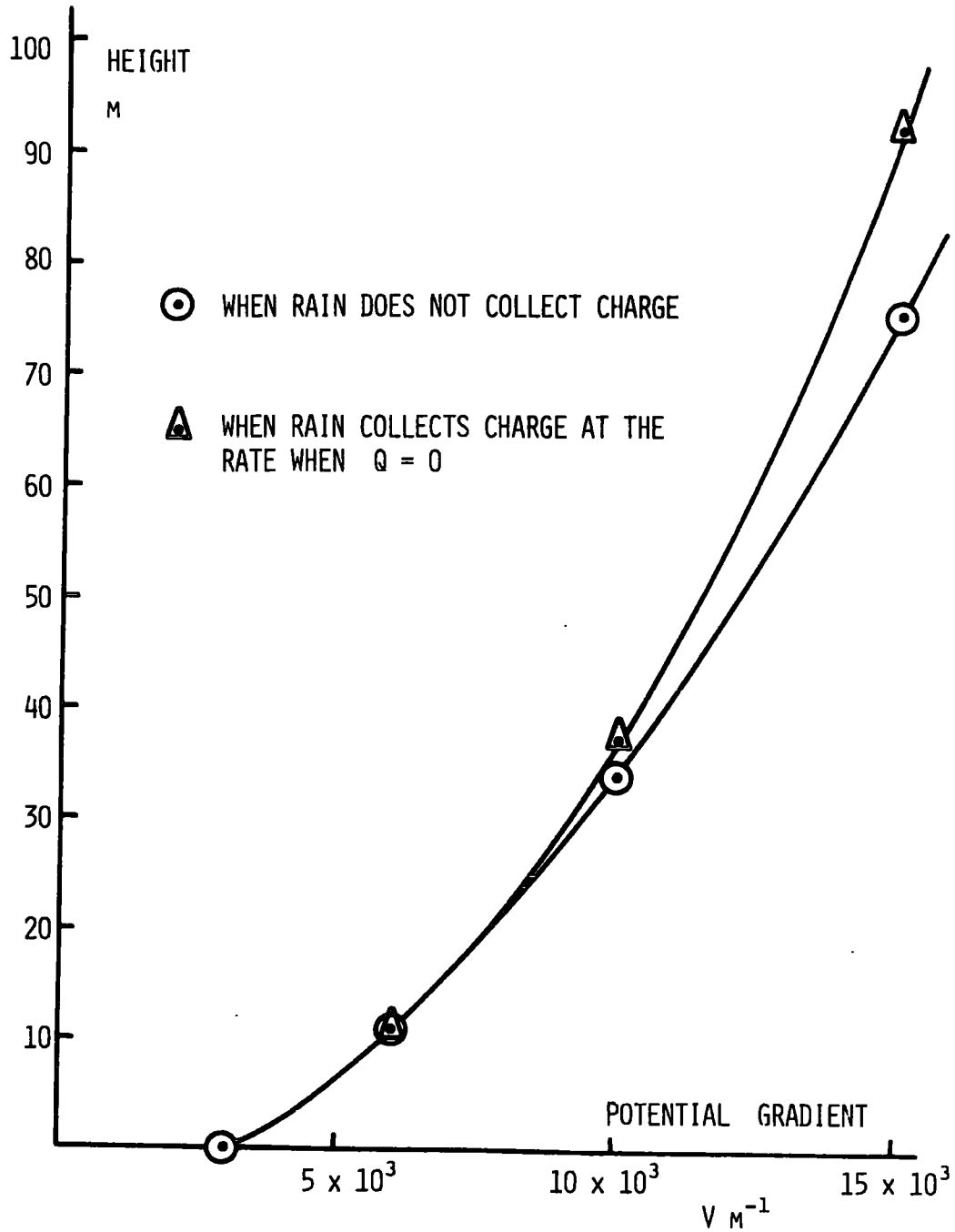

FIGURE 4.23a GRAPH OF HEIGHT AGAINST POTENTIAL GRADIENT

	(1)	{2}
Field	Height, $Q>4\pi\varepsilon_o 3a^2F$	Height, $Q = 0$
F Vm^{-1}	z m	z m
3×10^3	0	0
6×10^3	11.0	11.2
10^4	34.2	37.1
1.5×10^4	75.8	92.4
2×10^4	124.4	181.3

Corresponding values of negative electric field, F, and height, z, if rain, (1) captures no charge and {2} captures charge at the rate when Q = 0, for the storm of November 4, 1965.

Figure 4.23b

4.25 From Figure 3.30b, the time scale for the variation in precipitation current after lightning is of the order 3 secs, during which rain falls about 20m.

Figure 4.23a shows that the variation of the electric field with height up to about 20m is nearly independent of any charge transfer to the rain drops and therefore any assumption made concerning this will have little effect on the potential gradient profile.

Equation 4.24(ii) shows that the height at which the charge transfer becomes important is proportional to 1/P m where $P = 3\pi a^2 N$. The values chosen for a and N are typical of a heavy storm and give 1/P to be about 225 m. However, in very heavy rain, of the order 4×10^{-5} m sec^{-1}, 1/P would be reduced to about 50m and it would become important to assess the charge transfer to the rain and its effect on the potential gradient profile.

During the storm of November 4, 1965, the average peak positive potential gradient was about 1000 Vm^{-1}. From Figure 4.23a it can be seen that the potential at a height of only 3m will never go far positive and few or no negative ions will be produced by point discharge. The negative change in precipitation current would be

due, therefore, not to the collection of negative ions but to the failure to collect positive ions during the fall through the lowest few metres.

The initial slope of the precipitation current, Figure 3.30b, cannot therefore be greater than the rate of collection of charge at ground level as given in equation 4.25(i).

$$\frac{di}{dt} = \frac{d(NUQ)}{dz} U \qquad \text{at } z = 0$$

$$= NU^2\left(\frac{dQ}{dz}\right) \qquad z = 0 \qquad (4.25i)$$

if $$\frac{dQ}{dz} = \frac{-3\pi a^2 J_o}{U} \qquad z = 0$$

which assumes $\bar{Q}$ is effectively 0.

For the values chosen,

$$a = 1.1 \times 10^{-3} \text{ m}$$

$$N = 390 \text{ m}^{-3}$$

$$U = 7 \text{ m sec}^{-1}$$

$$J_o = 2 \times 10^{-9} \text{ amp m}^{-2}$$

$$\left(\frac{dQ}{dz}\right)_{z=0} = \frac{-3\pi\ 1.2 \times 10^{-15}}{3.5} \text{ coulomb m}^{-1}$$

$$= 3.23 \times 10^{-15} \text{ coulomb m}^{-1}$$

and $$\frac{di_o}{dt} = -6.17 \times 10^{-11} \text{ amp m}^{-2} \text{ sec}^{-1}$$

but the measured rate of change of i_o is -5×10^{-10} amp

m^{-2} sec^{-1} (see Figure 3.30b) a factor of ten times. This discrepancy is outside the limits of experimental error and is due to an effect ignored in the theory so far.

4.30 A Droplet Diffusion Model

4.31 The shape and magnitude of the precipitation current response to a lightning discharge demands that the rain pick up its charge in the last few metres before reaching the ground. There may, therefore, be a heavy concentration of charge at this low level, which has a low mobility and which can be collected by falling drops by other than the Wilson (1929) process. Such a charge could reside on droplets and the charged droplets could be produced by splashing. For 1 mm radius drops falling through 50 micron radius droplets the collection efficiency is nearly one and is practically unaffected by the presence of electric charges (Langmuir, 1948: Gunn and Hitchfeld, 1951).

There is another objection to the previous model concerning the interpretation of the rate of recovery of potential gradient after a discharge. The calculated current, called J_o, is actually $J_o + I_o$ where J_o is the

point discharge current density as before and I_o is the current density at the ground due to the production of space charge by splashing. If this space charge consisted of small ions, I would be identical in nature to J and the previous analysis would be valid.

Let J include all ionic current density.

I = current density due to charge residing on droplets — amp m^{-2}

S = number of droplets — m^{-3}

q = average charge per droplet — coulomb

ν = capture efficiency of droplets by drops.

h = rate of capture of droplets by one drop — sec^{-1}

ν is defined by the equation

$$h = \pi a^2 U S \nu \qquad (4.31i)$$

β = rate of flow of droplets upwards — $m^{-2}\ sec^{-1}$

b = a diffusion coefficient, defined by the relation

$$\beta = \frac{I}{q} = -b \cdot \frac{dS}{dz} \qquad (4.31ii)$$

b has little physical significance near the ground, but its use gives a convenient density profile for the droplets.

At equilibrium during steady heavy rain,

$$\frac{d\beta}{dz} = -hN$$

$$b\frac{d^2S}{dz^2} = \pi a^2 NU\nu \cdot S \qquad (4.3\text{iii})$$

so that $$S = S_o \exp\{-(\frac{\pi a^2 NU\nu}{b})^{\frac{1}{2}}z\} \qquad (4.3\text{iii})$$

where $$\gamma = \frac{\sqrt{\pi a^2 NU\nu}}{b}$$

$$S = S_o \exp(-\gamma z)$$

and $$\beta = +\gamma b \cdot S$$

$$I = \gamma bq \cdot S$$

The rate, ΔH_z, at which the rain drops sweep up the droplets from a layer of thickness dz and height z is given by

$$\Delta H_z = Nh\,dz$$

$$= Na^2U\nu \cdot Sdz$$

$$= b\gamma^2 S_o \exp(-\gamma z) \cdot dz$$

$$= -\frac{\partial\beta}{\partial z} \cdot dz$$

$$= -d\beta$$

The work of Adkins (1959) suggests that I_o will be proportioned to E for a given steady rainfall. β_o is a constant so q will be proportional to E.

Let $q = \phi E$

When E changes suddenly by ΔE there is a discontinuous change in I_o equal to $\phi \Delta E \beta_o$. The ideal model then shows a vertical discontinuity in the value of q lying in a rising, horizontal plane. This plane rises with a velocity β/s which is equal to γb.

If $\gamma b < U$, the initial rate of change of rain current is given by

$$di = \phi \Delta E b \gamma S_o (1 - \exp\{-\gamma^2 b \cdot dt\})$$

$$= \phi \Delta E b^2 \gamma^3 S_o \cdot dt$$

or $$\frac{di}{dt} = \phi \Delta E b^2 \gamma^3 S_o$$

$$= \phi \Delta E b \gamma^2 \beta_o$$

When the field is steady,

$$\Delta i = \phi \Delta E \beta_o$$

From Figure 3.30b,

$$\frac{di_o}{dt} = 0{\cdot}5 \cdot 10^{-9} \text{ Amp m}^{-2} \text{sec}^{-1}$$

and $$\Delta i_o = 2{\cdot}5 \cdot 10^{-9} \text{ Amp m}^{-2}$$

when $$\Delta E = 3{,}000 \text{ V m}^{-1}$$

From the results plotted in Figure 3.30b,

$$b\gamma^2 = 0{\cdot}3 \text{ sec}^{-1}$$

and $$\phi \beta_o = 10^{-12} \text{ Amp V}^{-1} \text{m}^{-1}$$

but $$b\gamma^2 = \pi a^2 NU\nu = 1{\cdot}3 \times 10^{-2} \nu \text{ sec}^{-1}$$

and is independent of b. This model is therefore also unable to explain the results as ν cannot be greater than 1.

4.32 If γb is greater than U, the initial rate of change of rain current is given by

$$di = \phi \Delta E b \gamma S_o (1 - \exp\{-\gamma U \cdot dt\})$$

or

$$\frac{di}{dt} = \phi \Delta E b \gamma^2 S_o U$$

$$= \phi \Delta E \beta_o U \gamma$$

The final steady field will still be $\phi \Delta E \beta_o$. So now $\gamma U = 0 \cdot 3 \text{ sec}^{-1}$

and $\phi \beta_o = 10^{-12} \text{ Amp } V^{-1} m^{-1}$

Therefore $\gamma = 0 \cdot 03 \text{ m}^{-1}$

Thus by this model the droplets will all be rising with a velocity greater than 7 m sec^{-1} and the number density will fall off exponentially to about 1/3 the ground value at a height of about 30 m.

While it is difficult to assign a value for b in the turbulent conditions, it is unreasonable to accept the mass motion of droplets with upwards velocities greater than 7 m sec^{-1}, up to heights above 30m. This second model is therefore also unable to explain the results.

4.40 A Droplet Blanket Model

4.41 Instead of a diffusion coefficient, a blanket of droplets, of thickness L, will be considered. It is

postulated that the droplets are projected into it by splashing.

To simplify the calculation it will be assumed that the rate of injection of droplets into the blanket is the same at all levels and equal to $\lambda m^{-3}sec^{-1}$. Other symbols remain the same as in 4.30 except that β is taken to be zero above ground level and β_o is the rate of production of droplets.

$$\beta_o = \lambda L$$

$$\lambda = hN = \frac{\pi a^2}{4} NU\nu S \qquad z<L \qquad (4.41i)$$

$$S = \frac{4\beta_o}{\pi L a^2 NU\nu} \qquad z<L$$

$$I_o = \phi E \beta_o$$

When E changes suddenly by an amount ΔE there is a discontinuous change in I_o equal to $\phi \Delta E \beta_o$.

The average charge at some time t is given by

$$\bar{q} = q + \Delta q\{1 - \exp(-\lambda t/s)\}$$

If $t<L/U$, the charge picked up by a drop reaching the ground at time t, during the previous t secs is given by

$$\Delta Q = h \int_{t=0}^{t} \bar{q} \cdot dt$$

$$= h\left(qt + \Delta qt - \frac{S\Delta q}{\lambda}\{1 - \exp(-\lambda t/s)\}\right)$$

The rain current at the ground,

$$i_{o(t=t)} = i_{o(t=0)} + NUh\Delta q\left(t - \frac{S}{\lambda}\{1 - \exp(-\lambda t/s)\}\right)$$

$$\frac{di_o}{dt} = NUh\Delta q\{1 - \exp(-\lambda t/s)\}$$

at $t = 0$,

$$\frac{di_o}{dt} = 0.$$

If $t>L/U$, the charge picked up by a drop reaching the ground at time t during the previous t seconds is given by

$$\Delta Q = h \int_{t-L/U}^{t} \bar{q} \cdot dt$$

$$= h\{(q+\Delta q)\frac{L}{U} - \frac{S\Delta q}{\lambda}(e^{\frac{-\lambda(t-L/U)}{s}} - e^{\frac{-\lambda t}{s}})\}$$

The rain current at the ground

$$i_{o(t=t)} = i_{o(t=0)} + NUh\Delta q(\frac{L}{U} - \frac{S}{\lambda}\{e^{\frac{-\lambda(t-L/U)}{s}} - e^{\frac{-\lambda t}{s}}\})$$

$$\frac{di_o}{dt} = NUh\Delta q\{e^{\frac{-\lambda(t-L/U)}{s}} - e^{\frac{-\lambda t}{s}}\}$$

at $t = L/U$,

$$\frac{di_o}{dt} = NUh\Delta q\{1 - \exp(\frac{-\lambda L}{SU})\}$$

at $t = \infty$,

$$i_o = i_{o(t=0)} + NUh\Delta qL/U$$

and $\beta_o = NhL$

The current at $t = L/U$ undergoes an inflexion. If L/U is small compared with S/λ this inflexion will not be seen in the record, Figure 3.30a and the maximum slope measured will be that at $t = L/U$.

If $\frac{di_o}{dt} = 0.5 \cdot 10^{-9}$ Amp m^{-2} sec^{-1}

and $\Delta i_o = 2.5 \cdot 10^{-9}$ Amp m^{-2}

when $\Delta E = 3{,}000$ Vm^{-1}

from equation 4.41(i),

$$\frac{S}{\lambda} = \frac{1}{\pi a^2 NU\nu} = \frac{80}{\nu}$$

$$= 100 \text{ sec, say.} \qquad (4.41ii)$$

Droplets will not be projected above 4m so that

$\frac{L}{U} < \frac{1}{10}\frac{S}{\lambda}$ and $1 - \exp\left(-\frac{\lambda L}{SU}\right) \rightarrow \frac{\lambda L}{SU}$

$$\frac{di_o}{dt} = NUh\Delta q \frac{\lambda}{S}\frac{L}{U} = \frac{\lambda}{S}\beta_o \Delta q$$

$$\Delta i_o = \beta_o \Delta q$$

From the records,

$$\frac{\frac{di_o}{dt}}{\Delta i_o} = \frac{\lambda}{S} = 0.2 \text{ sec}^{-1}$$

or $\frac{S}{\lambda} = 5$ sec $\qquad (4.41iii)$

4.42 The two values for S/λ (4.41ii) and (4.41iii), of $80/\nu$ and 5 secs respectively are obtained by considering in the first case the rate at which the rain is able to sweep any suspended matter out of the air, the time constant is nearly the same as that for wetting completely a horizontal surface, and in the second case the rate of recovery of precipitation current to a step change in field. Their gross difference shows

that a mere sweeping out of suspended charge alone can not be used to explain the effects observed.

4.43 Splash Trajectories

If the rain cannot sweep out the suspended charge quickly enough, the droplets may themselves precipitate out. Consider a droplet diameter d projected vertically with a velocity V_o m sec^{-1}.

$$m\ddot{g} + 6\pi\frac{d}{2}\eta\dot{x} + m\ddot{x} = 0$$

which is of the form,

$$A + B\dot{x} + C\ddot{x} = 0$$

whose solution is

$$x = \left(\frac{A}{B} + V_o\right)\frac{C}{B}\left(1 - e^{\frac{-Bt}{C}}\right) - \frac{At}{B}$$

Now $\frac{A}{B} = mg/6\pi\frac{d}{2}\eta = 2d^2\rho g/36\eta$

is the terminal velocity = V_t, say,

and $\frac{C}{B} = m/6\pi\frac{d}{2}\eta = 2d^2\rho/36\eta$

is the time constant with which the particle approaches the terminal velocity = V_t/g.

$$x = 0$$

when $$\frac{At}{B} = \left(\frac{A}{B} + V_o\right)\frac{C}{B}\left(1 - \exp\left\{\frac{-Bt}{C}\right\}\right)$$

The R.H.S. cannot be bigger than $\left(\frac{A}{B} + V_o\right)\frac{C}{B}$ so the maximum time of flight

$$= \frac{\left(\frac{A}{B} + V_o\right)\frac{C}{B}}{\frac{A}{B}} = \frac{\left(\frac{A}{B} + V_o\right)}{g}$$

and this will normally be less than one second as pointed out in paragraph 4.11 .

However, if the splashing occurs above ground level--on a leaf for instance--or if there is turbulent air flow over the ground, such droplets will be diffused upwards and take more time to precipitate down to ground level. The measured long time constant demands that either all splash droplets are diffused upwards before falling to ground or that only those convected upwards are charged or that only those that are convected upwards enter the rain receiver. The precautions to avoid direct splashing suggest that the third condition at least is true.

4.44 Magnitude of Splash Effect

The results of Gregory, Guthrie and Bunce (1959) suggest that each rain drop will produce of the order 200 droplets of diameter about 100 microns. 3,000 drops m^{-2} sec^{-1} will then produce 6×10^5 droplets m^{-2} sec^{-1}. If these were convectively distributed within the lowest 0.5 m, the time constant for settling out will be of the order 3 sec and there will be a density of 3.6×10^6 droplets m^{-3}. If they were initially uncharged, these droplets would acquire charge

by capturing the positive small ions at a rate derived by Whipple and Chalmers (1944).

$$\frac{dq}{dt} = \frac{-\pi ne\omega(3a^2F + q/4\pi\varepsilon_o)^2}{3a^2F}$$

If $q = 0$

$$\frac{dq}{dt} = -3\pi ne\omega a^2F$$

$ne\omega F_o = J_o$ cannot be estimated from the rate of recovery of electric field because the space charge never rises above the field mill. If the following values are taken for the storm of November 4, 1965,

$$e = 1.6 \times 10^{-19} c$$

$$F = -3 \times 10^3 \ Vm^{-1}$$

$$\omega = 2 \times 10^{-4} \ m^2 sec^{-1} \ V^{-1}$$

$$a = 5 \times 10^{-5} m$$

n is indeterminate but has an upper limit such that the space charge forms complete shielding for the electric field at the ground.

$$n_{max.} = 2E \frac{\varepsilon_o}{e} = 3 \times 10^{11} \ m^{-3}$$

$$ne = 5 \times 10^{-8} \text{ coulomb } m^{-3}$$

Thus, the maximum

$$\frac{dq}{dt} = 7.10^{-16} \text{ coulomb } sec^{-1}$$

The maximum charge, $q_{max.}$, is independent of n.

$$q_{max.} = 4\pi\varepsilon_o \cdot 3a^2F$$
$$= 25 \cdot 10^{-16} \text{ coulomb}$$

After 3 sec falling, the droplet charge may be as large as 10^{-15} coulomb if n is as large as 3×10^{11} m^{-3}. A production of 6×10^5 droplets m^{-2} sec^{-1} would produce a maximum current of 6×10^{-10} amp m^{-2} which is still too small to explain the observations.

However, the droplets may already be charged by splashing before they acquire additional charge by ion capture. If each droplet acts as a dipole with its reflection just before separation it will carry a charge q such that $E = 2q/4\pi\varepsilon_o h^2$ approximately, where h is the height of the charge centre. If E were 3×10^3 Vm^{-1} and h were 0.2 mm then q would be 10^{-14} coulomb which would be more than enough to explain the results. An initial charge of only 10^{-15} coulombs would be doubled by ion capture and would create a precipitation current of the right order of magnitude.

4.50 Further Considerations

4.51 A normal wind during a tropical thunderstorm is more than one metre per second--sometimes much more--so that droplets produced by the few drops which hit

the shielding rods will drift a few metres down wind in the seconds they take to fall and will not enter the receiver. If the precipitating splash droplet model is correct, those entering the receiver were produced a few metres upwind. At the site, a paved driveway was in just this position and may have been the source of the charged droplets.

The process of splashing on a paved driveway in heavy rain may well include the bursting of bubbles which is an effective method of projecting charged droplets with high velocities (Blanchard, 1963). This factor was not studied at the time the measurements were made and could be a profitable subject for future work.

Splashing on leaves of shrubs and atomization of surface water in the very high fields present must also be considered as likely contributors to the droplet blanket hypothesized.

4.52 Further analysis of the Whipple-Chalmers model would give a height when the charge on the rain drops changes sign. Everywhere except near the ground Q is much less than Q_1 and can be taken as 0. The charge collected will then be

$$Q = \int_{o}^{G} \frac{-3\pi ne\omega a^2 F}{U} \, dz$$

where G is the height of the sign change.

$ne\omega F = J$ which will never be greater than J_o and a value for G which is too low by a factor of the order 2 will be given by

$$G = \frac{UQ_o}{3\pi a^2 J_o}$$

$$= 7.10^8 \text{ m}$$

which is far too high to be an acceptable value and this strengthens the case that the charge is brought to earth by other than the Whipple-Chalmers model.

CHAPTER V

EVAPORATION CURRENT

5.1 Zero Drift

A drift in the zero reading of the rain current receiver was noticed when the bucket contained a little water. This drift returned to zero when the bucket dried out. The spurious current could be explained as either an evaporation current or as a thermoelectric current through dirty insulators caused by the temperature differences set up by the evaporation. An experiment was performed to investigate the possibility of an evaporation current though previous work suggests it is too small to be measured. For a review, see Chalmers (1967).

5.2 Apparatus

The apparatus was set up as in Figure 5.20a. A flat dish containing an aqueous solution at just less than 100°C was placed at the centre of a hole, in a large flat grounded sheet of aluminium, on a heated

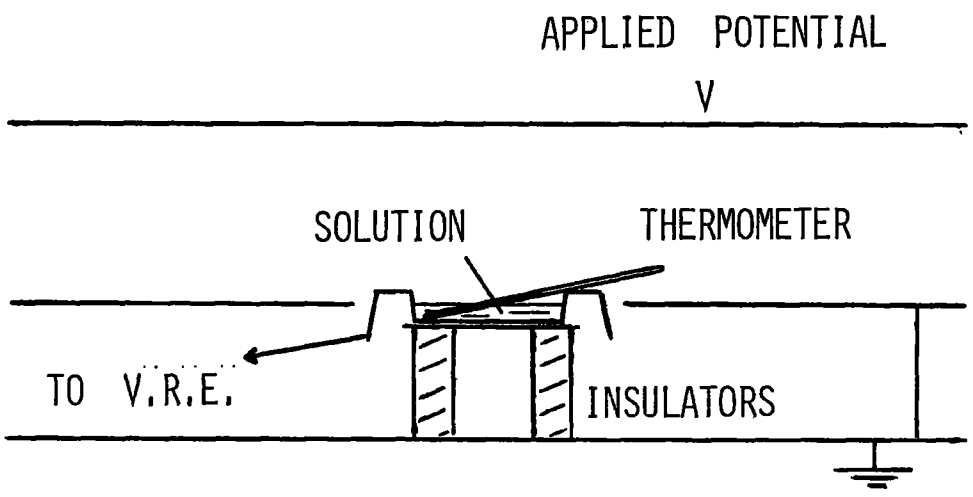

EVAPORATION CURRENT EXPERIMENT

FIGURE 5.20A

brass block standing on polystyrene insulators with an asbestos sheet protecting them. As the liquid slowly cooled, various electric fields were applied by raising the potential of a covering sheet to various voltages.

The different liquids investigated included distilled water, rain water and saturated salt solution.

5.3 Results

A current was measurable for fields greater than about 10 Vm^{-1}.

(The V.R.E. maximum sensitivity was 3 x 10^{-15} amp full scale deflection but noise prevented measurements below this value.) However, the current was always of the order 10^{-14} Ea where E is the field in Vm^{-1} and a is the area of the dish in m^2. 10^{-14} mho m^{-1} is the conductivity of air, approximately, and it was concluded that evaporation current, if any, must therefore be less than conduction current and could not be measured with the apparatus as set up. It was further concluded that any evaporation must also be too small to give a measurable deflection in the rain current detector.

Cleaning the insulators in the rain current detector eliminated the (thermoelectric) zero drift.

CHAPTER VI

THE PEPEL PROJECT

6.0 The Lane-Smith residence, K.22 Fourah Bay College, Figure 2.5b, is at a height of 350 m and has a panoramic view of the Sierra Leone river and the country beyond, Figure 6.1a. Thunderstorms can be observed building up and moving down the river. The occurrence of a warm thunderstorm initiated this project.

Many of the theories of thunderstorm electrification (Simpson and Scrase, 1937; Chalmers, 1943; Workman and Reynolds, 1950; Reynolds, Brook and Gourley, 1957; Latham and Mason, 1961) have invoked the presence of ice as a participant in the generation of electric charge, and numerous arguments in favour of these ideas have been brought forward.

However, there have been several reports of thunderstorms in which it would seem that the temperature everywhere inside the storm was above $0^{o}C$ and so

ice could not be present (Foster, 1950; Appleman, 1957; Moore, Vonnegut, Stein and Survilas, 1960; Pietrowski, 1960; Michnowski, 1963; Houghton, 1969).

Some of the protagonists of ice theories have thrown doubt on the accuracy of the identification of these storms as "warm" storms and it is highly desirable that examples of such storms should be fully authenticated. There appears little room for doubt in the following account.

6.1 The Warm Thunderstorm

At 17.15 on September 17, 1965, the sky was blue with some scattered cumulus and a single isolated thunderstorm over the port of Pepel at a distance of about 21 km to the E.N.E., Figure 6.1a. The location of the storm could be verified by the rain from it obliterating the view of the lights at Pepel, Figure 6.1b. Immediately in front of Pepel is Tasso Island and this was used as a 'yard stick' to measure the height of the visible top of the cloud, since the height of the cloud subtended, at the observer, an angle a little less than that subtended by the island, nearly the same distance away. This observation placed the top of the cloud at a height of 3,000 ± 600 m.

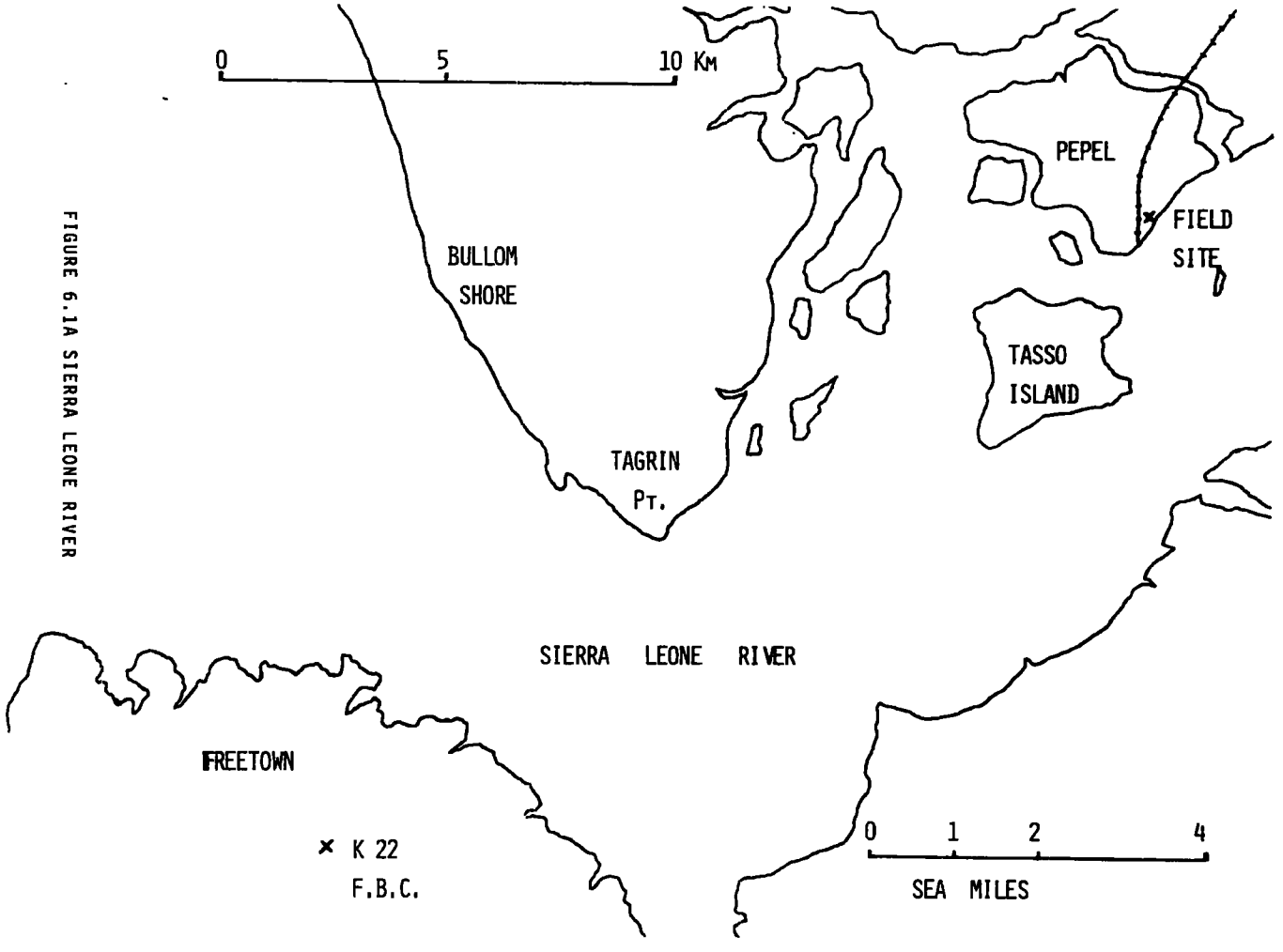

FIGURE 6.1A SIERRA LEONE RIVER

FIGURE 6.]b A WARM THUNDERSTORM

At this time of year in the early evening the ambient sea-level temperature is 27 ± 3°C. Assuming the cloud base to be at 300 m and assuming the saturated adiabatic lapse-rate within the cloud, the temperature at the top of the cloud comes to 11 ± 5°C. To reach a temperature of 0°C would require, under these conditions, a height of 5,300 ± 700 m. The normal freezing level is about 5,600 m, which helps to confirm the present calculations.

To reach the height for freezing and still subtend the same angle, the storm would have had to be 37 ± 7 km away and could not have produced precipitation only 21 km away.

The storm was observed to give one flash of lightning within the cloud. At 21 km, of course, the thunder was not heard. There may have been other flashes prior to the one observed.

6.2 Discussion of the Warm Storm

The storm described was certainly one in which lightning occurred and yet one in which no ice could have been present. The first question which arises is why such storms have been so rarely reported. One answer may be that the conditions under which they can be ob-

served and definitely characterised are not common; if other storm clouds had been present at the same time, the identification of this one as a "warm" storm might not have been possible. A second answer may be that these storms are themselves rare; if this particular storm had developed more intensely, it would have risen another 2,000 m and would no longer have been a warm storm; if it had developed a little less, no lightning might have occurred. Also, a similar-sized storm in a colder climate would have already reached the freezing level at 3,000 m.

The next question is that of the process of charge separation at work. If it is the same process as occurs in the main separation of charge in the normal thundercloud, then this must be quite independent of ice and all those theories which invoke ice must be wrong. If the process in the warm thunderstorm is the same as that which gives rise to the lower positive charge in the normal storm, then this process cannot be melting, as has sometimes been suggested.

If the polarity of a warm storm could be determined, one or other of these suggestions would be eliminated; but so far, nobody with instruments has been

able to get near enough to a warm thunderstorm even to measure its polarity. It was decided, therefore, to try to measure the polarity of others similar.

If it should turn out that the polarity is the same as that of the normal cloud, the problem then is whether the process at work is the same as that in the normal cloud, or different.

Another point to consider is that other clouds, of sizes similar to that described, have been observed to give heavy precipitation but no lightning. This suggests that electrical development requires some form of triggering which occurred in the storm described but not in other cases.

6.3 Experimental Project

When it was realized, after the calculations, that the storm observed was indeed warm, the possibility of another occurrence was considered and it was decided to make preparation for this event. From that day a diary of storm events was maintained and a sextant was kept in the house for more accurate height measurements.

A field site was negotiated with the Sierra Leone Development Company at Pepel where a field mill was set

up, Figure 6.3a, which recorded the field at 15 sec intervals. The intention was that at the next occurrence of a warm thunderstorm over Pepel there would be a record of the electric field beneath it.

A camera and sextant were taken aboard a light aircraft owned by the Sierra Leone Selection Trust, used for commuting from Freetown to Yengema, 200 miles up country, to look for warm thunderstorms and measure the height of their cloud tops.

A 16 mm movie camera was borrowed from Professor F.H. Ludlam for one year and, except when the supply of film ran out and there was no money to buy more, time-lapse ciné of interesting clouds over Pepel and the Sierra Leone River were taken. A copy of this film is deposited in the library with this thesis at the University of Durham. Another copy is with Professor F.H. Ludlam at Imperial College, London and another with the author. A schedule of filming, with some general comments, is included in Appendix D.

6.4 Results

At no time after September 17, 1965, was another warm thunderstorm observed. However, the movie film provided interesting insight into the flow patterns of

thunderstorms and one correlation of flow pattern with electric field.

The 'roller' clouds in front of, and just below, the thunderstorm cannot, it seems, be formed by air rising from below as condensation would not normally occur until the height of the main cloud base was reached. The clouds are rolling such that the lower surface is moving away from the storm which suggests that the downdraft is moving forward from below the storm and is deflected upwards to form these clouds. Such a flow would preclude the existence of an updraft from ground level in front of the downdraft as has been suggested (Auer, Veal and Marwitz, 1969).

The timing of the recorder at Pepel depended on the frequency of the supply which was not intended to operate electric clocks and therefore varied. The recorder gained 7 ± 1 minute per day. As the event on October 13, 1967, occurred 20 days after installing the chart, the record timing may be out by as much as 20 minutes.

At 18.30 that evening, a cloud in front of a storm mushroomed up, just by Pepel, from 4 to 11 km in 15 minutes with a sustained vertical velocity of the cloud top of about 8 m sec^{-1}.

The 1 hr. 58 min. filming on October 13, 1967,

used 962 frames at 0.1228 min. intervals. Figure 6.4b shows the height readings taken directly from the film. Tasso was 4.85 cm long on the film image used which corresponded to a distance of 4.35 km at a range of 22 km. This provided the height scale used. The horizon was taken to be 150 m above ground at the range of the cloud.

Frame Number from Beginning of Sequence	Time G.M.T.	Height of Cloud Top, km.
780	18.32	4.68
806	18.35	5.49
829	18.38	6.84
854	18.41	8.64
884	18.45	10.71
962	18.54	11.70

Figure 6.4b

It can be seen, Figure 6.4a, that the electric field grew as the cloud height grew. Such a behaviour is compatible with a convective theory of electrification (Vonnegut, 1965). Even if the field occurred as much as 20 minutes later, the growth would seem to be too rapid and too early for gravitational separation.

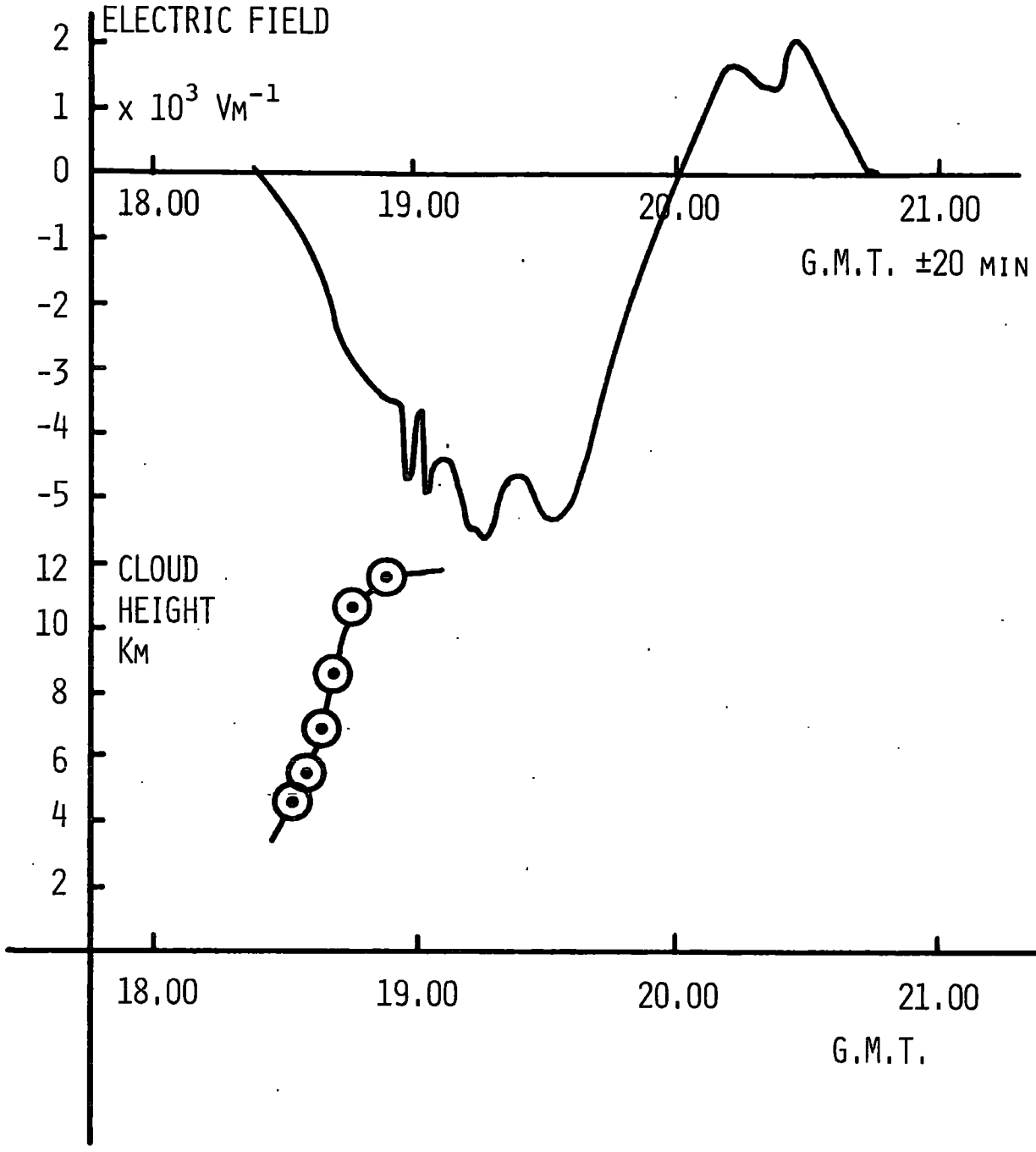

GROWTH OF ELECTRIC FIELD AND CLOUD HEIGHT WITH TIME

FIGURE 6.4a

CHAPTER VII

CONCLUSIONS

7.0 The conclusions are divided into topics and each topic is subdivided into what was achieved and suggestions for future work.

7.1 Instrumentation

Useful measurements were made with instruments designed to record electric field, precipitation current and rate of rainfall.

With present knowledge and technology, it would be easy to build a more sensitive amd more precise field mill. However, the importance shown by this thesis of processes occurring within the lowest half meter above the ground demand that, in heavy rain, a mill be positioned to measure the actual electric field at ground level. Such a mill would be situated in a pit in which splashing was eliminated.

Rain current density measurements were made with a shielded receiver which minimized the effects of displacement current, conduction current and direct splashing.

Such an instrument was very well adapted to detect and measure the important contribution made by the turbulent diffusion of splash droplets. To investigate the charge on the rain drops alone, it would be desirable to make measurements preferably on individual drops (Smith, 1955) or to use an exposed receiver (Ramsay and Chalmers, 1960) in which compensation may be made for displacement current and conduction current and where splashing off the receiver will be nearly equal to splashing into the receiver.

7.2 Precipitation Current

The results show that in addition to the rain current due to the charge carried on the rain drops, there is a large current i_o' due to precipitation of the droplet blanket and a significant current, i_o'', due to displacement current. To obtain the rain current alone, these two contributions must be subtracted from the overall current measured. The droplet current density at some instant may be expressed by the

equation

$$i_o' = \frac{1}{\tau} \int_{t=0}^{\infty} I_{o_{(t)}} \cdot e^{\frac{-t}{\tau}} \cdot dt$$

where t is time before the instant, τ is the time constant for droplet precipitation and $I_{o_{(t)}}$ is the current density into the droplet blanket by splashing and ion capture at time t.

$$I_{o_{(t)}} = \phi\beta_o E_{(t)}$$

where ϕ is the mean charge per droplet per unit electric field, β_o is the rate of injection of droplets into the droplet blanket and E_t is the electric field at time t.

$\phi\beta_o$ and τ would be expected to vary with rate of rainfall and wind speed and, perhaps, electric field. The mean values of $\phi\beta_o$ and τ for the three storms are shown in Figure 7.2a.

Date	τ	$\phi\beta_o$
October 24, 1965	3.6 sec	0.99×10^{-12} Amp $V^{-1}m^{-1}$
November 4, 1965	3.2 sec	0.87×10^{-12} Amp $V^{-1}m^{-1}$
June 7, 1966	2.5 sec	3.96×10^{-12} Amp $V^{-1}m^{-1}$

Figure 7.2a

The displacement current is significant only when

there is a large change in E in a time small compared with the time constant of the rain receiver, τ_2. The current, i_o'', to be subtracted is given by

$$i_o'' = \chi \sum_{t=0}^{\infty} \Delta E_{(t)} e^{\frac{-t}{\tau_2}}$$

where χ is the displacement current per unit potential gradient change at the time of the charge and t is the time prior to the instant in question.

$$\Delta E_{(t)} = E_{(t+\delta t)} - E_{(t)}$$

where $E_{(t)}$ is the field at time t and δt is any constant time interval small compared with τ_2.

For the rain receiver used, $-\chi$ had the value 2.15×10^{-13} Amp $V^{-1}m^{-1}$ and τ_2 was 1.5 sec.

It is not difficult to write a computer program to compute and subtract i_o' and i_o'' from the record of i_o and plot the resulting rain current density against electric field. Such a procedure is one suggestion for future work in precipitation electricity using either the author's results or new measurements in any part of the world, not only the tropics.

7.3 Splashing

The results show that in heavy rain in the presence

of a high electric field and a strong wind, charged droplets of probably about 100μ diameter are carried by turbulence to heights, above their trajectory in still air, of the order 0.5m and precipitate out downwind a distance of the order τ.(wind speed).

The current density into the ground due to the precipitation of these droplets is of the same order of magnitude as the rain current itself. The net contribution at a place where splashing takes place is on average, of course, nearly zero.

Specific suggestions for further work in this area include the following:

a) A thorough investigation, theoretical and experimental, of the turbulent transfer of slowly precipitating particles near the ground. Previous work has been done on blow sand, sediment transport in water and the diffusion of very fine particles (Allen, 1968; Bagnold, 1966; Chamberlain, 1966) but none is directly applicable to the transport of splash droplets.

b) Measurements of droplet mass, velocity, direction and charge for a range of drop sizes

and surfaces. The most satisfactory measurements published so far seem to be those of Gregory, Guthrie and Bunce (1959).

c) The difficult problem of measuring the droplet density, mass spectrum and charge spectrum at various heights in actual, heavy, thunderstorm rain. The author is not aware of any attempts to make these measurements.

An interesting development would be to construct a pit some 100 m diameter covered by wire mesh at ground level. This would provide a ground plane on which to make measurements in the absence of the blanket of splash droplets. Two purposes would be served; to avoid complications in measuring other parameters, such as rain current, and to provide a control experiment when investigating the splashing.

7.4 Evaporation

No significant electrification due to evaporation was detected.

7.5 Pepel Project

One warm thunderstorm was observed but never again. Some fascinating time lapse movie of developing

clouds and thunderstorms were shot. Electric field measurements made at Pepel during one sequence of filming suggest that a convective process rather than precipitation is responsible for the electrification.

The obvious suggestion for future work is more of it. The author hopes for the opportunity to return to Sierra Leone to set up more and better instruments at Pepel and more and better cameras at Fourah Bay College. This would enable a more definite relationship to be established between the electrical activity of a storm and the characteristics of the visible cloud.

APPENDIX A

THE EFFECT OF THE GROUNDED RODS

A.0 A finite conducting cylinder in an electric field is difficult to analyze because of the discontinuities. However, some aspects of a prolate spheroid have been treated in the literature (Smythe, 1950; Picca, 1968) but, to the author's knowledge, the shielding effect has not been calculated.

A.1 Background

The rod may be approximated to a conducting spheroidal boss of height c and base radius b. Using cylindrical coordinates such that $z = z$, $x = \rho \sin \phi$ and $y = \rho \cos \phi$, the rod is described by

$$\frac{\rho^2}{b^2} + \frac{z^2}{c^2} = 1 \qquad z>0 \qquad \text{(A.1i)}$$

This is one of a family of prolate spheroids described by

$$\frac{\rho^2}{b^2 + \theta} + \frac{z^2}{c^2 + \theta} = 1 \qquad z>0 \qquad \text{(A.1ii)}$$

Let $c^2 + \theta = (c^2 - b^2)\eta^2$

then Smythe (1950) shows that the potential, V, around the spheroid when placed in a uniform field, E, parallel to the z axis is given by

$$V = Ez\left(1 - \frac{\coth^{-1}\eta - \frac{1}{\eta}}{\coth^{-1}\eta_o - \frac{1}{\eta_o}}\right)$$

where $\eta_o = c(c^2-b^2)^{-\frac{1}{2}}$ and E is positive if V increases with z.

A.2 Potential Gradient at the Ground

At z = 0, the spheroidal surfaces and the electric field are both vertical so that η has a stationary value along a field line. The potential gradient, then, is given by

$$\frac{dV}{dz} = E\left(1 - \frac{\coth^{-1}\eta - \frac{1}{\eta}}{\coth^{-1}\eta_o - \frac{1}{\eta_o}}\right) \qquad \text{(A.2i)}$$

Let a form factor, β, equal the ratio of the rod radius to the rod height.

$$\beta = \frac{b}{c}$$

Then, $\eta_o = (1 - \beta^2)^{-\frac{1}{2}}$

For the family of prolate spheroids given by equation A.lii, the distance along the ground from the rod, d, is given by ρ when z = 0, so that

$$d^2 = b^2 + \phi$$

$$= \beta^2 c^2 + \phi$$

and $$\eta^2 = \frac{c^2 + \phi}{c^2 - b^2} = \frac{c^2(1 - \beta^2) + d^2}{c^2 (1 - \beta^2)}$$

From equation A.2i, the reduction in electric field is given by

$$\Delta E = E \left(\frac{\coth^{-1}\eta - \frac{1}{\eta}}{\coth^{-1}\eta_o - \frac{1}{\eta_o}} \right)$$

A table of values of $\Delta E/E$ for different values of β and d is set out in Figure A.2a and the results plotted in Figure A.2b.

Table of values of $\Delta E/E$ for different values of d and β.

d =	0.3c	0.5c	0.7c	c	2c
$\beta (=\frac{b}{c})$			$\Delta E/E$		
2×10^{-1}	0.718	0.410	0.249	0.128	0.025
10^{-1}	0.473	0.274	0.166	0.086	0.017
10^{-2}	0.219	0.127	0.077	0.041	0.008
10^{-3}	0.143	0.083	0.050	0.027	0.005

Figure A.2a

These results clearly show that for a typical rod whose height is 100 times the radius, the field on the ground at a distance equal to the height of the rod is reduced by less than 5%.

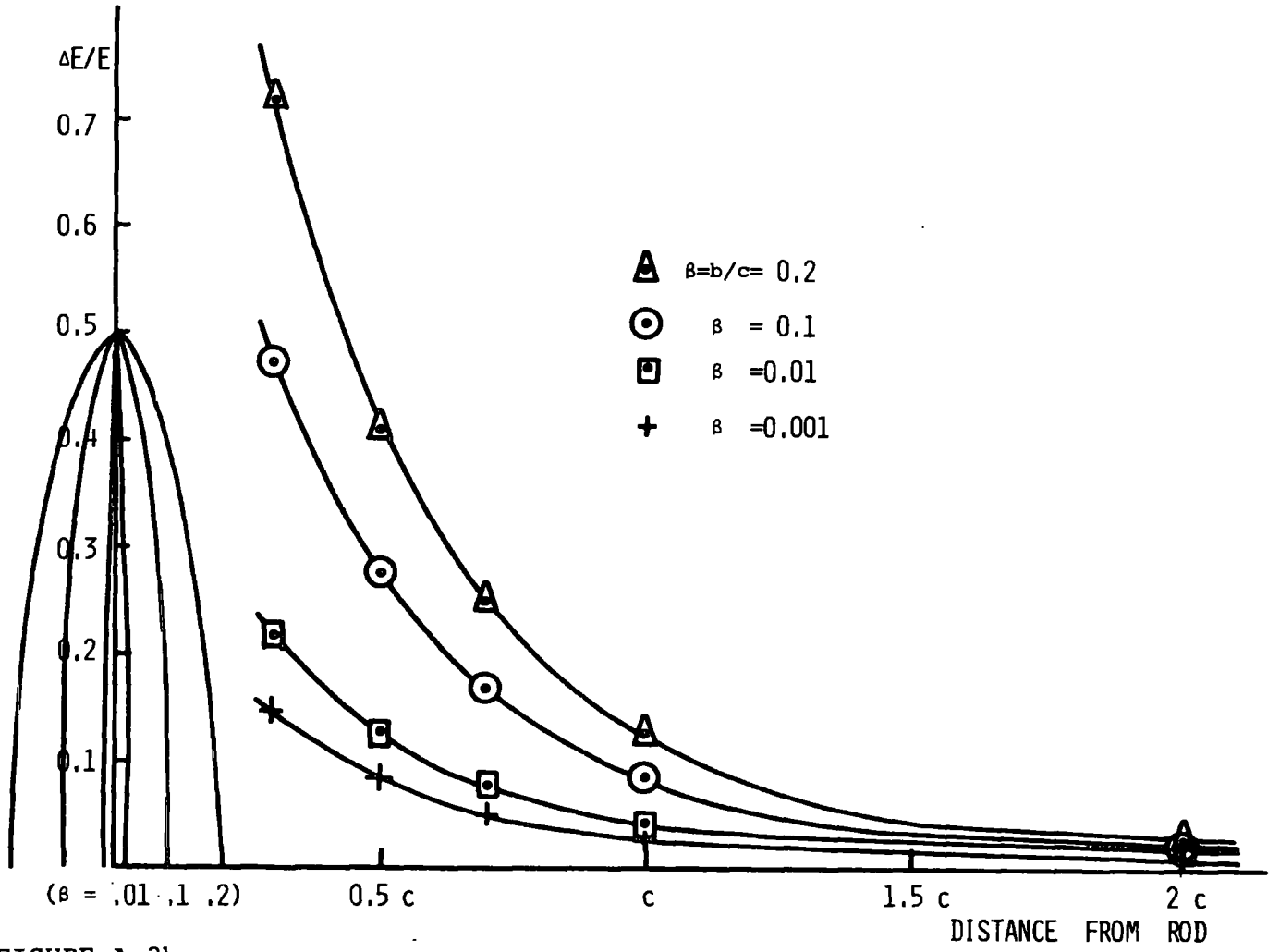

FIGURE A.2b GRAPH OF FRACTIONAL REDUCTION IN FIELD, $\Delta E/E$, AGAINST DISTANCE FROM ROD OF HEIGHT c FOR VARIOUS DIAMETERS, b .

However, it is easy to show (Picca, 1968) that the field at the tip of this same rod is over 2,000 times the ambient field and therefore in stormy weather point discharge will take place. There will, therefore, be a region downwind of the rod in which space charge gives a much more complete shielding for slow variations in electric field.

APPENDIX B

FURTHER INSTRUMENTATION

B.0 Considerable time and effort was spent in developing an automated system to measure and record the charge, mass and velocity of a vast number of drops together with sampled values of up to 10 different parameters immediately after each drop measurement. The system was completely designed and one of every circuit module was built and tested. A tape punch was purchased and the buffer electronics designed. Unfortunately, lack of the services of a technician to build the instrument prevented the completion of the project.

The project was revived when a Tektronix type 547 oscilloscope with a remote control single shot facility became available through U.S. A.I.D. and a camera with remote control film wind was purchased through U.K. technical assistance. It was hoped to

measure the charge mass and velocity of some single drops in a manner similar to Smith (1955).

Unfortunately, just as calibration was proceeding, the high voltage transformer in the oscilloscope burnt out and the project was once more brought to a halt. The replacement parts had not arrived when the author left Sierra Leone several months later.

This brief account is included in the thesis partly because of the time and effort spent in the project and partly because the idea of the experiment in this form is new and there are one or two novel solutions to problems which arise.

B.1 Single Drop Detector

The ironware was basically the same as that used by Smith (1955) with a collimator, two separate rings and a parallel plate capacitor between them. The only significant difference was that there were separate amplifiers for the two rings.

To make the charge pulse independent of the drop velocity it was necessary to ensure that the input time constant to the pulse amplifiers was much longer than the transit time of the slowest drop.

A long time constant, greater than 1 second, was

obtained by employing an M E 1400 electrometer valve at the front end of the preamplifier and capacitative 'Miller' feedback over the first three stages.

B.2 Oscilloscope System

A four trace plug-in unit was used. The two charge pulses were mixed together and displayed in the first trace. The 'mass' pulse from the change in frequency of the oscillator controlled by the capacitor between the two rings was displayed in the second trace. The output of an asymmetric field mill (Lane-Smith, 1967) was displayed in the third trace and the fourth trace was available for a precipitation current sampling. The four traces were chopped. The sweep control was set for single shot operation. The camera shutter was left open. The scope had to trigger on both positive and negative charge pulses so a trigger pulse generator, Figure B.2a, was constructed.

An output on the oscilloscope called +Gate B gave a 20V positive gating pulse during a sweep. A control circuit was built, Figure B.2b, operated by the back edge of the +Gate B pulse, which wound on the film and then reset the single sweep on the oscilloscope. The whole system worked perfectly and was being calibrated

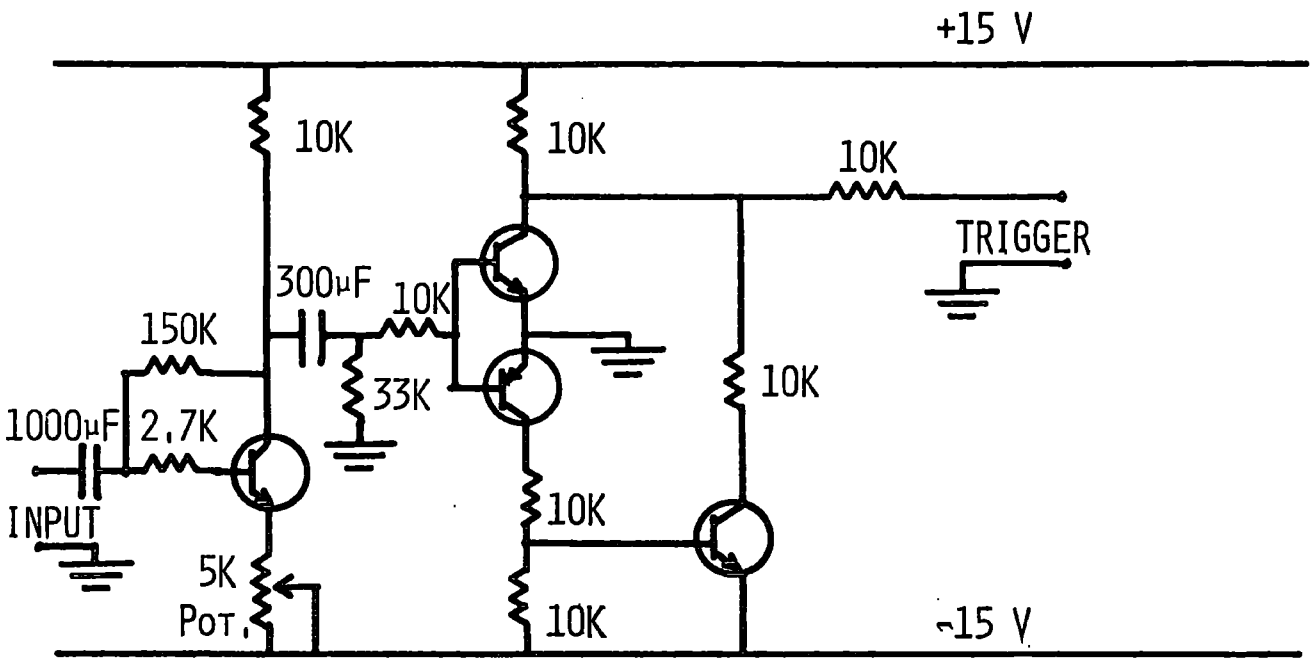

FIGURE B.2a TRIGGER PULSE AMPLIFIER

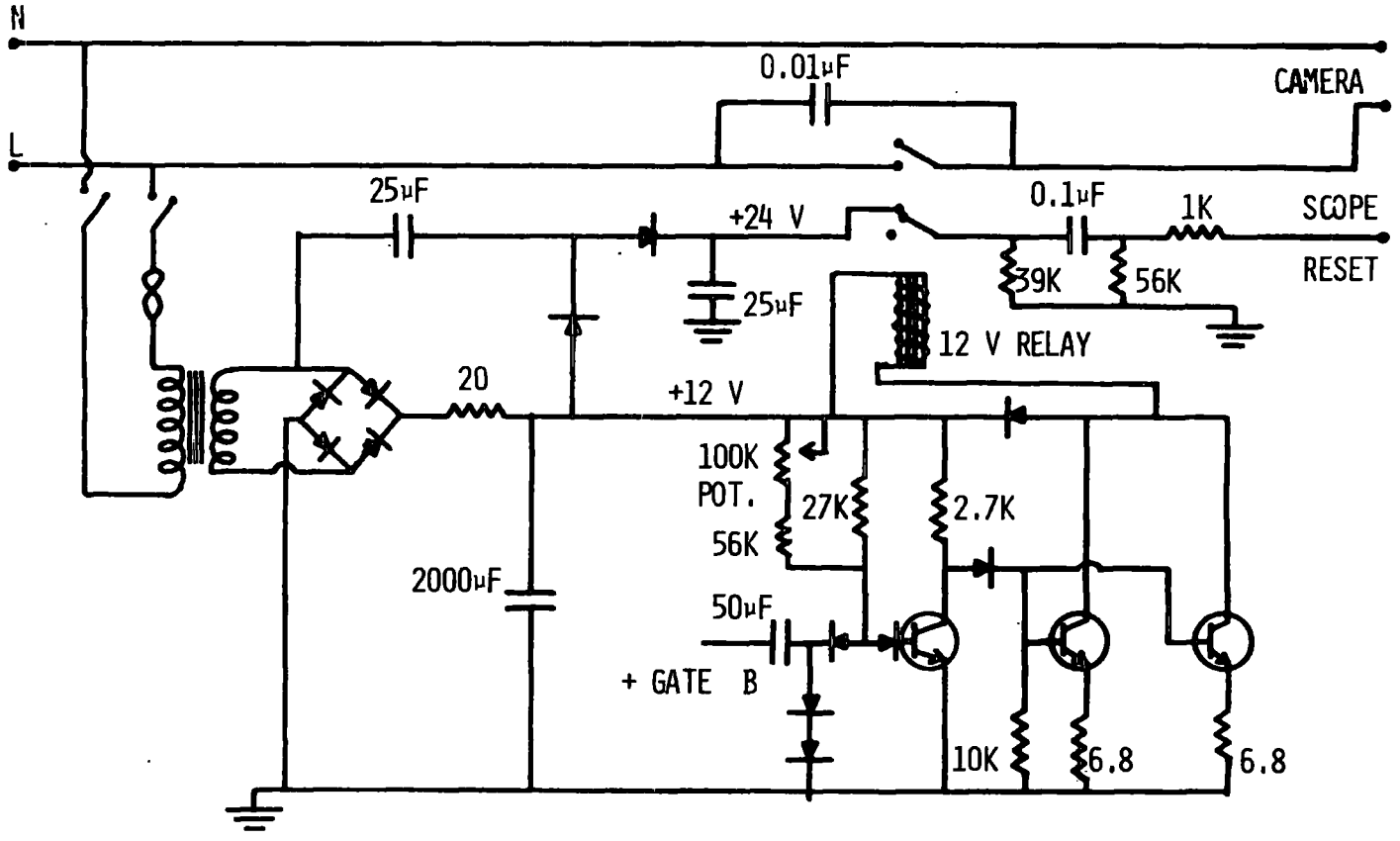

FIGURE B.2b CAMERA CONTROL CIRCUIT

when the oscilloscope broke down.

B.3 Analogue to Digital Converter

During four months spent in the computer building of the department of electrical engineering at the University of Manchester an A/D converter was designed, and partly built, to do the following:

1. To reset itself and wait for a positive or negative pulse from the first induction ring of the single drop receiver.
2. To start a clock when the first pulse reaches a maximum.
3. To measure the height of the first pulse.
4. To measure the height of the pulse from the 'mass capacitor.'
5. To measure the height of the pulse from the second ring.
6. To stop the clock when the pulse from the second ring reaches a maximum and record the time interval between this and the first pulse.
7. To sample, rapidly and consecutively, a number (the design was flexible and any number could be accommodated just by adding modules)

of different ambient parameters--such as electric field, wind speed, precipitation current, rate of rainfall, time, temperature and so on.

8. To punch all the above information on paper tape, using enough buffer storage to accommodate data waiting to be punched.

The complete system used about 1,000 semi-conductor devices and would require many pages of text and diagrams for a full description.

Most of the circuitry and the logic, though complex, used standard procedures described in the literature, see for example Zacharov (1968), and will not be described in detail here. A simplified block diagram is shown in Figure B.3a.

After completing a measurement cycle, or after switching on, the control waits until there is no signal on channel 1 and then selects that channel. When a signal is detected, the sign detector operates the switch to select the signal or its inverse, whichever is negative, to drive the amplifier which charges the storage capacitor. At the signal peak, the time register is started and the A/D conversion performed. The channel

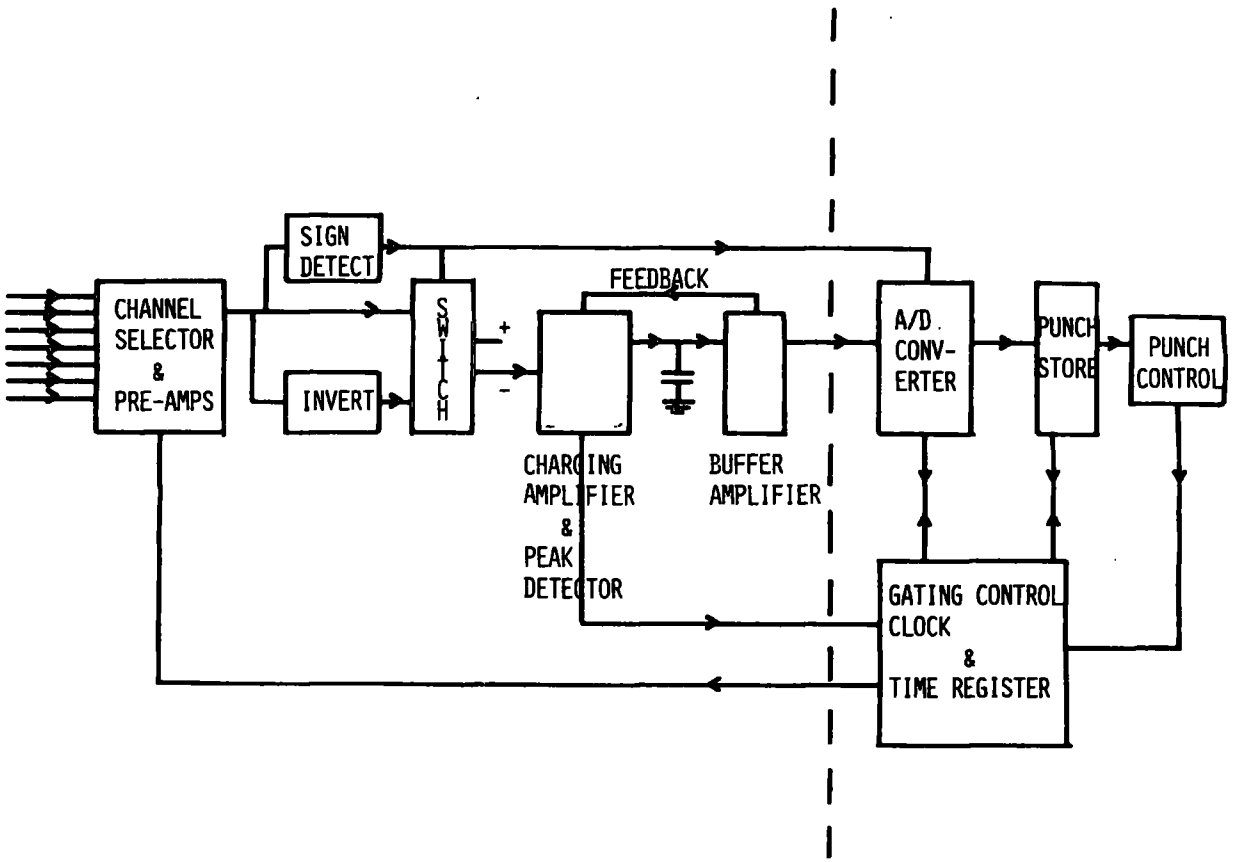

FIGURE B.3a BLOCK DIAGRAM OF ANALOGUE TO DIGITAL CONVERTER

number, the signal magnitude and sign are placed in the punch store, if it is not being read by the punch control, and the tape punch records the information at its own speed.

As soon as the information is placed in the punch store, the storage capacitor is discharged and the control selects channel 2 and waits for the raindrop to reach the 'mass capacitor.' At the signal peak a similar process takes place except the time register is not affected and there must be room in the punch store before transfer of information from the A/D register.

The signal peak on channel 3, the second induction ring of the single drop receiver, is used to stop the time register. When the channel number, signal magnitude and sign have been punched, the time interval between peaks 1 and 3 is recorded.

The gating control then cycles the remaining channels which carry information, sampling the steady values and not looking for a peak. It finally resets in channel 1 to repeat the process.

There are many contingency controls which take care of

i) asynchronism of the tape punch,

ii) uncertainty of the content of registers when first switched on, and,

iii) the possibility of a drop entering the first ring but missing the other one.

The process chosen for the A/D conversion was one of successive approximation. This is because it is fast (100 μsec), every conversion takes the same time and the method is inherently linear and capable of high accuracy. The buffer amplifier provides a current directly proportional to the signal being digitalized. Current sinks weighted according to the binary system used, in this case pure binary, are successively switched in, balanced against the source and left in if too small or switched out. A register, indicating which sinks are finally left in to balance the source, gives the signal directly in digital form according to the binary or other code adopted.

B.4 Peak Detection

In order to time the interval between pulses from the two induction rings, it was necessary to detect the occurrence of the peak. One significant innovation made by the author was in the method of peak detection. The two systems normally used were found to

be unsuitable and a new principle of operation had to be devised.

The most obvious approach was simply to differentiate the signal and when the derivative changed sign this would indicate a peak. Unfortunately, noise in the signal would produce a large number of reversals in the slope and, therefore, spurious peak detection. This system, therefore, could not be used.

A method adopted in some commercial instruments when a peak has to be detected is to delay the signal by about a tenth of the pulse length, invert it and subtract it from the original signal. When this quantity changes sign, after having a value larger than the noise, a peak is detected. This system overcomes the problem of noise but depends on all the pulses having about the same length. The raindrop velocities, and hence the pulse lengths in the receiver, varied by a factor of more than ten. It was not possible, therefore, to use this system to time the interval between the pulses from the two induction rings.

The system adopted, Figure B.4a, involved the storage capacitor and the buffer amplifier. As the signal rose so the charge on the storage capacitor

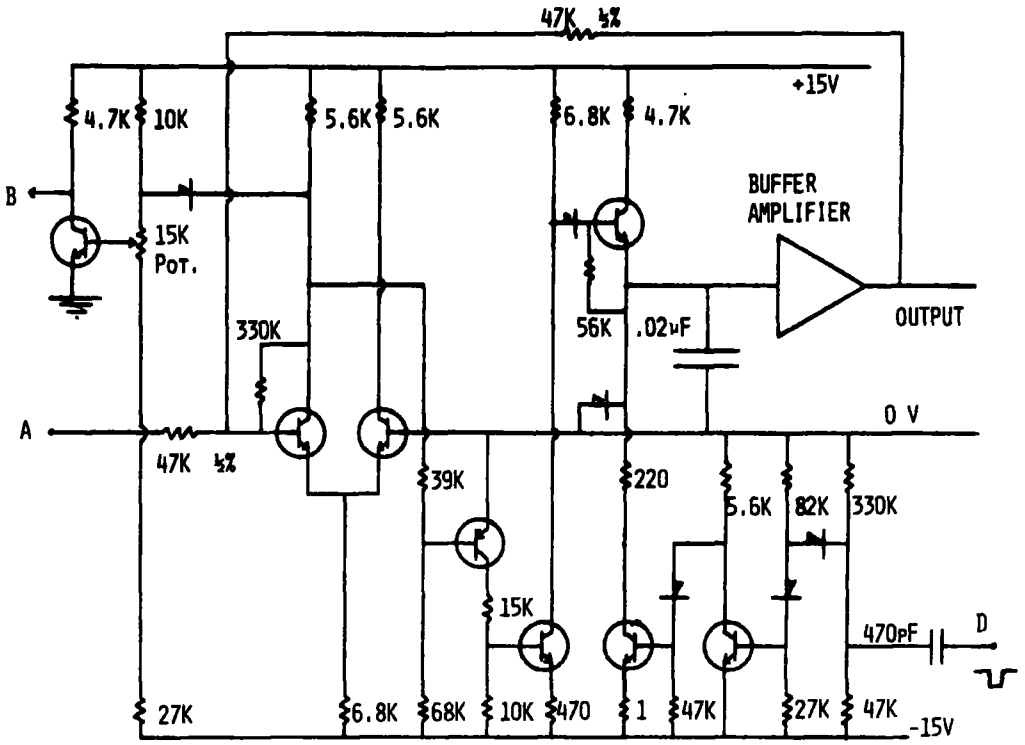

SAMPLING CAPACITOR CHARGING AND DISCHARGING CIRCUIT AND PEAK DETECTOR

All diodes are silicon switching diodes. All transistors are silicon medium gain transistors and the differential pair are matched. The buffer amplifier has a gain of nearly one and an imput impedance of more than 10 megohm.

The negative going signal is applied to the input, A. The level at B goes high positive when the signal peak is past. The buffer amplifier output is applied to the analogue to digital converter. A negative going pulse is applied to D after the conversion to discharge the sampling capacitor.

FIGURE B.4A

rose. Feedback from the buffer amplifier ensured that its output was equal to the signal. When the signal started to diminish, the charge on the storage capacitor remained steady and the buffer amplifier output then exceeded the signal. When the difference between the two was greater than some pre-determined amount, which must be greater than the noise, a peak was detected.

This system avoided the problems of both the previous methods. The delay between the peak occurring and its detection varied with height and length of the pulse. But since both pulses were identical in these parameters, the time interval measurement was accurate.

B.5 Future Development

In the field of Atmospheric Physics, it is usually desirable to accumulate large amounts of data and its recording and processing is always a problem. The device described in this appendix, had it been constructed, would have provided an excellent solution. However, although the facilities are now available, the author does not intend to build the system as described. Present day technology offers alternative methods which, though more expensive in capital equipment, are more

flexible and easier to use. An 8-channel F.M. tape recorder which is compatible with an A/D converter in the computer centre may become the core of a new system. Even so, analogue peak detection may still be desirable.

APPENDIX C

MATHEMATICAL DERIVATIONS

C.0 Some of the results stated in the body of the thesis are here derived in detail.

C.1 Nomenclature

a = area of stator exposed at some instant.

$e(t)$ = potential of the stator at some time t

f = frequency of the true signal

k = Boltzmann constant

t = time

A = maximum area of stator exposed

B = a representative bandwidth

C = effective capacitance across the amplifier input

D = separation between the stator and the rotor

E = applied electric field

H = Hum parameter defined by equation C.3i.

I = current to the pre-amplifier from the stator

K = conductivity of the air

P = an integer

R = effective resistance across the amplifier input

T = true signal period

V = output from the detector

γ = signal to noise ratio

δ = incremental phase change

ε_0 = permittivity of free space

θ = absolute temperature of input resistor

ω = a representative angular frequency of the spurious signal or noise

C.2 Conduction Current (page 17)

Conduction supplies a current, $I_2 = KEa$. Figure C.2a shows how this current varies with time by comparison with the displacement current, for a symmetrical field mill. The peak conduction current has a value KEA. The triangular current wave can be considered as a steady current of value KEA/2 together with what may be approximated to a sinusoid of amplitude KEA/2 and frequency f.

When the displacement current, $\varepsilon_0 E(da/dt)$, is

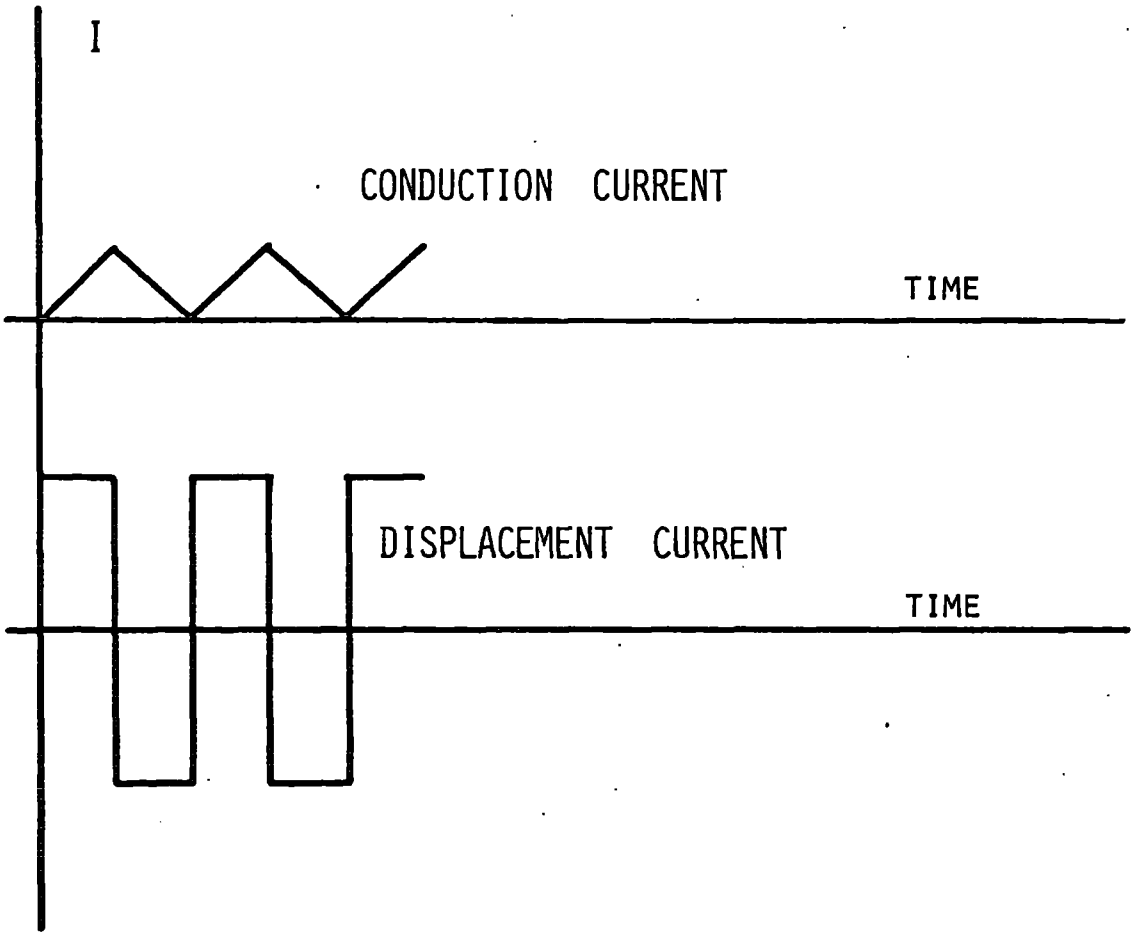

VARIATION OF CONDUCTION CURRENT AND DISPLACEMENT CURRENT WITH TIME

FIGURE C.2a

integrated by the input characteristics of the pre-amplifier, it produces a triangular voltage wave of amplitude $\varepsilon_0 EA/2\ C$ (Lane-Smith, 1967) which peaks at the instant maximum area is exposed. The conduction current wave, integrated by the same input characteristics, produces a nearly sinusoidal voltage wave of amplitude $\frac{KEA}{2\pi f.2C}$ whose phase is $\pi/2$ behind that of the current which peaked at the instant maximum area was exposed. Because of this phase change, with a phase sensitive detector, the signal due to this component of the conduction current will be zero. Without a phase sensitive detector, the ratio of the signal to spurious signal will be given by

$$\gamma_{(a)} = \frac{\varepsilon_0 EA}{2C} \cdot \frac{4\pi fC}{KEA}$$

$$= \frac{2\pi f\varepsilon_0}{K}$$

which will normally exceed 10^5.

The steady component of the conduction current will raise the average potential of the stator to a value KEAR/2.

However, the capacitance to ground of the stator is changing at a rate equal to $\frac{-\varepsilon_0 da/dt}{D} = dC/dt$.

The rate of change of input potential is given by

$$\frac{de}{dt} = \frac{-KEAR}{2C}\frac{dc}{dt}$$

$$= \frac{\varepsilon_0 KEAR}{2CD}\frac{da}{dt}$$

so that the deviation from the mean potential due to the variation of capacitance is $\frac{\varepsilon_0 KEAR.\ A}{2DC.\ 2}$.

This is in phase with the true signal of amplitude $\frac{\varepsilon_0 EA}{2C}$, so that the ratio of the signal to the spurious signal will be given by

$$\gamma(b) = \frac{\varepsilon_0 EA}{2C} \cdot \frac{4DC}{KEA^2R\ \varepsilon_0}$$

$$= \frac{2D}{KAR}$$

for any method of detection.

C.3 Hum and 'Pick-up' (page 18)

If the exposed part of the input circuit is much shorter than the electromagnetic wavelength, a quasi-static theory can be used and then the induced charge on the input is proportional to the applied field, E′. At any particular frequency the charge is given by

$$q = HE' \cos \omega t \qquad \text{(C.3i)}$$

The input current is given by

$$I_3 = -\omega HE' \sin \omega t$$

This current is applied to the parallel RC input circuit and the resultant potential variation has an amplitude equal to $\frac{\omega RHE'}{(\omega^2C^2R^2 + 1)^{\frac{1}{2}}}$.

The signal to noise ratio will, in general, be given by

$$\gamma_{(c)} = \frac{\varepsilon_o EA}{2C} \cdot \frac{(\omega^2C^2R^2 + 1)^{\frac{1}{2}}}{\omega RHE'}$$

If $\omega CR >> 1$ the expression simplifies to

$$\gamma_{(c)} = \frac{\varepsilon_o EA}{2HE'}$$

If $\omega CR << 1$ the expression simplifies to

$$\gamma_{(c)} = \frac{\varepsilon_o EA}{2HE\ \omega CR}$$

RC must be kept larger than T so to benefit from the second expression, to have ωCR small, T must be as small as possible.

C.4 Thermal Noise (page 19)

The input resistor, R, may be considered as a noiseless resistor in series with a voltage source whose mean square value is $4k\theta R$ per unit frequency bandwidth. This noise signal is decoupled by the input capacitance, C, so the total noise input signal is given by

$$\overline{e^2} = 4k\theta R \int_{\omega_1}^{\omega_2} \frac{1}{(1 + \omega^2C^2R^2)} \cdot \frac{d\omega}{2\pi}$$

where $\frac{\omega_2 - \omega_1}{2\pi}$ is the bandwidth, B, accepted by the amplifier and detector.

$$\overline{e^2} = \frac{4k\theta R}{2\pi CR} (\tan^{-1}\omega_2 CR - \tan^{-1}\omega_1 CR)$$

If $\omega_2 CR$ and $\omega_1 CR$ are both much bigger than 1,

$$\overline{e^2} \simeq 4k\theta RB$$

The signal to noise ratio then becomes

$$\gamma_{(d)} = \frac{\varepsilon_0 EA}{2C} (4k\theta RB)^{-\frac{1}{2}}$$

$$= \frac{\varepsilon_0 EA}{4RC} \cdot \frac{\sqrt{R}}{\sqrt{k\theta B}}$$

If $2\pi RCf$ is of the order 1, then,

$$\gamma_{(d)} \simeq \frac{\varepsilon_0 EAf\sqrt{R}}{\sqrt{k\theta B}}$$

However, if $\omega_2 CR >> 1$ and $\omega_1 CR << 1$,

$$\overline{e^2} = \frac{4k\theta R}{2\pi CR} \cdot \frac{\pi}{2}$$

$$= k\theta/C$$

The signal to noise ratio is then

$$\gamma_{(d)} = \frac{\varepsilon_0 EA}{2C} \cdot \frac{\sqrt{C}}{\sqrt{k\theta}}$$

$$= \frac{\varepsilon_0 EA}{2\sqrt{CR}} \cdot \frac{\sqrt{R}}{\sqrt{k\theta}}$$

$$\simeq \frac{\varepsilon_0 EAf\sqrt{R}}{\sqrt{k\theta f}}$$

which is similar to the former equation except that the signal frequency is substituted for the noise bandwidth.

C.5 Phase Sensitive Detector Type 1 (page 23)

The detector is switched in for half a period each cycle. The average output, $\overline{\Delta V}$, from the detector during a cycle ending at a time PT is given by

$$\overline{\Delta V} = \frac{1}{T} \int_{(P-\frac{1}{2})T}^{PT} (e_t - e_{(P-\frac{1}{2})T}).dt$$

If $e_t = - e_o \sin (2\pi t/T)$

then, $$\overline{\Delta V} = \overline{\Delta V_o} = \frac{1}{T} \int_{(P-\frac{1}{2})T}^{PT} \{0 - e_o \sin(\frac{2\pi t}{T})\}.dt$$

$$\overline{\Delta V_o} = \frac{e_o}{2\pi} \left[\cos (\frac{2\pi t}{T})\right]_{(P-\frac{1}{2})T}^{PT}$$

$$= e_o/\pi$$

If $e_t = - e_o \sin (\frac{2\pi t}{T} + \delta)$

then, $$\overline{\Delta V} = \frac{1}{T} \int_{(P-\frac{1}{2})T}^{PT} \{e_o \sin \delta - e_o \sin(\frac{2\pi t}{T} + \delta)\}.dt$$

$$= \left[\frac{e_o \sin \delta}{2} + \frac{e_o}{2\pi} \cos(\frac{2\pi t}{T} + \delta)\right]_{(P-\frac{1}{2})T}^{PT}$$

$$= \frac{e_o \sin \delta}{2} + \frac{e_o}{\pi} \quad \text{if } \delta \text{ is small.}$$

So that, $\overline{\Delta V} = \overline{\Delta V_o}(1 + \frac{\pi}{2} \sin \delta)$

and for a steady field, the total output will be

$$V = V_o(1 + \frac{\pi}{2} \sin \delta)$$

C.6 Phase Sensitive Detector Type 2 (page 24)

The average output, $\overline{\Delta V}$, from the detector during a cycle ending at a time PT is now given by

$$\overline{\Delta V} = \frac{1}{T} \int_{(P-\frac{1}{2})T}^{PT} e_t \cdot dt$$

If $e_t = - e_o \sin (\frac{2\pi t}{T})$

then, $\overline{\Delta V} = \overline{\Delta V_o} = \frac{1}{T} \int_{(P-\frac{1}{2})T}^{PT} - e_o \sin (\frac{2\pi t}{T}) . dt$

and $\overline{\Delta V_o} = \frac{e_o}{\pi}$

If $e_t = - e_o \sin (\frac{2\pi t}{T} + \delta)$

then $\overline{\Delta V} = \frac{1}{T} \int_{(P-\frac{1}{2})T}^{PT} - e_o \sin (\frac{2\pi t}{T} + \delta) . dt$

$$= \left[\frac{e_o}{2\pi} \cos (\frac{2\pi t}{T} + \delta)\right]_{(P-\frac{1}{2})T}^{PT}$$

$$= \frac{e_o}{2\pi} \{\cos(2\pi + \delta) - \cos(\pi + \delta)\}$$

$$= \frac{e_o}{2\pi} \cdot 2 \cos \delta$$

$$= \frac{e_o}{\pi} \cdot (1 - \sin^2 \delta)^{\frac{1}{2}}$$

$$= \overline{\Delta V_o} \left(1 - \frac{\delta}{2} \sin \delta\right) \quad \text{if } \delta \text{ is small.}$$

So that $V = V_o \left(1 - \frac{\delta}{2} \sin \delta\right)$

APPENDIX D

16mm FILMING SCHEDULE

D.1 Preamble

The 16 mm film consists of seven 50-foot magazines. All shots except Mag 1 were taken at the same speed, a nominal 7 secs per frame, from the verandah of the Lane-Smith residence (K22, Fourah Bay College) which has an elevation of 1,050 feet, the camera facing approximately N.E. Tagrin point and Tasso island are both clearly visible on most frames so that the exact azimuth can be determined by reference to the map, Figure 6.1a. Some white splicing tape was left between the 50-foot lengths to aid in location of specific shots. The film is virtually unedited--as will be immediately apparent to the viewer.

Comments in the schedule in round brackets () were written at the time of filming. Comments in square brackets {} have been added later.

At Pepel there is a jetty for loading iron ore into cargo boats. This is the only place in the field of view of the camera where there are lights visible from Fourah Bay College and it therefore provides a landmark in the evening when the ground is in shadow.

D.2 Schedule

Mag 1

May 25, 1967

18.35-18.56 21 min. 5½ sec per frame N.E.
F 2.8 (no lightning)

May 26

15.12-17.31 2 hr. 19 min. 7 sec per frame N.E.
16.06 precipitation
17.05 lightning
{notice typical distant thunderstorm towards the end}
18.28-18.41 33 min.
18.49-19.07 18 min.

Mag 2

June 5

17.38-17.59 21 min. 7 sec per frame N.E.
F 11

18.55-19.20 approx. F 4.

(Under surface of low cloud before storm.

Thunder and lightning)

June 12

17.15-18.05 50 min.

June 14

13.45-14.05 20 min. F 11

(Squall line approaching)

June 15

13.15-15.05 1 hr. 50 min.

13.15 F 11 (Squall approaching)

13.25 F 5·6 (rain)

13.35 F 8

14.03 F 11

June 17

13.15-14.09 54 min. F 16

(Much cloud and some showers)

Mag 3

September 15

15.16-17.30 2 hr. 14 min. F 8

(Developing cumulus over Pepel)

{Then storm umbrella from South}

September 17

17.48-18.33 45 min. F 5·6

(shower cloud N of Pepel)

{rollers in front of hill side}

September 19

15.58-before 18.00 less than 2 hours F 8

(2 storms beyond Pepel)

Mag 4

September 23

13.08-17.18 4 hr. 10 min. F 11

(Heavy shower N of Pepel)

{Notice at the back of the storm a diffuse trail of small cumulus}

Jumping is due to the camera running down and stopping.

Mag 5

October 8

16.27-17.46 1 hr. 19 min.

(Heavy shower N of Pepel)

16.27 F 11

17.15 F 8

{Field at Pepel <500V/M (no visible record)}

October 9

16.09-16.24 15 min. F 11

(Small cumulus N of Pepel, storm coming from South)

October 11

18.24-18.44 20 min.

18.24 F 4 (Sunset on a storm)

18.30 F 2·8

18.35 F 1.8

October 13

16.56-18.54 1 hr. 58 min.

16.56 F 11

(Scattered cumulus prevented from growing by strong shear)

17.30 F 8 (Magnificent cumulus range 4 miles, estimated from shadow on water)

17.50 F 5·6 18.15 F 4 18.27 F 2.8

18.35 F 1.8 (Storm approaching Pepel, 18.37½ filter off)

18.40 (Superb towering cumulus with lightning occurring with 3 minutes of the height reaching 6 miles)

{Pileus which appears above the cloud, is penetrated and remains around the cloud like

a skirt.}

18.54 Finish (Storm reaches Pepel)

Mag 6

October 18

16.54-18.42 1 hr. 48 min.

16.54 F 11

17.33 F 8

{cumulus over Pepel at sunset}

October 22

17.40-18.15? ?35 min. F 8

(shower over Pepel)

October 25

13.20-16.39 3 hr. 19 min. F 11

(small growing cumulus behind Pepel)

Mag 7

16.39-18.27 1 hr. 48 min. F 11 - F 1·8

(storm over Pepel)

October 31

16.17- ? ? F 11

16.28 F 8 (Scattered cumulus)

REFERENCES

Adkins, C.J.	1959	Small ion concentration near the ground. Q. J. Roy. Met. Soc., 85, 237-252.
Allen, J.R.L.	1968	J. Sed. Petro, 38, 621-633.
Appleman, R.	1957	J. Met., 14, 89.
Auer, A.H. Jr., Veal, D.L. and Marwitz, J.D.	1969	Proc. 6th Severe Local Storms Conf., A.M.S., 16-19.
Bagnold, R.A.	1966	U.S. Geol. Surv., Prof. Paper 422-1.
Beneteau, P.J. and Riva, G.	1963	S.G.S. Fairchild. Application Report, 51.
Blanchard, D.C.	1949	G.E. Res. Lab. Proj. Cirrus Occ. Rep., 16.
_____	1963	Progress in Oceanography Vol. 1, Pergamon.
Blaser, L. and MacDougall, J.S.	1964	S.G.S. Fairchild. Application Report, 138.
Browne, I.C., Palmer, H. P. and Wormell, T.W.	1954	Q. J. Roy. Met. Soc., 80, 291-327.
Chalmers, J.A.	1943	Phil. Mag., 34, 63.
_____	1951	Q. J. Roy. Met. Soc., 77, 249-259.

_____	1967	Atmospheric Electricity (2nd ed.) Pergamon.
Chamberlain, A.C.	1966	Proc. Roy. Soc. A, 296, 45-70.
Chaplin, G.B.B. and Owens, A.R.	1957	Proc. Inst. E. E. 105B, 258-266.
Fletcher, N.H.	1962	The Physics of Rain-clouds, Cambridge.
Foster, H.	1950	Bull. Amer. Met. Soc., 31, 140.
Gregory, P.H., Guthrie, E.J. and Bunce, M.E.	1959	J. Gen. Microbiol. 20, 328-354.
Gunn, K. and Hitsch-feld, W.	1951	J. Met. 8, 7.
Harnwell, G.P. and van Voorhis, S.N.	1933	Rev. Sci. Inst. 4, 540-541.
Harris, D.J.	1967	Nature, 214, 585.
Houghton, D.	1969	Weather, 24, 2-18.
Humphreys, W.J.	1929	Physics of the Air. Mc-Graw-Hill (1964, Dover Pub. Inc., New York).
Kelkar, V.N.	1968a	Ind. J. of Met. & Geo-phys. 19, 143-148.
_____	1968b	Ind. J. Met. & Geophys. 19, 29-38.
Landon, V.D.	1941	Proc. Inst. Rad. Engr. 29, 50-55.
Lane-Smith, D.R.	1965	Wireless World 71, 402.
_____	1967	J. Atmos. & Terr. Phys. 29, 687-699.

Langmuir, I.	1948	J. Met. 5, 175.
Latham, J. and Mason, B.J.	1961	Proc. Roy. Soc., A. 260, 537.
Lenard, P.	1892	Ann. Phys., Lpz. 46, 584-636.
Michnowski, S.	1963	Ind. J. Met. Geophys., 14, 320.
Moody, N.F.	1956	Electron. Engr. 28, 94-100.
Moore, C.B., Vonnegut, B., Stein, B.A., and Survilas, H.J.	1960	J. Geophys. Res., 65, 1907.
Picca, R.	1968	Fourth Int. Conf. on Univ. Aspects of Atmos. Electricity. Tokyo. Sect.1.3.
Pietrowski, E.L.	1960	J. Met. 17, 562-563.
Ramsay, M.W. and Chalmers, J.A.	1960	Q. J. Roy. Met. Soc., 86, 530-539.
Reynolds, S.E., Brook, M., and Gourley, M.F.	1957	J. Met., 14, 426.
Schonland, B.F.J.	1928	Proc. Roy. Soc. A., 118, 233-251.
Simpson, G.C. and Scrase, F.J.	1937	Proc. Roy. Soc., A. 161, 309.
Simpson, G.C.	1949	Geophys. Mem., Lond. 84, 1-51.
Sivaramakrishnan, M.V.	1961	Ind. J. Met. Geophys. 12, 447-464.
_____	1965	Ind. J. Met. & Geophys. 16, 13-32.
_____	1967	Ind. J. Met. & Geophys. 18, 13-26.

Smith, L.G.	1951	Dissertation Rain Electricity, Cam. Univ.
_____	1955	Q. J. Roy. Met. Soc., 81, 23-47.
Smythe, W.R.	1950	Static & Dynamic Electricity, McGraw-Hill.
Volta, A.	1782	Phil. Trans. Roy. Soc., 72, 237-280.
Vonnegut, B.	1965	Problems of Atmos. and Space Electricity, S.C. Coroniti(ed.), Elsevier, Amsterdam, 285-292.
Whipple, F.J.W. and Chalmers, J.A.	1944	Q. J. Roy. Met. Soc., 70, 103-120.
Wilson, C.T.R.	1929	J. Franklin Inst. 208, 1-12.
Workman, E.J. and Reynolds, S.E.	1950	Phys. Rev., 78, 254.
Wormell, T.W.	1953	Q. J. Roy. Met. Soc., 79, 3-50.
Zacharov, B.	1968	Digital Systems Logic & Circuits, George Allen & Unwin Ltd., London.

Journal of Atmospheric and Terrestrial Physics, 1967, Vol. 29, pp. 687–699. Pergamon Press Ltd. Printed in Northern Ireland

A new design of sign-discriminating field mill

D. R. LANE-SMITH
Fourah Bay College, University of Sierra Leone

(*Received* 14 *November* 1966)

Abstract—A design of field mill is presented which, while giving the sign of the field as well as the magnitude, uses only one rotor and one stator and no other form of pick-up. The simplicity of design also extends to the electronics which does not include the phase sensitive detector normally required.

An asymmetric waveform is generated. The sign of the asymmetry depends on the sign of the field and this is detected as a steady, positive or negative direct current.

1. INTRODUCTION

THE field Mill (HARNWELL and VAN VOORHIS, 1933) works on the basic principle of alternately exposing an insulated plate to, and screening it from an electric field. As the area of plate exposed changes, charge is induced on the plate. The displacement current, I, supplying this charge, is given by:

$$I = -\varepsilon_0 E \frac{dA}{dt} \tag{1}$$

where E is the potential gradient and A is the area of plate exposed. MAPLESON and WHITLOCK (1955) have shown that, for a normal sector type mill,

$$I = \pm \varepsilon_0 E A \omega / \pi$$

where ω is the angular velocity of the rotor.

The equivalent circuit of the stator-rotor assembly, including leaks and strays in the first stage of the amplifier, is shown in Fig. 1. The only limitation in the value of R is that it must be made small compared with any leakage resistance, R_L, from a current source which would otherwise deposit charge on the stator. The effect of such a charge would be that as the capacitance to ground of the stator varied with the position of the rotor, so its potential would vary. This is the same action as a condenser microphone. (On the other hand, such an effect could be used to off-set the zero of the field mill and would be one way of discriminating the sign.)

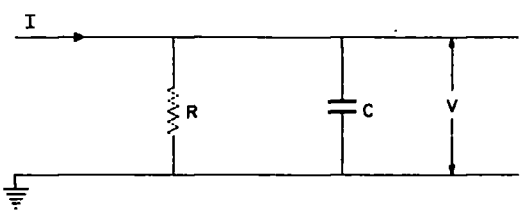

Fig. 1.

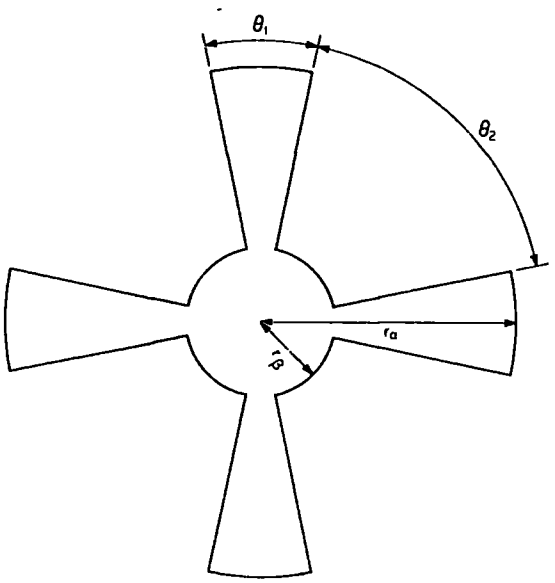

Fig. 3.

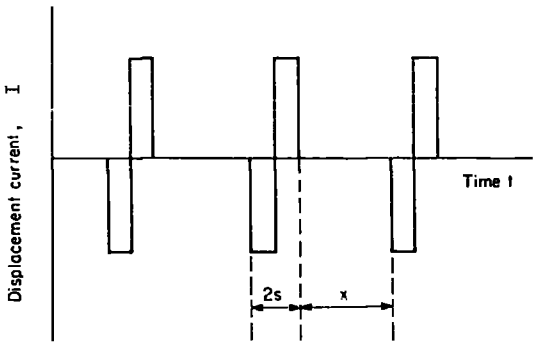

Fig. 4.

The current, I, flowing into the input circuit is therefore a periodic function shown in Fig. 4, which can be divided in three parts, (a), (b) and (c):

(a) $$I = -J \qquad 0 < t < s \tag{3}$$

where

$$J = \varepsilon_0 E N \omega (r_\alpha^2 - r_\beta^2)/2 \tag{4}$$

ε_0 is the permittivity of air

E is the potential gradient, called positive when the direction is downwards

$t = 0$ at the beginning of the period when the rotor is just about to start covering the stator

$s = \theta_1/\omega$ where θ_1 is the angular width of a vane.

The expression for $V_{(n-1)}$ would include a term $V_{(n-1)} \exp(-2T/RC)$ so the effect of the value of $V_{(n-1)}$ on subsequent values of V falls off exponentially with a time constant RC. Therefore the value of E', which determined V_0, will have negligible effect on V_n when nT becomes large compared with RC. For such values of n, V_n is equal to $V_{(n-1)}$.

$$V_n - V_{(n-1)} = V_{(n-1)}(\exp(-T/RC) - 1) + JR(1 - \exp(-s/RC))^2 \exp(-x/RC).$$

When there is a steady potential gradient, E, and when

$$n \gg \frac{RC}{T}, \qquad V_n - V_{(n-1)} = 0$$

so

$$V_{(n-1)} = -\frac{JR(1 - \exp(-s/RC))^2 \exp(-x/RC)}{\exp(-T/RC) - 1}. \tag{15}$$

The solution of equation (15) depends on whether RC is much less than, nearly equal to, or much greater than T. For the field mill described it is necessary that RC be much greater than T because only then is the wave form the right shape for the detector, and also only then is the amplitude of the signal independent of the rotor angular velocity. In this case, $\exp(-T/RC)$ becomes $(1 - T/RC)$ and equation (15) becomes

$$V_{(n-1)} = +(1 - x/RC)Js^2/CT \approx +\frac{Js}{C} \cdot \frac{s}{T}. \tag{16}$$

From equation (9)

$$V_a = \frac{+Js^2}{CT} - \frac{Jt}{C} \qquad 0 < t < s \tag{17}$$

so

$$V_a' = \frac{Js}{C}\left(\frac{s}{T} - 1\right) \tag{18}$$

and

$$V_b' = V_c' = V_n = \frac{Js}{C} \cdot \frac{s}{T}. \tag{19}$$

This gives the waveform shown in Fig. 5.
The amplitude of the signal, ΔV, is given by

$$\Delta V = V_b' - V_a' = \frac{Js}{C}$$

$$= \frac{\varepsilon_0 EN\omega}{2C}(r_\alpha^2 - r_\beta^2) \cdot \frac{\theta_1}{\omega}$$

$$= \frac{\varepsilon_0 EA}{C} \tag{20}$$

where A is the total area of the exposed plates.

3. The Electronics Circuits

The amplifier

The requirements for the amplifier are a high input impedence, low output impedance and gain sufficient for the sensitivity required. If the input impedence is low, a larger capacitor, C, must be used to give a sufficiently large time constant, RC, which in turn means a smaller signal. Provided the noise level is not high the product of the gain required and the input impedance is sensibly constant for a

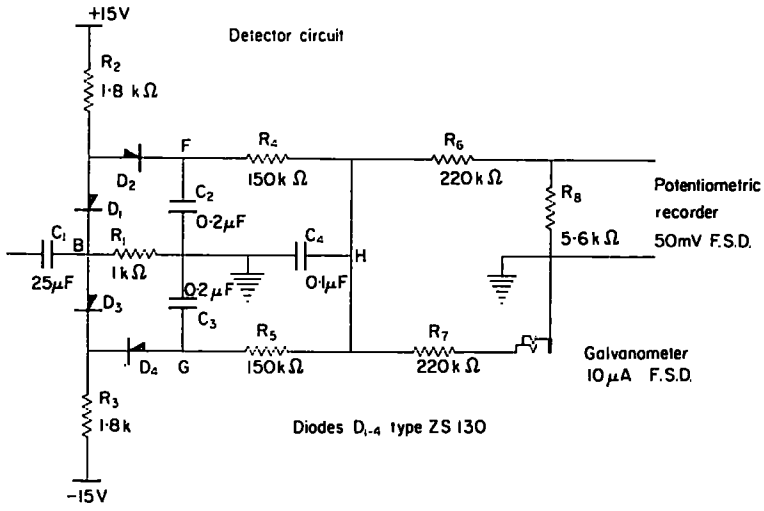

Fig. 6.

given signal frequency so that the high input inpedence requirement can be traded for a high gain requirement. The output impedance must be low compared with the input impedance of the detector circuit.

Any amplifier satisfying these requirements would be adequate. If the amplifier produces a phase reversal, a positive field will give a positive final output.

The detector (Fig. 6)

The detector measures the amplitude of the positive and negative peaks and adds them algebraically, that is, if the largest positive excursion were +6V and the largest negative excursion were −2V, the output would be proportional to +4V. This d.c. signal is then put into suitable form for the recorder used.

Operation

As the potential at the point B rises above the potential of F, some of the current flowing down R_2 is diverted from D_1 to flow through D_2 to charge the 0·2 μF condenser C_2. When C_2 is fully charged, F will be at a slightly higher potential than B because, with only the small current flowing through R_4 to keep it 'alight', the forward drop across D_2 will be less than that across D_1. When B begins to fall in potential D_2 becomes reverse biased and F remains at a slowly dropping potential as C_2

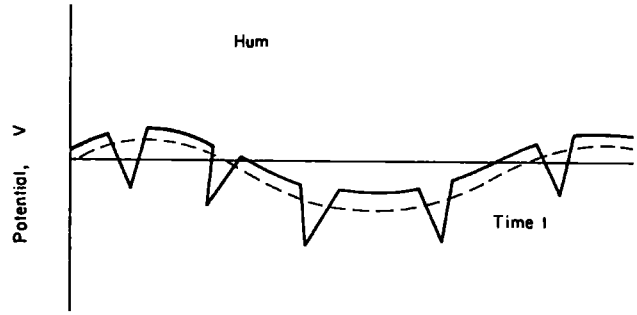

Fig. 8.

negative excursions by the amplitude of the hum. As for noise, this does not affect the final output.

The off-set zero system and the phase-sensitive detector system also react to hum in the same way that they react to noise.

If the hum or noise is picked up on the stator of the field mill so that its amplitude depends on whether the plate is screened or not, the effect is to change the sensitivity of the mill for signals of the same order of magnitude as the hum. With no field, the hum signal appears as in Fig. 9.

When a small field is applied the signal changes to that of Fig. 10 where it can be seen that the difference between the maximum positive and negative excursions is less than it would be if no hum were present.

The calibration curve then takes on the shape of Fig. 14. For high accuracy at low fields, it is therefore necessary to calibrate the field mill under similar hum and noise conditions to those under which it will be used.

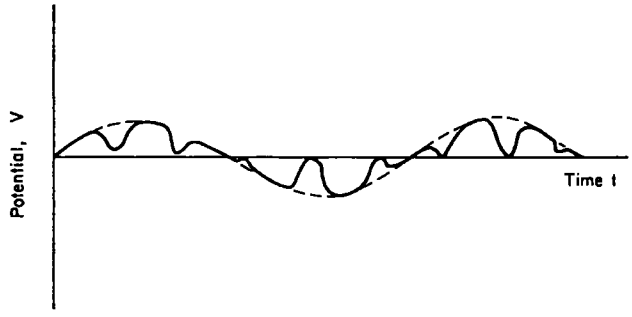

Fig. 9.

The off-set zero system and the phase sensitive detector system also both change their sensitivity for small signals in the presence of this type of pick-up.

(iii) *Temperature and supply variations*

The potential at B (Fig. 6), for zero signal, controls the output zero level. It is determined by resistors R_1, R_2, and R_3, the supply voltages and the forward potential drop across diodes D_1 and D_3. To avoid too heavy a load on the amplifier, R_1 is made quite high which means that changes in the supply rail potentials will have more effect on the output potential. For the design presented, a change of

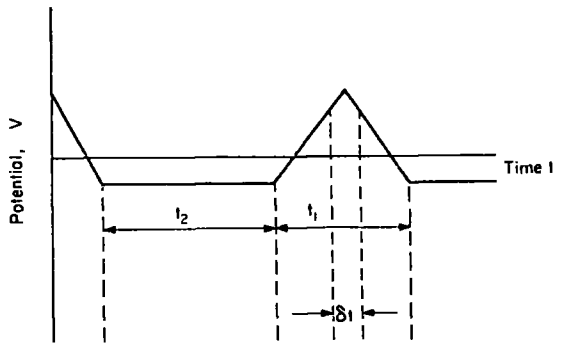

Fig. 12.

approaches 5 per cent of t_1 ($\approx 2\%$ of a period, say) then there will be about a 5 per cent reduction in the potential at F. This situation is reached when the current through R_4 is $\frac{1}{50}$th the current through R_2 and happens when F reaches some potential $+V_{max}$. At this time H will be at about $+\frac{2}{3}V_{max}$. So:

$$\frac{15 - V_{max}}{1{\cdot}8} \approx \frac{50 \times \frac{2}{3}V_{max}}{150}$$

and

$$V_{max} \approx 10{\cdot}7 \text{ V} \tag{23}$$

The output circuit is designed to give full scale deflection when the peak voltage reaches 6 V, or $\Delta V = 8$ V, which ensures that errors due to non-linearity are always less than 5 per cent.

Increasing the charge current, perhaps using the modified circuit of Fig. 9 or Fig. 13, will further reduce the errors due to non-linearity. If the vanes of the rotor are made 10 per cent wider than the vanes of the stator, the peak will cease to be a sharp point but will have a flat top of duration 5 per cent of t_1. The error introduced by the charging time of C_2 now becomes less than 1 per cent.

The response time of the detector, determined by C_1R_1, $C_2R_4C_3R_5$ and C_4, R_6 and R_7, should be longer than the response time of the field mill, RC, which, in turn, should be longer than the signal period $1/f$. If a rapid response is required then a fast field mill must be used to give a high signal frequency.

5. Performance

Several field mills working to this principle have been constructed. The performance of a simple demonstration model is described. The mill is of very simple design with four blades each of radius 2 in. and angular width 22°. Into the space between the stator blades were inserted earthed plates to reduce the effect of stray fields.

The rotor was driven at about 3000 rev/min, giving a signal frequency of about 200 c/s.

Hum pick-up of the type shown in Fig. 9 was present with an amplitude of the same order of magnitude as that of the signal due to a field of about 300 V/m. This hum level in the laboratory was far greater than that to be expected in the open and

clearly evident. On the X1 range with full scale deflection for a field of 600 V/m, the curve is found to be continuous and well behaved.

6. Conclusion

The field mill described has many of the advantages of the system using a phase sensitive detector with the added advantage of extreme simplicity. No extra pick-up on the field mill is required, there is only one amplifier and the detector is simple in design and requires few components.

The principle is well suited for specialised applications where previously far more complex devices have been used. One example would be the compensation for displacement current (Adamson, 1960; Hutchinson, 1966), where the negative feedback would be easily applied. Another application is for use in radio-sondes or other inaccessible places. A double field mill has been designed in which one rotor has $\theta_1 = 3\theta_2$ while the other has $\theta_2 = 3\theta_1$ (see Fig. 3). The outputs from the two identical stators are connected together and amplified as one signal. With this double field mill, the effects of self charge are eliminated, Currie and Kreielsheimer (1960), and the output signal gives the magnitude and sign of the field when detected as shown above.

The signal which carries the information of both magnitude and sign of the field (Fig. 5) can be transmitted over just two wires or could be used to modulate a carrier wave. Thus only one signal need be transmitted and the detector can be housed in the recording station.

References

Adamson J.	1960	*Q. Jl R. Met. Soc.* **96**, 252.
Collin H. L.	1962	*J. Atmosph. Terr. Phys.* **24**, 743.
Currie D. R. and Kreielsheimer K. S.	1960	*J. Atmosph. Terr. Phys.* **19**, 126.
Groom K. N.	1965	*J. Atmosph. Terr. Phys.* **27**, 775.
Harnwell G. P. and van Voorhis S. N.	1933	*Rev. Scient. Instrum.* **4**, 540.
Higazi K. A. and Chalmers J. A.	1966	*J. Atmosph. Terr. Phys.* **28**, 327.
Hutchinson W. C. A.	1966	*J. Atmosph. Terr. Phys.* **28**, 823.
Kilinski E. von	1950	*Z. Met.* **4**, 677.
Malan D. J. and Schonland B. F. J.	1950	*Proc. Phys. Soc. Lond.* **B63**, 402.
Rangs	1942	*Zentr. Wiss. Ber.* No. 699.